Three Essays on Dynamical Processes on Networks

Daniele Cassese

Supervisor: **Prof. Paolo Pin**

Department of Economics and Statistics
University of Siena

This dissertation is submitted in partial fulfillment for the degree of
Doctor of Philosophy

July 2016

To my mum and dad.

Declaration

I hereby declare that except where specific reference is made to the work of others, the contents of this dissertation are original and have not been submitted in whole or in part for consideration for any other degree or qualification in this, or any other university. This dissertation is my own work and contains nothing which is the outcome of work done in collaboration with others, except as specified in the text and Acknowledgements.

Daniele Cassese
July 2016

Acknowledgements

Forthcoming

Abstract

Networks are an useful abstraction to model complex systems: the set of nodes represents the fundamental units, and the set of links constitutes the constraint to interactions among these units. This simple but powerful abstraction provides a framework for studying how interactions among the micro components of the system generates its macroscopic properties, or in other words for understanding the emergence of complexity.

Modeling a dynamical process on a graph structure may be a hard task, and it is often necessary to implement computer simulations to study the emerging dynamics. Simulations can be very useful, and can give lots of insights about the emerging properties of a complex system but it is always preferable to have equation based models, not necessarily as a substitute of agent based models, in fact to complement the former and give a clearer framework inside which the results of the agent based model can be better understood.

Chapter 1 introduces the minimal background material on network theory and provides a brief introduction to pair approximation.

Chapters 2 and 3 develop equation-based models to study dynamical processes on networks, using a mean field approach based on pair approximation. Chapter 2 provides a version of the replicator equation for a family of graphs with local homogeneity and global heterogeneity, here called multiregular graphs. This replicator equation on graphs is applied to the study of the evolution of cooperation, finding a relationship between the cost of cooperation and the graph topology that ensures the sustainability of cooperation in equilibrium.

Chapter 3 studies the dynamics of ideological conflict in a population structured on a graph, using the framework of epidemiological compartmental models. We develop a new typology of epidemic dynamics, where the surveillance against the diffusion of the disease is performed by a specific class of nodes instead that being exogenously imposed *via* death or vaccination, resulting in a novel dynamic behaviour. The dynamic is analyzed on a complete, a static regular and an adaptive network, and the epidemic thresholds for the three models are compared.

Chapter 4 studies an Edgeworth process on a weighted graph, that is a simple dynamics of pure exchange among nodes placed on a complete graph with weighted edges. The main result of this paper is determining the conditions under which the set of topologies can be mapped one-to-one to the set of stable equilibria of the trade dynamics. Under a minimal set of assumption we provide a version of the Second Welfare Theorem for networks.

Table of contents

List of figures **xiii**

List of tables **xvii**

1 Basic Concepts **1**
1.1 Graphs and networks 1
1.2 Pair Approximation 4
1.3 Dynamical Systems 5

2 Replicator Equation on Multiregular Graphs **7**
2.1 Introduction 9
2.2 Replicator Equation on Regular Graphs 12
2.3 Derivation of Replicator Equation 14
2.4 Extensions 16
2.5 Evolution of cooperation 20
2.6 Multi-Regular Random Graph 23
2.7 Generating a Random MR Graph 27
2.8 Further research and Conclusions 28

3 Surveillance on Networks, a Pair Approximation Model **29**
3.1 Introduction 31
3.2 Epidemiological Models 34
3.3 The Complete Graph Model 35
3.4 The static regular graph model 37
3.5 Equilibria Stability and Basic Reproduction Number 44
3.6 Adaptive Networks 49
3.7 Basic Reproduction Number 54
3.8 Numerical Analysis 56
3.9 Best Response Maps 63

3.10 Conclusions 65

4 Edgeworth Process on Networks **67**
4.1 Introduction 69
4.2 The model 74
4.2.1 Pure Exchange 74
4.2.2 Trading 76
4.3 *Fair trading* between two agents 78
4.4 More agents 80
4.4.1 The network environment 81
4.5 Analogous of the second welfare theorem for networks 82
4.5.1 A numeric example: the Cobb-Douglas case 84
4.6 Conclusions 92

References **95**

Appendix A **103**
A.1 Evolutionarily Stable Strategy 103

Appendix B **105**
B.1 Pair Equations, static network 105
B.2 Pair Equations, adaptive network 106
B.3 Eigenvalues 106

Appendix C **109**

List of Abbreviations **111**

List of figures

2.1 *Multi-regular* graph with three $\mathcal{V}$ of degrees 3,4 and 6. The gray vertices are the frontier vertices which create a bridge with an adjacent $\mathcal{V}$ of different degree. The blue vertices are interior vertices. 18

2.2 *Multi-regularity* not satisfied. Removing the edge between the two red vertices the regularity condition does not hold anymore, and adding one or more edges between each of the red vertices and any of the non-red vertices violates [b_1] - [b_2]. 19

2.3 Regularity is restored in each subgraph but connectedness is lost. There are only interior vertices and the graph is not *multi-regular*. 20

2.4 Trajectories of a multi-regular graph (3,4,9) as the frequencies of the three subgraphs change. Blu lines for defectors, red for cooperators 22

2.5 Rest points of a multi-regular graph (3,4,9), the black points are the stable ones 23

2.6 Trajectories of a multi-regular graph (3,5,7,9), $b/c = 6$. Cooperators prevail for most of the possible topologies 24

2.7 Trajectories of a multi-regular graph (3,5,7,9), $b/c = 3.5$. Defectors prevail on most of the topologies 25

3.1 Example of indirect effect changing a pair RS into RI 40

3.2 *[Endemic Equilibrium]* Threshold map for endemic equilibrium as β, ϵ and k vary. The space above the blue curve is where the endemic equilibrium is unstable, while in the space below is stable. As connectivity increases the EE is stable only for very low infection and exit rates. 45

3.3 *[Endemic equilibrium]* Here for a given level of exit rate, $\epsilon = 0.17$, the contour functions of the highest eigenvalue $\hat{\lambda}_{EE}$ as function of k and β. As k increases the endemic equilibrium becomes unstable (the red area at $\hat{\lambda}_{EE} = 0$) even for very low infection rates. 46

3.4 *[Endemic Equilibrium]* The maximum eigenvalue $\hat{\lambda}_{EE}$ as a function of β and ϵ: most of the points are unstable (red area) while the set of stable points is a cloud around the locus $\beta = \epsilon$. 46
3.5 *[Disease Free Equilibrium]* Map of the epidemic threshold as a function of β, ϵ and k (right) and corresponding contour functions (left). $\mathscr{R}_0 > 1$ in the space above the curve, where the DFE is unstable, viceversa it is stable in the space below. 49
3.6 *[Disease Free Equilibrium]* Maximum eigenvalue of the DFE, $\hat{\lambda}_{DFE}$ when β and k vary and when ϵ and k vary respectively. The gray shaded plane is the level where the maximum eigenvalue is zero, red points indicate stability, green points instability. 50
3.7 $\mathscr{R}_0$ for $\epsilon = 0.1, \mu = 0.1, P_S = 0.5$ (a) and $\epsilon = \mu = 0.1, \beta = 0.5$ (b). The red area indicates instability of the DFE, the blue area stability. 55
3.8 $\mathscr{R}_0$ for $\epsilon = 0.1, k = 10$, $\beta = 0.5$ (a) and $\epsilon = \mu = 0.1, k = 10$ (b). The red area indicates instability of the DFE, the blue area stability. 55
3.9 Trajectories of x_I for different initial values of x_R, with $\epsilon = \mu = 0.1, k = 5$, $\beta = \gamma = 0.5$, $P_S = P_I = 0.5$ and $0.15 \leq x_R(0) \leq 0.7$. The higher the initial value of x_R, the lower the equilibrium value of x_I. 56
3.10 Trajectories of x_I for different initial values of x_S, with $\epsilon = \mu = 0.1, k = 5$ $\beta = \gamma = 0.5$, $P_S = P_I = 0.5$. The lower the initial value of x_S, the higher the equilibrium value of x_I. 57
3.11 Trajectories of x_I for different initial values of x_I, with $\epsilon = \mu = 0.1, k = 5$ $\beta = \gamma = 0.5$, $P_S = P_I = 0.5$. The lower the initial value of x_I, the higher the equilibrium value of x_I. 57
3.12 Whenever $P_S > 2P_I$ the population of infected oscillates in the proximity of the low disease equilibrium. Trajectories here have all initial values of $x_I = 0.01, x_S = 0.3, x_R = 0.2$ While P_S and P_I change. The amplitude of the oscillation increases with $P_S - P_I$. 59
3.13 Dependency of x_I^* as the arrival rates change. In the equilibria in figure (b) initial conditions were $x_R(0) = 0.01$, $x_S(0) = 0.3$, $x_R = 0.2$. Figure (a) maps the point in the (P_S, P_I, P_{NS}) unitary simplex to colors. 60
3.14 Change of x_I^* as λ and β change for (a) $x_R(0) = 0.01$, (b) $x_R(0) = 0.1$ 61
3.15 Impact of node arrival rate (a) and average connectivity (b) on x_I^*. With high κ x_I^* approaches zero, but never touches it if $P_I > 0$. 61
3.16 Dependency of x_I^* on homphily (a) and spontaneous exit rate (b) 62
3.17 Diverging oscillations caused by low ϵ and high homophily (b) 62

3.18 Modified logistic for $x_R \in (0,1)$, $b\gamma = 50$, $Q = 4 \cdot 10^3$, $v = 2$. In blue the values on the interval $x_R \in (0, R^)$ 64
3.19 Best Response map (fully-mixed) when $\gamma = \beta = 0.5$: red corresponds to instability of DFE, blue to stability. (a) depicts how x_R choice impact on ρ, given $\epsilon = 0.1$, (b) shows the best response map when also ϵ can vary. 65
3.20 Best Response map (adaptive) for the DFE (a) at $\mu = 0.1 = \epsilon$, $\beta = 0.5$, $k = 10$ and for the LEE (b). Blue indicates BR. 66

4.1 Example of the difference between a Walrasian equilibrium and a fair equilibrium in the Edgeworth box and in the space of utilities. 75
4.2 Modified from Shoham and Leyton-Brown [112], shows the Cartesian product of two 1-simplices. Notice the analogy with the Edgeworth Box. 75
4.3 Probability simplex (left) and corresponding simplex of topologies (right). Red corresponds to $p_1 = 1$, blue to $p_2 = 1$, green to $p_3 = 1$. The magnitude of the component of green, blue and red for each point is proportional to the magnitude of the corresponding probability. 86
4.4 Mapping between simplex of topologies and the corresponding equilibria. Only the three vertices are shown, map is according to colors 87
4.5 Projection of equilibria in the space of utility on agents' planes 87
4.6 Equilibria of the fair trading represented on the space of utilities for the case $\alpha_1 = \alpha_2 = \alpha_3 = 0.5$ (left) and projection on two-agents' planes. 89
4.7 Set of equilibria of a fair trading on the space of one commodity only 90
4.8 $\alpha_1 = \alpha_2 = \alpha_3 = 0.5$, extreme inequality: agent 1 is rich agents 2,3 are poor. . . 91
4.9 $\alpha_1 = \alpha_2 = \alpha_3 = 0.2$, extreme inequality: agent 1 is rich agents 2,3 are poor . . 92
4.10 $\alpha_1 = \alpha_2 = \alpha_3 = 0.2$ moderate inequality: agent 1 richer than agents 2 and 3. . 93

B.1 Examples of $\mathscr{GL}$ varying the parameters. 107

C.1 Taken from Lovison and Pecci [67], shows the case of the Pareto Set as in the convex case, respectively for 2 functions (leftmost graph), 3 functions and 4 functions. 109

List of tables

3.1 Summary of parameters effect on the infection level at equilibrium. 61

Chapter 1

Basic Concepts

Networks are

1.1 Graphs and networks

A network is a system that can be represented by a set of nodes (vertices) and a set of connections among them, links (edges), where the nodes constitute the elements of the system, while the links between them represent the existence of some form of interaction. Clearly many systems can be described using this abstract framework, where the network provides the conceptual basis that allows to represent complex interactions between the different components of the system. Networks are applied and studied in many disciplines, and are the core subject of mathematical graph theory, which provides a rigorous framework and a large set of theorems for analyzing the properties of these beautiful abstract objects. The origin of the discipline of graph theory is usually attributed to Euler's famous paper on the Königsberg Bridge problem, presented to St. Petersburg Academy in 1735 [35]. Here we present a very brief review of the basic concepts of network theory, in order to provide the reader with a set of definitions that will be later used in the following papers. The terminology adopted is from [7] and [13], that we recommend to the interested reader for a more extensive introduction.

Basic Definitions

A graph $G = (V, E)$ is an ordered pair of disjoint sets, V being the set of nodes or vertices and $E = V \times V$ the cartesian product of the vertex set, giving all the possible pairs of edges, called links or edges. If a couple of vertices $i, j \in V$ is joined by an edge $(i, j) \in E$ they are called *adjacent* or *connected*. If the link represents a bidirectional relation then the

graph is *undirected*, otherwise it is directed, and (i, j) means there is a link from i to j (not necessarily a link in the opposite direction). All the graph treated in this thesis are *undirected*. The set of nodes connected with a i is usually called the *neighbourhood* of i, denoted $V(i)$ and we will often refer to adjacent nodes as $neighbours$. A very useful mathematical representation of the graph is given by the *adjacency matrix*, a square symmetric (in the undirected case) matrix of dimension equal to the number of nodes in the graph with entries 0 or 1, defined $A = a_{ij}$, where $a_{ij} = 1$ if $(i, j) \in E$ and $a_{ij} = 0$ if $(i, j) \notin E$. If the graph is *simple*, that is presents no loops or multiple edges, the main diagonal of the adjacency matrix is made of all zeros. The adjacency matrix can be particularly useful in describing the graph properties. For example the entry a^k_{ij} of A^k, kth power of A represents the number of *paths* of length k between i and j, that is the number of consecutive edges connecting the two nodes. If the path starts and ends in the same node we have a *cycle*. Given a set of vertices according to characteristics of the set of edges we can classify different families of graphs. When the number of edges equals the number of vertices, hence all vertices are connected, the graph is called *complete*. If every vertex has the same number of adjacent vertices d, then it is called a *d-regular graph*. A graph is said to be *connected* if there exists a path between any two vertices. A minimal connected graph, that is a graph that after the removal of any of its edges is disconnected, it is called a *tree*. A special tree, with an internal node to which all the remaining nodes are connected (its k *leaves*) is called a *star*. A *subgraph* $G' = (V', E')$ of $G = (V, E)$ is a graph such that $V' \subset V$ and $E' \subset E$. We define an *induced subgraph* of a graph $G = (V, E)$ a subgraph $G[S] = (S, \hat{E})$ over a subset of the vertex set $S \subset V$ such that for any two vertice in S, if $(i, j)_S \in E$ then $(i, j)_S \in \hat{E}$. A subset of vertices of a graph is called a *clique* if its induced subgraph is complete.

Some graph metrics

Here we define some of the basic metrics that help in classify nodes in terms of their importance. The most obvious metric is the number of connections a node has, which is called *degree*. In undirected graphs the *degree centrality* of a node is hence simply given by the sum of its adjacent vertices, or alternatively by the sum of the elements of the corresponding row in the adjacency matrix. Nodes are hence classified according to how well they are connected, but this measure stops at the neighbourhood level, without considering the contribution of its neighbours' connections to the importance of the node. There are more refined measures of centrality that take in consideration also the degree of neighbouring nodes, like the *Bonacich centrality*, for a definition and discussionof this and other centrality measures see [57]. By aggregating the information about the degree

of all the nodes it is possible to obtain a powerful statistical measure of the entrire graph, namely the *degree distribution*. The degree distribution P_k is the probability that any randomly chosen vertex has degree k [7]. An important degree distribution is the *power law* [6], that emerges in many real networks, the typical example is the *world wide web*, where there are very few highly connected nodes and many with low degree. Graphs showing a power law degree distribution are called *scale free*. Another useful statistic is the *average degree*, which is just defined as the sum of the degree of all nodes divided by their numerosity. Calling κ the average degree and k_i the degree of node i:

$$\kappa = \frac{1}{|\mathcal{V}|}\sum_i k_i = \sum_k P_k = \frac{2|\mathcal{E}|}{|\mathcal{V}|} \tag{1.1}$$

where $|\mathcal{V}|$ and $|\mathcal{E}|$ represent the cardinality of the vertex and edge set respectively.

Clustering

An important measure of the local structure of neighbourhoods in a graph is called *clustering*. This captures a common characteristic observed in social networks, that two friends of someone tend to be friends with each other. Topologically these three nodes form a triangle, or a closed triple. There are different definitions of clustering, but they are all version of "counting triangles in the graph", or more precisely:

$$C_\Delta = \frac{3 \times \text{number of closed triples}}{\text{number of triples}} \tag{1.2}$$

Weighted Graphs

The graph structure can be enriched by attributing labels to vertices (for example representing different states, or types), or the structure can be modified by attaching a scalar to each edge, measuring the intensity of the relationship this represents. This is the case of *weighted graphs*. The analogous to the adjacency matrix in this case is a matrix whose w_{ij} entry represents the weight attached to the (i, j) edge, a zero weight corresponding to the absence of a connection. In the last chapter of this thesis we will use a simple undirected weighted graph where the weights are normalized so that the sum of all the weights of a node is equal to 1. The adjacency matrix in this case is a symmetric doubly stochastic matrix (a matrix whose rows and columns sum up to 1).

Random Graphs

Random graph theory is an important branch of graph theory that originates with some papers of Erdős Pál who discovered the important methodological approach that graph existence can be proved by using probabilistic methods without necessarily constructing the graph [13]. The interest of random graph theory is on determining what are the characteristics of *most* graphs inside a family, in other word discovering if there is a *typical* graph, in the sense a graph with some clear properties that has a high probability over the space of graphs in a given family. The existence of such typical graph was discovered by Erdős and Rényi in their early works, [31], [32]. A random graph can be defined as a probability space whose points are graphs [13]. A simple example considers a set of n vertices, V, defining the complete graph over these vertices as K_n . The space $\mathcal{G}(n,M)$ is made of all the subgraphs of K_n with M edges, where $M \in [0,N]$ and $N = \binom{n}{2}$ is the number of edges of K_n. The number of elements in the space $\mathcal{G}(n,M)$ is $\binom{N}{M}$. By attaching a probability to any of the elements of this space, $\mathcal{G}(n,M)$ becomes a probability space. The simplest way of doing this is assuming that all elements have the same probability, then the probability of a random graph $G_{n,M} \in \mathcal{G}(n,M)$, so the probability that a graph taken at random in the space has exactly *that* precise structure on the given vertices and with the given number of edges, is simply $1/\binom{N}{M}$. There are other ways of defining a RG, see [13] for an extensive and rigorous analysis. The construction of this probability space is the basic building block to explore the properties of *most* graph in a family and those of *almost every graph* in a probability space, hence those asymptotic property that occur almost everywhere in the space.

A specific type of such probability space is made of graphs where the degrees of vertices are restricted [125], that is the uniform probability space of $d-regular$ graphs over n vertices, $\mathcal{G}_{n,d}$ with the necessary restriction of nd being even. In the contest of this thesis we are particularly interested the enumeration of regular graphs of a given degree over a given number of vertices, that is in finding an asymptotic formula for the computation of this number. To this scope we will make use of some well-assessed results in random graph theory, that will be presented in the first paper.

1.2 Pair Approximation

Pair approximation is a specific form of moment closure approximation, a technique used for obtaining equation-based models of complex systems. The idea of the moment closure method in the context of dynamical systems is to derive a set of moment equations (typically differential or difference eqution), describing the behaviour of the moments

(we will use the mean) of the random variable generated by the stochastic dynamical system. This moment equations will typically depend on possibly infinite chains of higher order correlations, that will be approximated by a function of lower order correlations, that is a moment closure, in order to allow analytical tractability [63].

Pair approximation was introduced by [45] to study the spatial dynamic od Lotka-Volterra models, and have had a great diffusion in theoretical biology for the study of several phenomena on spatially structured populations [75], [**?**], [**?**], [**?**], [8].

The dynamics of such systems can be studied by analysing the rate of changes of some average quantites, which in turn can be predicted with good accuracy [4]. This can be done by deriving the expected rate of change of, say, the proportion of agents which are in a certain state, as an average of all the possible events that affects this proportion over the network. So for example the expected global change of the proportion of terrorist agent (f) in a regular network can be written as

$$\frac{dE(f)}{dt} = E\Big(\frac{df}{dt}\Big) = \sum_{\text{all sites } i} \sum_{\text{all events } e_i} r(e_i)(f_{e_i} - f) \tag{1.3}$$

where $r(e_i)$ is the probability of an event e at vertex i that affects the average f by f_{e_i}. The rates $r(e_i)$ depend on the spatial configuration of the network. Now, if the quantity of interest f is, as above, the proportion of sites occupied by terrorists, then the above is a simple non-spatial model. If, instead, f tracks some other spatial configuration (pairs of vertices, triangles, and so on) then we can analyze how the configuration of the structure change given the dynamical process. Pair approximation analyzes pairs of neighbouring sites, and it is the simplest possible spatial configuration that can be studied with a master equation like (1.3).

1.3 Dynamical Systems

Chapter 2

Replicator Equation on Multiregular Graphs

Abstract

Evolutionary graph theory studies evolutionary dynamics among agents whose interactions are determined by a graph structure. While the evolutionary dynamics of simple and homogeneous graphs is relatively easy to study, there is a gap in the literature regarding closed-form solutions of dynamics on complex , inhomogeneoug graphs, as topological complexity often endangers analytical tractability. Real world networks usually show complex structures, hence it is necessary to develop techniques to study evolutionary dynamics on non trivial topologies. The replicator equation is one of the fundamental mechanism to study selection, this paper provides a version of the replicator equation for a family of complex graphs using the method of pair approximation and proposes an algorithm for the generation of such graphs.

Keywords: Replicator equation, Multi-regular graph, Random Graph, Algorithm

2.1 Introduction

Evolutionary Game Theory [EGT] studies the behaviour of large populations of agents who repeatedly interact strategically [104]. EGT was introduced in 1973 by Maynard-Smith and Price[56] in the contest of the study of animal conflict. One of the building blocks of EGT is that fitness (which in genetics is the level of reproductive success relative to some baseline level) of a phenotype does not depend simply on the quality of the phenotype itself, but on the frequencies of different phenotypes in the population. Fitness is hence frequency dependent [83] In EGT, as opposed to Classical Game Theory, rationality plays no role: when individuals play a game with other individuals in the population, they do not choose their strategies as their strategy is the manifestation of their inheritance and it is determined (think of a phisical trait as simple example, you don't get to choose your height). For the same reason the other individuals against whom she plays have fixed strategies. The payoffs of the game are in terms of fitness, so if a trait offers an evolutive advantage over another, this would translate in a better fitness for the individual who has inherited that trait. The dynamics resulting from interactions between individuals

carrying different traits capture the process of natural selection: the strategy (phenotype, cultural trait) that performs better gives an advantage in term of reproductive success, hence it will reproduce at a higher rate and eventually take over the entire population [83].

EGT stem from the field of evolutionary biology, intended as an application of game theory to biological context, and succesively finds applications in many other fields, such as sociology, economics, anthropology, where it is applied for the study of cultural evolution [20], that is to say the change of behavioural norms over time, or to evolution of language [86]. Modifications of the originary concept allow to extend the study from completely non-rational players (in a purely biological setting) to players that are boundedly rational, and whose decision process is infuenced by other factors beyond rationality, such as myopic behaviour, imitation or (anti-)conformism. For an inspiring exposition of its various application to economics and social sciences see [15]. The weaker rationality assumption that characterize EGT models is often more appropriate for the study of social system than the strong rationality assumptions on which classical game theory is based, the latter being largely disproved by a huge literature on experiments showing the systematic fallacy of preference axioms. Another reason for the success of EGT in social sciences is that it is a dynamical theory, where classical game theory has a powerful concept of equilibrium and multiple refinements, but lacks a dynamical model that explains how these equilibria are reached, limitation that was already clear to Von Neumann and Morgenstern in their fundational work [78].

One of the basic assumptions of EGT is that every individual interacts with everyone else in the population with the same probability. This assumption is clearly limitative, since in every kind of population (bacteria, cells, animals, human) the relational structure is constrained by some underlying architecture, whether representing physical or social distance in social networks, rather than biochemical events in protein networks. When a population is fully mixed the probability of interaction between individuals carrying different traits is just given by the product of the frequencies of the two traits in the population, which is equivalent to say that matching is random. If matching is not random, for example because there is a positive (negative) correlation between the type of the individual and those with whom she interacts, then we say there is positive (negative) assortative matching, due for example to kin selection [84] or to geographic proximity [85]. When matching is non random the focus is not only on individual but on group selection, and on the competition among groups whose fitness depends ultimately on the group composition. Group selection has been used to model extensively the evolutionary fundation of human cooperation in [16]. [58] give a general framework for evolutionarily stable strategy under arbitrary matching rules. Evolutionary Graph Theory [EGrT] takes a

different approach, as individuals are placed a graph, that determine not only with whom the individual interacts to play the evolutive game, but also where a new born offspring will be placed (even if the interaction and the replacement graph don't need to coincide, see for example [90]). The interest of EGrT is to study the impact of the topology on evolutionary dynamics. It was introduced by [66], who showed in their seminal paper the role of different topologies in suppressing or amplifying selection. Among the interesting contribution in the field there have been applications to the study of the evolution of cooperation on different kinds of graphs [36], finding the relation between the cost of cooperation and the connectivity of the interaction and replacement graph that favors cooperation.[88] determine an analytical condition for the Evolutionary Stable Strategy for regular graphs under different updating rules. [89], on which the present work is based, find the replicator equation on a regular graph proving that it corresponds to a transformation of the payoff matrix of the evolutive game. One of the problematic aspects of EGrT is that, as soon as the complexity of the structure increases, the computational complexity explodes, making often impossible to obtain closed form solutions for the dynamical process, hence many works in the field rely on an algorithmic approach. It is important to stress that the complexity of many problems of the evolutionary dynamics of structured populations is not completely understood. Recently [54] showed that the complexity classes used in computer science to classify problems and the algorithms to solve them can be used to classify some of the problems of interest of EGrT. They prove that for some of these problems (for example finding the fixation probability of a structured population) it is simply not possible to find a solution expressed by equations (unless P=NP).

There are lot of interesting open questions in EGrT that needs to be explored, as suggested in [110] . The two more promising lines of research appears to be the study of the effect of complex topologies on the dynamics, and the study of the dynamics with endogenous structure, when the graph is not fixed but can itself change due to evolution.

The contribution of this paper is a replicator equation under different updating rules for a family of complex graphs that are characterized by local degree homogeneity and global degree heterogeneity, that we call a multi-regular graph.

The paper is structured as follows: the first part introduces the replicator equation on regular graphs, explaining the result obtained by [89] and showing in some detail how it is derived. Then a new family of graphs is introduced, and using the framework of [89] the replicator equation for these graphs is introduced. This equation is then applied to study a simple example of evolution of cooperation on a multiregular graph. A formula for

computing the expected degree distribution of a random multiregular graph is proposed, and finally an algorithm to generate graphs belonging to this family.

2.2 Replicator Equation on Regular Graphs

The Replicator Equation is one of the fundamental tools for the study of evolutionary dynamics. Take an evolutionary game with n strategies and a payoff matrix Π, where π_{ij} denotes the payoff that strategy i obtains against strategy j. Say that the frequency of each strategy $i \in n$ is given by x_i, where $\sum_{i\in n} x_i = 1$. Define as $f_i = \sum_{j\in n} x_j \pi_{ij}$ the fitness of strategy i and as $\phi = \sum_{i\in n} x_i f_i$ the average fitness of the population, then the replicator equation is:

$$\dot{x}_i = x_i(f_i - \phi) \text{ for } i \in n \tag{2.1}$$

According to this equation the time evolution of the frequency of strategy i in the population depends on the relative advantage that i has in term of fitness with respect to the average fitness of the population. It is deterministic, does not consider mutation and assumes a well-mixed population. The trajectory of this equation lies entirely on the $(n-1)$dimensional unitary simplex.

If the population is placed on a graph, then this equation cannot be used to describe the evolutionary dynamics. Under certain assumption on the population topology it is possible to derive an equivalent version of a replicator equation on graph. This fundamental result is obtained by [88], considering an infinitely large population placed on a regular graph of degree k, in which each vertex is occupied by an individual, and all the vertices are occupied. A regular graph is characterized by degree homogeneity: every vertex has the same number of neighbours, k. Each individual play an evolutionary game with his k neighbours and obtains an accumulated payoff P. The usual way [66] to translate payoff into fitness, that is reproductive success, is through the following formula:

$$F = (1 - w) + wP \tag{2.2}$$

where $0 \leq w \leq 1$ is a parameter representing the intensity of selection, with $w = 0$ the case in which fitness is constant and independent on the payoff, and $w = 1$ the other extreme case in which fitness is exatcly equal to the payoff. On what follows w is assumed small and strictly less than 1.

As it is common in the literature, three updating rules are considered for the evolutionary dynamics: 'birth-death', 'death-birth' and 'imitation'.

[BD: Birth-Death] An individual is chosen for reproduction with probability proportional to fitness. The offspring replaces one of the k neighbour chosen randomly.

[DB: Death-Birth] An individual is randomly chosen to die. One of the k neighbours replaces it with probability proportional to their fitness.

[IM: Imitation] An individual is randomly chosen to update his strategy. He can imitate one of his k neighbours proportional to their fitness.

[88] prove that for small w the dynamics of the frequencies of strategies in an $n \times n$ game can be described by a simple modification of the common replicator equation. Using pair approximation method[1] the authors derive this equation for the replicator dynamics on a regular graph:

$$\dot{x}_i = x_i \left[\sum_{j=1}^{n} x_j(\pi_{ij} + b_{ij}) - \phi \right] \tag{2.3}$$

where $\dot{x}_i$ is the derivative of frequency of the *i-th* strategy with respect to time, π_{ij} is the payoff a player with strategy i gets when the other player adopts j, and $\phi = \sum_{ij=1}^{n} x_i x_j(\pi_{ij} + b_{ij})$. The b_{ij} term is the key parameter that is obtained as a transformation of the initial payoff matrix, which form depends on the updating process followed. In the three updating process considered it is given by:

$$\begin{aligned}
&\text{[BD]:} \quad b_{ij} = \frac{\pi_{ii} + \pi_{ij} - \pi_{ji} - \pi_{jj}}{k-2} \\
&\text{[DB]:} \quad b_{ij} = \frac{(k+1)\pi_{ii} + \pi_{ij} - \pi_{ji} - (k+1)\pi_{jj}}{(k+1)(k-2)} \\
&\text{[IM]:} \quad b_{ij} = \frac{(k+3)\pi_{ii} + 3\pi_{ij} - 3\pi_{ji} - (k+3)\pi_{jj}}{(k+1)(k-2)}
\end{aligned} \tag{2.4}$$

Equation (2.3) is a transformed version of the classic replicator equation [117]. Ohtsuki and Nowak [88] call (2.3) the *replicator equation on graphs*. This equation says that evolutionary dynamics on a regular graph can be analyzed by simply transforming the payoff matrix $\Pi = [\pi_{ij}]$ $i, j = 1, ..., n$ in $\hat{\Pi} = \Pi + B = [\pi_{ij} + b_{ij}]$ where the value of b_{ij} will depend on the updating rule considered. Moreover, given the structure of b_{ij} in each of the updating rule, we can easily see that $B = [b_{ij}]$ is an antisymmetric matrix with $0s$ on the main diagonal, given that $b_{ii} = 0$ and $b_{ij} = -b_{ji}$. This matrix captures local

[1] Pair Approximation method was first used in the contest of population dynamics by [45] who proposed a statistical physics approach to the study of the evolution of populations.

competition on a graph taking account of the gain of $i-th$ strategy from i and j players and the gains of $j-th$ strategy from i and j players [87].
The same transformed payoff matrix can be used to derive the conditions for an Evolutionary Stable Strategy (ESS) on regular graphs [89]. A strategy is an ESS if, when most of the members of a population adopt it, there is no mutant strategy that can invade the population [56] (for a rigorous definition of ESS and its derivation on a regular graph see Appendix). An ESS if the population is well-mixed can be seen as a refinement of the Nash Equilibrium: it is important to notice that depending on $\hat{\Pi}$, the ESS depends on the topology, while Nash Equilibrium does not. A strategy is a strict Nash Equilibrium if there can be no strict gain in payoff in switching to another strategy, irrespective of the topology. This implies that the condition for a strategy to be NE on a graph are exactly the same as those in a well-mixed population. As a consequence, when the population is structured the relation between Nash and ESS does not hold anymore: an ESS may not be a NE and and a NE may not be an ESS.

2.3 Derivation of Replicator Equation

The following section presents a rigorous derivation of the replicator equation on regular graph in the case of BD updating, following [88]. The procedure for the derivation of the replicator equation for the two other updating mechanisms is analogous to the procedure for BD.

Remind that in the BD updating the player chosen for reproduction is picked with probability proportional to fitness, then his offspring replaces a random neighbour. The idea is to analyze local frequencies and global frequencies separately, which is possible given that local dynamics and global dynamics have different time scales. Given (2.2) and considering weak selection (w far from 1), the global frequencies change at a rate w, while local frequencies change at a rate of order 1. So local frequencies change can be derived considering glogal frequencies constant. Define as $q_{i|j}$ the conditional probability that the player considered uses strategy i given that adjacent player adopts strategy j. This is the *local frequency of strategy i around strategy j.* In terms of global frequencies this is given by $q_{i|j} = x_{ij}/x_j$ that is to say the global frequency of pairs $i-j$ adjusted for the global frequency of strategy j. The local frequency may be more complex, being conditioned not only on the adjacent player's strategy but also on the strategy of a two-step adjacent player. For the sake of tractability [88] uses the pair-approximation method, which has as a crucial assumption that the strategies of players that are more than one step adjacent do not affect the local frequency.

The first step is to derive local frequencies at equilibrium. If a player is chosen for reproduction on average once per step, the dynamics of the local frequencies are then:

$$\dot{q}_{i|j} = \frac{\dot{x}_{ij}}{x_j} = \frac{2}{k}\Big[\delta_{ij} + (k-1)\Big(\sum_s q_{i|s}q_{s|j}\Big) - kq_{i|j}\Big] + O(w) \tag{2.5}$$

where δ_{ij} is the Kronecker delta, $\delta_{ij} = 1$ if $i = j$, $\delta_{ij} = 0$ otherwise. Using the fact that $q_{i|j}x_j = q_{j|i}x_i$ the local frequencies in equilibrium are given by:

$$q^*_{i|j} = \frac{(k-2)x_i + \delta_{i|j}}{k-1} \tag{2.6}$$

These equilibrium conditions highlight the fact that players with the same strategy tend to form clusters, as can be seen by the inequality $q^*_{i|i} > x_i > q^*_{i|j}$. Now let the $(i;k_1,...,k_n)$-player be the player adopting strategy i with k_s, $s = 1,\dots,n$ denotes the number of neighbors playing strategy s and $k = k_1 + \cdots + k_n$. The number of i-players increases when a $(i;k_1,...,k_n)$-player is chosen for reproduction (event A) and his offspring replaces one of the k neighbor who is not an i-player (event B). The probabilities of these events are:

$$\mathbb{P}[A] = \Big[x_i\Big(\frac{k!}{k_1!\cdots k_n!}q_{1|i}^{k_1}\cdots q_{n|i}^{k_n}\Pi_{(i;k_1,...,k_n)}\Big)\Big]\Big/\bar{\Pi} \tag{2.7}$$

where

$$\Pi_{(i;k_1,...,k_n)} = 1 - w + w\Big(\textstyle\sum_s k_s\pi_{is}\Big) \tag{2.8}$$

is the fitness of the $(i;k_1,...,k_n)$-player and $\bar{\Pi}$ is the average fitness in the population.

$$\mathbb{P}[B] = 1 - (k_i/k) \tag{2.9}$$

On the other hand the number of i-players decreases when a $(j;k_1,...,k_n)$-player ($j \neq i$) is selected for reproduction and the offspring replaces an i-player. Name these two events C and D respectively, their probabilities are:

$$\mathbb{P}[C] = \Big[x_j\Big(\frac{k!}{k_1!\cdots k_n!}q_{1|j}^{k_1}\cdots q_{n|j}^{k_n}\Pi_{(j;k_1,...,k_n)}\Big)\Big]\Big/\bar{\Pi} \tag{2.10}$$

and

$$\mathbb{P}[D] = k_i/k \tag{2.11}$$

Considering each updating step takes Δt, call the global expected increment in the frequency of i-players $\mathbb{E}[\Delta x_i]$. In infinite populations we can have the global dynamics of strategy i as

$$\begin{aligned}\dot{x}_i &= \frac{\mathbb{E}[\Delta x_i]}{\Delta t} \\ &= \sum_{k_1+\cdots+k_n=k} \left[x_i \left(\frac{k!}{k_1!\cdots k_n!} q_{1|i}^{k_1} \cdots q_{n|i}^{k_n} \Pi_{(i;k_1,\ldots,k_n)} \right) \right] \left[1 - \frac{k_i}{k} \right] \Big/ \bar{\Pi} \\ &- \sum_{\substack{k_1+\cdots+k_n=k \\ j\neq i}} \left[x_j \left(\frac{k!}{k_1!\cdots k_n!} q_{1|j}^{k_1} \cdots q_{n|j}^{k_n} \Pi_{(j;k_1,\ldots,k_n)} \right) \right] \frac{k_i}{k} \Big/ \bar{\Pi} \\ &\approx w \frac{(k-2)^2}{k-1} x_i (f_i + g_i - \phi)\end{aligned} \tag{2.12}$$

where

$$\begin{aligned} f_i &= \sum_j x_j \pi_{ij} \quad \text{[average payoff of strategy } i\text{]} \\ \phi &= \sum_i x_i f_i = \sum_{i,j} x_i x_j \pi_{ij} \quad \text{[average payoff of the population]} \\ g_i &= \sum_j x_j b_{ij} \quad \text{[local competition among strategies]} \\ b_{ij} &= \frac{\pi_{ii} + \pi_{ij} - \pi_{ji} - \pi_{jj}}{k-2} \end{aligned} \tag{2.13}$$

The constant factor $w(k-2)^2/(k-1)$ is equivalent to a change of time scale, hence can be neglected, rewriting (2.12) simply as

$$\dot{x}_i = x_i (f_i + g_i - \phi) \tag{2.14}$$

which can be written as (2.3).

2.4 Extensions

A regular graph of degree k is more complex than a full-connected graph, still the complexity of the structure is minimal. In this section the results obtained above are extended to a structure of increased complexity. The approach followed is to isolate the relevant graph properties that are necessary in order to use the pair approximation method, and to relax other assumptions that do not harm the mathematical tractability. The necessary conditions that have to hold are regularity and connectedness, but relaxing in some way regularity is pivotal to add some complexity to the structure. We don't want all the vertices to have the same degree, hence it is necessary to introduce some degree heterogeneity.

In order to construct the desired structure it is necessary to provide some preliminary definitions. First, define as *maximal degree-homogeneous vertex subset* a subset of vertices with the same degree such that from each vertex in this subset there exist a path to any other vertex in the subset that traverses only vertices in the subset.

Definition 1 *Define $\mathcal{V}(d_i)$ as a maximal degree-homogenous (of degree d_i) vertex subset of the set of vertices V of the multi-regular graph, a vertex subset obtained in this way: pick a vertex of degree d_i, add it to $\mathcal{V}(d_i)$. Then add all its neighbours with degree d_i. For each neighbour add all its neighbours of degree d_i that are not yet in the vertex subset. Continue until no remaining neighbour of the added vertices has degree d_i.*

Definition 2 *Define as* multi-regular *graph G the graph with the following properties:*

[a] *the degree of each vertex is some integer d_i where $d_i \in [3,\dots,m]$.*

[b_1] *each of the d_i neighbours of each vertex has degree d_i (interior vertex) or, alteratively*

[b_2] *$d_i - 1$ neighbours have degree d_i and the remaining one degree $d_j \neq d_i$ (frontier vertex).*

[c] *each $\mathcal{V}(d_i)$ has a number of vertices $n_i \geq d_i + 1$ and $n_i k_i$ even.*

[d] *each $\mathcal{V}(d_i)$ has an even number of frontier vertices.*

[e] *G is connected.*

First of all notice that for each possible degree d_i there can be more than one $\mathcal{V}(d_i)$, the only case in which the $\mathcal{V}(d_i)$ is unique being when there is no other vertices of degree d_i on the graph that is not directly connected with any of the vertices in $\mathcal{V}(d_i)$. Clearly different $\mathcal{V}(d_i)$s of the same degree have different vertices (if $v \in \mathcal{V}(d_i)' \iff v \notin \mathcal{V}(d_i)'' \,\forall\, v$), because only neighbouring vertices of degree d_i can belong to a certain degree homogeneous vertex subset. Hence we can say that all the subgraphs of G which vertices are all in one of the $\mathcal{V}(d_i)$ for given i (so have degree d_i) belong to the class of d_i-homogeneous subgraphs of G.
Properties [b_1] and [b_2] ensure the form of regularity condition required. Consider that both interior and frontier neighbouring vertices of the same degree d_i belong to the same $\mathcal{V}(d_i)$. The induced subgraph of $\mathcal{V}(d_i)$ is a regular graph of degree d_i provided that we consider also the edges that from the frontier vertices of $\mathcal{V}(d_i)$ goes outside $\mathcal{V}(d_i)$. This is a key point because under the assumption of [88], in particular the assumpion of independence of local frequencies from strategies of players that are more than one

step adjacent, we can use (2.5) for computing local frequencies on a *multi-regular* graph. Properties [d] and [e] ensure that the graph is at least 2-connected, or in general, e-connected with e even. Property [c] simply guarantees the existence of a regular graph of degree d_i on the vertices of $\mathcal{V}(d_i)$. So a *multi-regular* graph keeps the requirement of regularity, and allows to extend the analysis to a more complex population structure, in which vertices belonging to the same $\mathcal{V}(d_i)$ have the same number of interactions, but this number can vary among different $\mathcal{V}(d_i)$s.

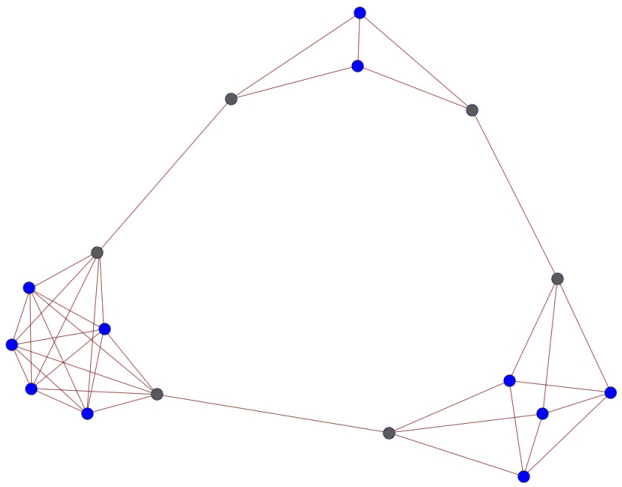

Fig. 2.1 *Multi-regular* graph with three $\mathcal{V}$ of degrees 3,4 and 6. The gray vertices are the frontier vertices which create a bridge with an adjacent $\mathcal{V}$ of different degree. The blue vertices are interior vertices.

A *multi-regular* graph is represented in Figure 1. Here there are three $\mathcal{V}(d_i)$s, respectively $\mathcal{V}_3$ of degree 3, made by the four vertices on the top of the figure, $\mathcal{V}_4$ of degree 4 made by the 6 vertices on the right and $\mathcal{V}_6$ of degree 6 made by the 7 vertices on the left. The blue vertices are inner vertices, and the gray are frontier vertices. This graph is 2-connected. As can be seen in Figure 2, if we remove one edge between two frontier vertices, the graph is still connected, but regularity condition holds no more. If we try to "restore" regularity by adding an edge between any of the two red vertices and one of the blue or gray vertices, we violate conditions [b_1], [b_2]. The only way to obtain a regular graph is removing also the other two edges between the remaining frontier vertices, obtaining a regular graph which is not connected, hence is not *multi-regular* as depicted in Figure 3. In order to see how a $\mathcal{V}(d_i)$ is constructed, imagine we pick vertex b in Figure 2. It has degree 4, so we create $\mathcal{V}_4$ and add b to it. Then we add all b's neighbour with degree 4 to $\mathcal{V}_4$, that is to say a, e, f, c. Then we see that a has no neighbour of degree 4 that is not yet in $\mathcal{V}_4$, while any of e, f and c has d. Add d to the set. Then no other neighbours have degree 4. $\mathcal{V}_4 = \{a, b, c, d, e, f\}$ is complete.

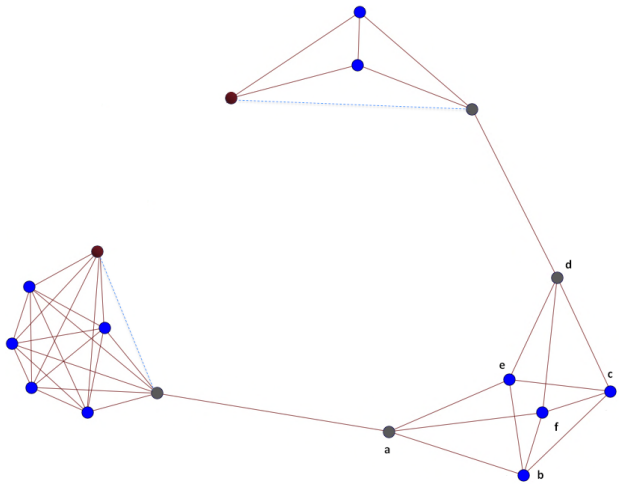

Fig. 2.2 *Multi-regularity* not satisfied. Removing the edge between the two red vertices the regularity condition does not hold anymore, and adding one or more edges between each of the red vertices and any of the non-red vertices violates [b$_1$] - [b$_2$].

Now consider the local dynamics on a *multi-regular* graph. Under the assumption that the strategies of players that are more than one step adjacent do not affect local frequency, equations (2.5)-(2.12), with d_i instead of k, hold for vertices in the same $\mathcal{V}(d_i)$. The event that an $(i;k_1,...,k_n)$-player (recall, a player adopting strategy i where k_h, $h=1,\ldots,n$ denotes the number of neighbors playing strategy h and $d_i = k_1 + \cdots + k_n$) is selected for reproduction is still given by (2.7) in each of the d_i-homogeneous subgraphs, and the probability that the offspring replaces one of the neighbour that is not an i-player is still biven by (2.9) in each of the d_i-homogeneous subgraphs. The same applies for events C and D above defined. The local dynamics described by these equations are not the same on the whole *multi-regular* graph, but vary with d_i for each different $\mathcal{V}(d_i)$. So each different class of d_i-homogeneous subgraphs with sufficiently large number of vertices, has a different replicator equation as in (2.12). Hence, in order to compute the global dynamics it is necessary to take account of the distribution of each class of degree-homogeneous subgraphs of G.

Knowing the frequency of each class of degree-homogeneous subgraphs of G, the global dynamics on a *multi-regular* graph is obtained by weighting each class-specific replicator equation for the probability of this class of subgraphs. Call $\mathbb{P}[\mathcal{G}_{d_i}]$ the probability that subgraph belongs to the class of d_i-homogeneous subgraphs, the global dynamics on a *multi-regular* graph is then:

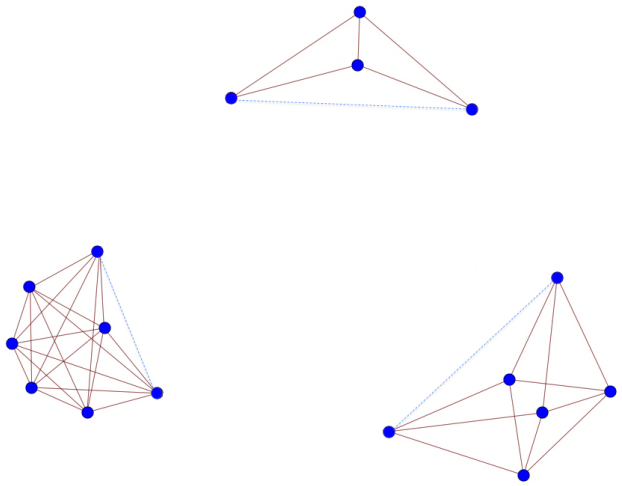

Fig. 2.3 Regularity is restored in each subgraph but connectedness is lost. There are only interior vertices and the graph is not *multi-regular*.

$$
\begin{aligned}
\dot{x}_s &= \frac{\mathbb{E}[\Delta x_s]}{\Delta t} \\
&= \sum_{d_i \geq 3} \sum_{k_1+\cdots+k_n=d_i} \left[x_s \left(\frac{d_i!}{k_1! \cdots k_n!} q_{1|i}^{k_1} \cdots q_{n|i}^{k_n} \Pi_{(s;k_1,\ldots,k_n)} \right) \right] \left[1 - \frac{k_s}{d_i} \right] \mathbb{P}[\mathscr{G}_{d_i}] \Big/ \bar{\Pi} \\
&- \sum_{d_i \geq 3} \sum_{\substack{k_1+\cdots+k_n=d_i \\ j \neq i}} \left[x_j \left(\frac{d_i!}{k_1! \cdots k_n!} q_{1|j}^{k_1} \cdots q_{n|j}^{k_n} \Pi_{(j;d_1,\ldots,d_n)} \right) \right] \frac{k_s}{d_i} \mathbb{P}[\mathscr{G}_{d_i}] \Big/ \bar{\Pi} \\
&\approx w \Big(\sum_{d_i \geq 3} \frac{(d_i-2)^2}{d_i-1} \mathbb{P}[\mathscr{G}_{d_i}] \Big) x_s (f_s + \sum_{d_i \geq 3} \sum_j x_j b_{ij}(d_i) \mathbb{P}[\mathscr{G}_{d_i}] - \phi)
\end{aligned}
\tag{2.15}
$$

Given the graph, hence its degree distribution, the factor $w\left(\sum_{d_i \geq 3} \frac{(d_i-2)^2}{d_i-1} \mathbb{P}[\mathscr{G}_{d_i}]\right)$ is a constant, and again just represents a change of time scale, so we can rewrite (2.15) as:

$$
\dot{x}_s = x_s (f_s + \sum_{d_i \geq 3} \sum_j x_j b_{ij}(d_i) \mathbb{P}[\mathscr{G}_{d_i}] - \phi) \tag{2.16}
$$

(2.16) is the replicator equation on a *multi-regular* graph.

2.5 Evolution of cooperation

One of the largely studied topics in the literature on EGT is the evolution of cooperation. This can be studied with a 2×2 game, in which the two strategies are Cooperator and Defector. The Cooperator is a guy who make some effort in order to produce a benefit for

the opponent. This effort has a cost, say c, and the benefit his opponent receives is b. The Defector just take the benefit from the Cooperator and does no effort in exchange. The payoff matrix is:

	C	D
C	$b-c$	$-c$
D	b	0

This represents a typical instance of the Prisoner's dilemma game [95]. Given that Defector is a strictly dominating strategy, D is a strict NE and an ESS, and the solution of the replicator equation as in (2.14) is at a point in which everybody in the population is a defector. Things change on a regular graph [88]: while under BD updating there is no difference with well-mixed populations, under DB updating cooperation is a stable state if $b/c > d$ where d is the degree of the regular graph. Analogously in the case of IM updating cooperation prevails if $b/c > d+2$. In both cases what emerges is that in order to sustain cooperation when agents are highly connected, the benefit/cost ratio has to be very high. Let's now examine how the replicator equation on a multi-regular graph looks like in this case: call x_c the frequency of cooperators, $(1-x_c)$ the frequency of defectors

$$\dot{x}_c = x_c\Big(x_c(b-1+c) - c + (1-x_c)\sum_{d_i\geq 3}\frac{d_i(b-c)-2c}{(d_i+1)(d_i-2)}\mathbb{P}[\mathscr{G}_{d_i}]\Big) \tag{2.17}$$

is the replicator equation for the PD under DB updating. In this case cooperation will be sustainable if the inequality $b/c > \sum_{d_i\geq 3} d_i\mathbb{P}[\mathscr{G}_{d_i}]$ holds. So as long as the highly connected subgraph have a low frequency, the benefit/cost ratio doesn't need to be too high to sustain cooperation. For example if $\mathbb{P}[\mathscr{G}_{d_i}]$ is a power-law distribution, with law $Cd_i^{-\alpha}$, then cooperation prevails for $b/c \geq \frac{C}{\alpha-1}d_i^{-(\alpha-1)}$.
Equilibria in which both cooperators and defectors coexist are possible on a multi-regular graph. Consider for example the Prisoner's Dilemma:

	C	D
C	5	0
D	8	1

The multi-regular graph in this example has subgraphs of degree 3,4 and 9. The following figures (generated in Python, see [23, 97]) show how the trajectories and the rest points change as the three frequencies (not represented in the graphs) change: on the trajectory plot the cooperators' trajectories are in red and the defectors' in blue, x-axis is time, y-axis is the frequency. As the frequency of the subgraph is higher for degrees 3 and 4 cooperators

and defectors coexists almost in equal proportions. As the frequency on 9 increases the number of equilibria in which the two strategies coexist decreases and the density around the point where all are defector increases.

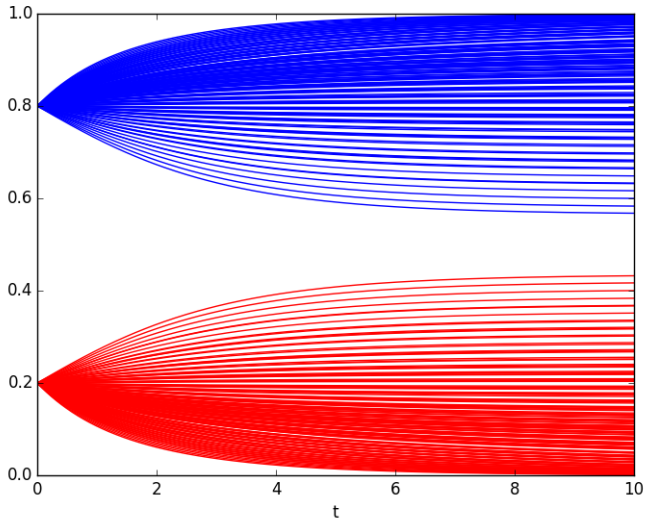

Fig. 2.4 Trajectories of a multi-regular graph (3,4,9) as the frequencies of the three subgraphs change. Blu lines for defectors, red for cooperators

Other two examples of Prisoners' Dilemma are illustrated, corresponding to the following payoff matrices:

	C	D
C	10	-2
D	12	0

In one case $b/c = 6$, in the other $b/c = 3.5$. Both games are played on a multi-regular graph with subgraphs of degree 3, 5, 7, 9. As before cooperators are red and defectors blue.

	C	D
C	5	-2
D	7	0

Where $b/c = 6$ for most of the topologies cooperators prevails, as can be seen by the concentration of red and blue trajectories respectively towards 1 and 0. There is some equilibrium in which they coexists, and few if not none where defector prevails, correspondance of the points where the frequency of 7 and 9 is very high.

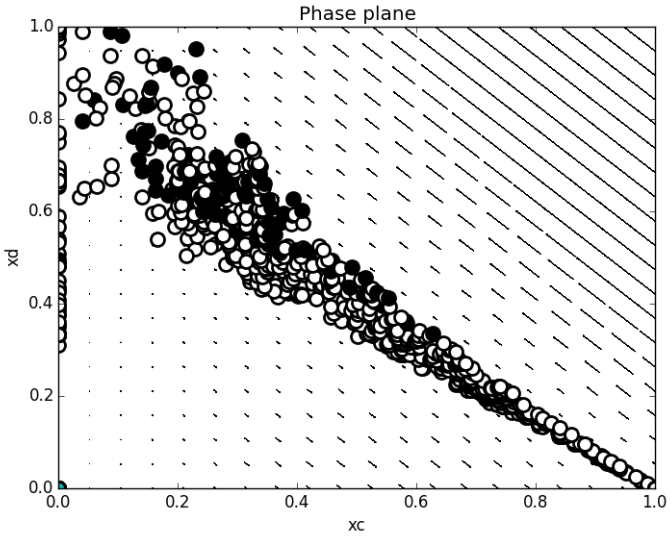

Fig. 2.5 Rest points of a multi-regular graph (3,4,9), the black points are the stable ones

The picture is the opposite where $b/c = 3.5$: the topologies for which defectors prevail are more, even if there is some "outlier" trajectory where subgraphs of degree 3 are the majority.

2.6 Multi-Regular Random Graph

As can be seen from (2.15) the difference in the probability distribution of $\mathscr{G}_{d_i}$ will affect the global dynamics. In particular, considering sub-populations numerosity being large enough and the difference in numerosity irrelevant between the sub-populations, the speed of the dynamics increases with d_i, so the dynamic is faster in those sub-populations which members have a higher number of interactions. The speed of the dynamic increases with $\mathbb{P}[\mathscr{G}_{d_i}]$, and its marginal effect increases with d_i.
Instead of assuming specific probabilities distribution of the class of degree-homogeneous subgraph, it is possible to investigate which kind of structure is more likely to emerge if we consider that such a kind of *multi-regular* graph can be randomly formed. Random graph theory is used to answer this question in order to obtain an estimate of the relative frequency of each class of degree-homogeneous subgraphs.

The variable of interest is the expected number of $\mathscr{V}(d_i)$ over the total number of $\mathscr{V}(d_i)$ with degree that goes from 3 up to a fixed m,

$$\rho[\mathscr{G}_{d_i}] = \frac{|\mathscr{V}_i|}{\sum_{i=3}^{m} |\mathscr{V}_i|} \tag{2.18}$$

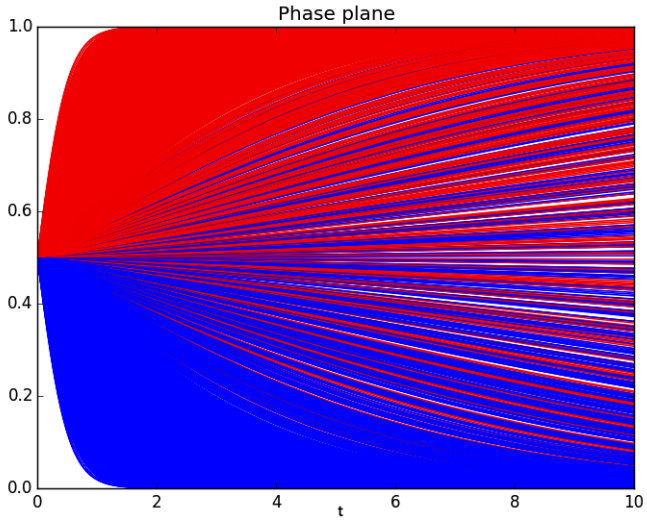

Fig. 2.6 Trajectories of a multi-regular graph (3,5,7,9), $b/c = 6$. Cooperators prevail for most of the possible topologies

where $|\mathcal{V}_i|$ is the number of possible random maximal d_i-homogenous vertex subsets.

The subgraph induced by $\mathcal{V}(d_i)$ on a *multi-regular* graph is not exactly a regular subgraph, because in this induced subgraph the frontier vertices will have degree $d_i - 1$. Recall that a subgraph induced by a subset of vertices is the considered subset of the vertices of the graph together with any edges whose endpoints are both in this subset, so the graph induced by $\mathcal{V}(d_i)$ has all the vertices of $\mathcal{V}(d_i)$ and all the edges that are between those vertices, that is to say all the edges between interior vertices except those connecting the frontier vertices to the outside. Nonetheless, as can be seen from Figure 3, any $\mathcal{V}(d_i)$ can induce a regular connected graph of degree d_i. Here there is a conjecture about the number of possible d_i-homogeneous graphs induced by $\mathcal{V}(d_i)$s.

Conjecture 1 *The number of possible d_i-homogeneous graphs on n vertices is at least the number of possible d_i-regular random graphs on n vertices.*

There still is no formal proof, but intuition suggests the validity of this conjecture. Suppose we have a regular graph of degree k on $k+1$ vertices. Only one such regular graph is possible. The kind of graph of degree k we are interested in (recall, a graph homogeneous in degree, connected, with at least two frontier vertices) can be obtained from the regular connected graph, removing (at least) one edge, so that in the graph there will be two vertices with degree $k-1$, and add to each of these vertices an edge to the outside. In this case we can see that we have $\binom{k+1}{2}$ different ways in which the two vertices can go to the

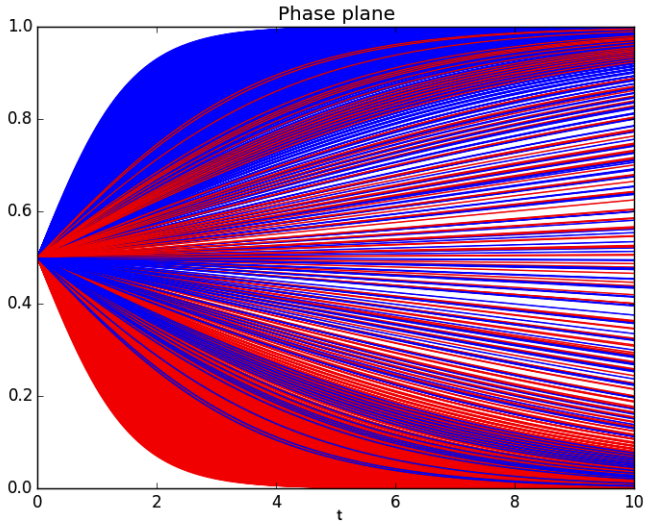

Fig. 2.7 Trajectories of a multi-regular graph (3,5,7,9), $b/c = 3.5$. Defectors prevail on most of the topologies

outside. More in general f is the (even) number of frontier vertices and n the total number of vertices in the regular graph, there are $\binom{n}{f}$ possible degree-homogeneous graphs. With $n = k+1$ we have only a regular graph, hence the proof is trivial. With $n \geq k+1$ the number of regular graphs increases, but as long as it increases more slowly than $\binom{n}{f}$, with f small enough with respect to n, the conjecture is true.

Using a result from random graph theory it is possible to compute asymptotically the number of random regular graphs of degree d to compute (2.18).
As in [125] Let $\mathcal{G}_{n,d}$ be the uniform probability space of d-regular graphs on n vertices, where we require dn to be even. The *pairing model* introduced by Bollobás allows to prove properties of the elements of $\mathcal{G}_{n,d}$ computing in the unifrom probability space of pairings. This probability space is so define: suppose dn even, and $d > 1$. Then take dn points partitioned into n blocks, each containing d points. A *pairing* is a perfect matching of the points into $\frac{1}{2}dn$ pairs, and corresponds to a multigraph in which blocks are vertices and pairs are edges. Each simple graph corresponds to exactly $(d!)^n$ pairings, so a regular graph can be chosen uniformly at random by picking uniformly at random a pairing. Being interested in simple graphs (with no loops nor multiple edges), the randomly chosen pairing will be accepted only if it has no loops or multiple edges. In order to obtain results for random regular graphs of degree d with n vertices, it is enough to do computations in the probablity space of the corresponding pairings and then condition on the event that the multigraph has no loops or multiple edges (e.g. it is simple). Call this event $\mathbb{P}(Simple)$.

The pairing model gives a simple way for counting the number of d-regular graphs asymptotically, given by the formula:

$$|\mathscr{G}_{n,d}| = \frac{(dn)!\mathbb{P}(Simple)}{(dn/2)!2^{dn/2}(d!)^n} \tag{2.19}$$

Hence (2.19) will depend on the way $\mathbb{P}(Simple)$ is computed, and different researchers obtained different estimates of $\mathbb{P}(Simple)$ under different conditions. A particularly easy to apply formula is the so called Bender and Canfield's [9] asymptotic formula:

$$\mathbb{P}(Simple) \sim \exp\Big(\frac{1-d^2}{4}\Big) \tag{2.20}$$

for d fixed and $n \to \infty$ and dn even. Using Stirling's formula Bender and Canfield obtain

$$|\mathscr{G}_{n,d}| \sim \sqrt{2}e^{(1-d^2)/4}\Big(\frac{d^d n^d}{e^d (d!)^2}\Big)^{\frac{1}{2}n} \tag{2.21}$$

The problem related with this formula is that it works for $d = d(n) \leq \sqrt{2\log n} - 1$ as proved by [11], so it is not very useful if we want the degree to grow faster with n. An useful refinement of (2.21) is here presented, which consent to extend the range of d, even if it is not so compact as (2.21). [72] obtain the formula for $d = o(\sqrt{n})$:

$$|\mathscr{G}_{n,d}| \sim \frac{(dn)!}{(\frac{1}{2}dn)!2^{dn/2}(d!)^n}\exp\Big(\frac{1-d^2}{4} - \frac{d^3}{12n} + O\Big(\frac{d^2}{n}\Big)\Big) \tag{2.22}$$

According to [72] , this is the best result obtained for the counting of the number of random regular graph on a larger range of d.

Another important result that turns to be useful in this contest, proved by Bollobás [12], says that when $d \geq 3$ and constant, the random regular graph $G(n,d)$ is *a.a.s.* connected. This result is useful in deriving an estimation of (2.18). The expected frequency of a subgraph belonging to the d_i-homogeneous class of subgraphs and having n vertices is given by:

$$\rho[\mathscr{G}_{d_i}] = \frac{|\mathscr{G}_{n,d_i}|}{\sum_{d_i=3}^{m}|\mathscr{G}_{n,d_i}|} \tag{2.23}$$

where the population n is fixed for each subgraph. The formula for counting the number of graphs that will be chosen will depend mainly on how large d is with respect to n. Whenever is possible, it is preferable to use Bender and Canfield's formula.

So, using (2.23) in (2.15) the replicator dynamics of a population that is structured in a random *multi-graph* can be computed. Moreover, given that both (2.21) and (2.22) depend on both d and n, it would be interesting to analyze different kind of dynamics of

the population for different numerosity of the single subpopulations of different degree. In further research this aspect will be analyzed through numerical simulations.

2.7 Generating a Random MR Graph

In this section an algorithm for the construction of a Random Multiregular Graph is proposed. The algorithm is based on a modified version of the pairing model.

Fix the number of vertices to n and let $d_i \geq 3$ the degree. Define as $\mathbb{P}(d_i)$ the fraction of vertices with degree d_i. The nearest integer $[n\mathbb{P}(d_i)]$ is the number of vertices with degree d_i; as in the pairing model, assume this number to be even. Define also as r the ratio of vertex degree to vertices with the same degree to vertices with other degrees.

1. Create a set of $[n\sum_{d_i}\mathbb{P}(d_i)d_i]$ points.
2. Divide them in n buckets in the following way.
   (a) Take $[n\mathbb{P}(d_i)]$ points and put them in $[n\mathbb{P}(d_i)]$ different buckets.
   (b) Add $d_i - 1$ points to each of these buckets.
   (c) Repeat the same procedure for all the other d_i. In this way for each d_i there will be $[n\mathbb{P}(d_i)]$ buckets with d_i points.
3. Pick a random point, say it is in a bucket with d_i points.
4. Join it with probability r to a random point among those in one of the $[n\mathbb{P}(d_i)]$ buckets with d_i points, and with probability $1-r$ to any of the other points at random. Continue until a perfect matching is reached.
5. Collapse the points, so that each bucket maps onto a single vertex of the original graph. Retain all edges between points as the edges of the corresponding vertices.
6. Check if the corresponding graph is simple.

Step 4 can also be changed by joining the picked point with any other point at random. The reason for imposing the ratio of connections with other-degre-vertices is because for some applications could be useful to control the formation of dense degree-homogeneous subgraph with few "bridge" connections with the outside. Here the the fraction of frontier vertices is assumed uniform along the subgraphs, while it could be reasonable to make r vary with the degree d_i, depending on the models considered. A version of the proposed alogrithm has been implemented in Python, using Networkx which builds random multi-regular graphs with specified number of frontier vertices.

2.8 Further research and Conclusions

This paper provides a version of the replicator equation on graphs. A specific graph structure is constructed, called *multi-regular* graph, that keeps the relevant properties of regularity and connectedness, and the replicator equation for this kind of graph is derived. The extended replicator equation depends on the probability distribution of the degree-homogeneous subgraphs in a *multi-regular* graph. Following a random regular graph approach a formula for computing these probabilities under random graph formation is provided. For the construction of a random regular graph it is proposed an algorithm based on the pairing model. There are interesting research lines to be followed in future to extend these result in order to satisfactory describe real networks evolutionary d As regards further developments of this work, the analysis of the proposed replicator dynamics will be extended to different games under different updating rules. A further research line that worths consideration is investigating if the proposed replicator equation can be a good approximation for a population which does not exhibit a *multi-regular* structure. The idea is to take the degree distribution of this population, and generate a *multi-regular* graph where the probability distribution of the homogeneous subgraphs follows the degree distribution of the population. This aspect is still under analysis, and requires further study.

Chapter 3

Surveillance on Networks, a Pair Approximation Model

Abstract

This paper develops a recruitment model on a social network in presence of surveillance. The recruitment process is described as a change of state of those nodes that are likely to be recruited to the state of the recruiter itself if there is a link between the two nodes. There is surveillance on the network, there are nodes that can change the status of the recruiters or eliminate them from the network (in the adaptive model). Pair approximation is used to derive a dynamical systems describing the dynamics among the classes of nodes, and this allows to find a threshold for the recruitment process that depends on the parameters. This dependency is used as a guide for a social planner who has the objective of minimizing the diffusion of the recruiters' class. Three instances of the model are presented: the non-spatial case, the static network case and the adaptive network case.

Keywords: Compartmental model, Pair Approximation, Reproduction Number

3.1 Introduction

Individuals in a society can be classified according to their adherence to a set of beliefs or principles. One of the phenotypical manifestations of the complex interaction of these beliefs can take the form of affiliation with a political party, with a religion, or more in general with a group of similar-minded individuals who share the common objective to spread their beliefs and to make them dominant in their society. This generates competition among different groups, each trying to enlarge the number of its members, as the probability of succeeding in their scope is increasing in the number of adepts (both if we think of a political election or an armed revolution). Once one of the groups becomes dominant, they will try to stay dominant, hence to hinder the enlargement of other groups. This very minimal and abstract representation of an ideological conflict is used to build a mathematical model of recruitment in a society where an initially small group of people who disagree with the dominant group and aims at eventually overthowing them, try to recruit new members, while the dominant group actively tries to obstacle this process through a surveillance system.

The model was originally developed having in recrutiment activities of a terroristic group that may bring radicalization in a society, hence there may be an emphasis on the surveillance aspect, as if we were on the point of view of the social planner. Given that the process described is not specific of terrorism, but could be applied to a vaste range of ideological conflicts[1], it is important to stress that this does not want to be a model of social control, and the author is not implying at any point that the actions of the group trying to subvert the leading authority are not legitimate. This work is not about the merit, not even the reasons of this form of conflict, but merely on the description of an abstract version of its mechanics: a process of affiliation to an illegal group (so that individual who are discovered to members are liable to suffer punishment) that is actively counteracted by the leading authority. The objective of the authority is to minimize or eventually annihilate the subversive group, while the objective of the group is to recruit as many people as possible, to reach a significative number that is sufficient to overtrhow the leading authority.

Looking more specifically at terroristic warfare, it has probably reached an unprecedent diffusion and the number of fatalities caused is increasing. The necessity to develop effective counterterrorism measures is catalyzing numerous studies, both qualitative and quantitative, to try to better understand the psychological, sociological and political motivations of terrorism and provide models of its diffusion in a society. Among them [107] provides a systematic approach to terrorism using economic methodology, where terrorists are modeled as ractional-actors, where game theory is used to analyze terrorist strategies and to suggest countermeasures [106, 105, 73]. Without disregarding the importance of a rational actor approach, it is legitimate to ask whether some extreme activities (like suicide bombing for example) enter the realm of rational behaviour. On this line [34] suggests an evolutionary approach to understand the psychological motivations of terrorists, and how their behaviour can be rational in an evolutionary sense, even if extremely costly for the individual and [109] proposes a predator-prey model to predict the behaviour of terrorist groups, as these explicitly models life and death competitions.

Another stream of the literature on terrorism concentrates mainly on activity of terroristic groups, without necessarily dig into the motivations and the behavioural aspects beyond those. These studies often starts from data, and use mathematical modeling as well as agent based simulations to try to generate models that are a good predictor of

[1]The same mechanism could be used to analyse consent to a revolutionary group in an autocratic state, the evolution of a heretic group trying to emerge against the dominant religious authority. By way of example consider the Pauperistic Movements during the Middle Age, like the Dolcinians, that were brutally persecuted by the Catholic Inquisition, or the Anabaptist movements during the Reformation in Central Europe

terrorist behaviour. Among the others, [22] use simulations to study the frequency of attacks by terrorist groups and [102] investigates spatio-temporal patterns of terroristic attacks by the Provisional Irish Republican Army, providing a map of the probabilities of attack depending on the various organizational phases of the IRA terroristic group.

To the author knowledge there aren't many papers using a network approach to terrorism, an attempt in this direction in [1] who propose a mechanism of radicalization, where the transmission of ideology is modeled as a contact process on a network. [64] discusses how the knowledge of the terrorist network can help in identifying the critical node that may lead to network disruption. Along the same line, even if not focused on terrorist networks, [18] use a measure of centrality to address optimal reduction of the criminal networks.

The use of mathematical modeling in this work follows a generative approach: we propose a simple mechanism to explain the process and analyze the dependency of the model on the parameters. To validate the mechanism we should then see if the parameters can be calibrated to generate realistic patterns. An interesting work using the generative approach is [119] who model violence escalation during the 2011 London riots. Their model is built on several levels: individual decisions of participating into riots are taken on the basis of a benefit-cost analysis mechanism, individual involvement in the riot is modeled as a contagious (Susceptible-Infected-Removed, SIR) model, and finally they consider also rioters' interaction with police and suggest strategies for violence deterrence. Even if the phenomenon modeled is different, as well as the mathematical formulation adopted, we use a similar modeling strategy: a (minimal) individual rule of decision making, then a (modified) SIR model as diffusion mechanism.

The only other work that uses an epidemical model to study terrorism, to our knowledge, is [121]. They divide the population in three groups, Terrorist, Susceptibles and Non Susceptibles. The number of terrorists can increase for direct recruitment among the susceptibles and can decrease for natural death or death in action and military intervention. Susceptibles may be recruited, so they become terrorists, or they may become Non Susceptibles as a consequence of pacifist propaganda led by the authority. Their number may also increase because of terrorist propaganda that convinces previously Non Susceptible individuals. Together with this processes there is also an underlying birth/death process of the population that affects the dimension of the three groups. There are similarities between our model and this approach, a fundamental difference is that in [121] the population is not structured, hence there is a random matching mechanism that determines the interaction between susceptibles and terrorists. Here we model both the case of a non structured population and the case of a social network.

3.2 Epidemiological Models

The spread and establishment of infectious diseases has been largely studied by mathematical epidemiologists, hence there is a variety of mathematical tools available for building and testing theories. The first mathematical model of disease spread dates back to 1760 [10], but it's the 20th century that we had an exponential growth in the number of models and in their applications. Starting in 1926 Kermack and McKendrick [62] published a series of papers that can be considered foundational to the modern approach to epidemiological models, introducing the idea of compartmentalization. In compartmental the population is stratified in compartments according to individual status (Susceptible, Infected, Recovered), then the transitions among these compartments is modeled following the assumptions on the phenomenology of the disease, so that the evolution of the infection can be described by a set of differential equations. This constitutes the basic block of many models (both deterministic and stochastic) that can be complicated by adding new compartments, introducing the possibility of vaccination, differentiating for age, social and sexual groups [49]. The main results of compartmental models are threshold theorems that define under which conditions an infection will establish in a population. The most important measures are the "basic reproduction number", average number of secondary infections produced when one infected individual is introduced into a host population where everyone is susceptible [81], the "contact number", average number of contacts of a typical infective during the infectious period and the "replacement number", average number of secondary infections produced by a typical infective during the period of infectiousness [49].

One of the most relevant assumption of the basic model is to consider that the population is well-mixed, meaning that every individual can spread the disease to any other individual with the same probability, not incorporating the contact structure that is key for the disease spread pattern. This assumption allows mathematical tractability, but lacks a key element in understanding disease spreading patterns, namely population topology [79]. A particularly revealing example of the relevance of population topology is [92] who study a Susceptible-Infected-Susceptible (SIS) model on scale free graphs finding absence of an epidemic threshold and associated critical behaviour, meaning that scale free networks are prone to spreading whatever the spreading rate. The (analitic or numeric) determination of epidemic thresholds under various topologies is the subject of several papers [25, 21, 19, 108, 2]. Incorporating a network in the model avoids the random mixing assumption, as now each individual has a fixed set of contacts, its neighbours, and can only infect/be infected by them [61].

There are different approaches to network models of epidemics, which are summarized briefly in [51, 74, 96], here we focus on pariwise approximation models, that study the dynamics of pairs in the population, disregarding higher-order network structures: the density of pairs depends on the density of triplets, and the density of triplets on the density of higher order structure, but it is not possible to keep track of the infinite chain of interdependencies, so we need to stop at some point and approximate the remaining correlations. Pair Approximation is a special case of a moment closure, where pairs of individuals are the state variables and triplest are approximated by a function of pairs, this way capturing the effects of the topology without explicitly dealing with the entire network structure. PA has been largely used in mathematical epidemiology because it allows to capture some structural properties of the population still keeping the model relatively tractable [116]. Models have been used to find one of the basic quantities in epidemic models, the reproduction number [120], [126] study the stability of PA on regular and random networks, the transmission of STD [8], can be complicated by allowing for loops in the structure [55] random rewiring of susceptible individuals [26]. It is clear that PA models are still far from giving a representation of real networks, nonetheless it has been shown that numerical simulations agree very well with PA epidemic models[80], and they have also been applied in the case of the foot and mouth epidemic in UK [82] childhood [75]. [43] proves that PA is highly accurate on infinite uncorrelated networks with negligible clustering, which we do not expect for real world networks, so the assumption may result particularly harmful, nevertheless [44] show how simple Mean Field are quite accurate for some real world networks (in particular those with high mean degree), and infer that the same result hold for UPA

3.3 The Complete Graph Model

This section proposes an epidemic model to study affiliation to an illegal group as an infection process. Notation and terminology of epidemic models are kept for simplicity. The population is divided in four compartments: those who are part of the organization will be called the Infected I, while individuals who are unsatisfied but not part of the organization are the Susceptible S. The remaining part of the population cannot be infected, and is divided in Non Susceptible NS and Repressors R. The I individuals behave as recruiters, when they interact with a S, with some probability β she change her state to I. R individuals are responsible of surveillance, and when they interact with an I

individual, with some probability γ they are successfull and I individual goes back to the S state[2]. The model variables and parameters are:

1. β the rate of infection, that is the rate at which S $\rightarrow I$ if the two interact
2. γ the efficacy of surveillance, that is the rate at which $I \rightarrow S$ because of the interaction with a repressor R.
3. ϵ recovery rate at which $I \rightarrow S$ spontaneously (think of it as leaving the organization).
4. x_i with $i \in \{S, I, NS, R\}$ the fraction of the population in each compartment
5. $\rho = x_I + x_S$ the total fraction of S and I individuals.

The simplest version of the model, with fixed, fully mixed population is described by the differential equations:

$$\begin{aligned} \dot{x}_S &= \epsilon x_I - \beta x_S x_I + \gamma x_R x_I \\ \dot{x}_I &= \beta x_S x_I - \epsilon x_I - \gamma x_R x_I \end{aligned} \tag{3.1}$$

The assumption of a fully mixed population is equivalent to say that individuals are placed on a complete, non-weighted graph: everybody has a link to everybody else in the population, and the probability of interaction between any two individuals in different states is proportional to the fraction of these states in the population. In (3.1) the probability of interaction between an individual in state i and an individual in state j is just given by $x_i x_j$. Assuming that there are only flows between the I and S states, both x_R and x_{NS} are constant and can be treated as parameters. Using $x_S = 1 - \rho - x_I$ we can then just study $\dot{x}_I = \beta(1 - \rho - x_I)x_I - \epsilon x_I$. There are three fixed points, the trivial $x_S = x_I = 0$, the Disease-Free Equilibrium [DFE] $x_I = 0, x_S = 1 - \rho$ and the Endemic Equilibrium [EE]: $x_I = \frac{1-\rho-\epsilon-\gamma x_R}{\beta}, x_S = \frac{(1-\rho)(\beta-1)+\epsilon+\gamma x_R}{\beta}$. An interesting question is whether we can determine under which conditions the population will be resistent to the invasion of an epidemic, in other words if we can find a threshold that divides the parameter space where the population will always be disease free and parameter space where the population will, in equilibrium, have a positive fraction of infected individuals. We can answer this question by determining the basic reproduction number. The basic reproduction number $\mathscr{R}_0$ is

[2]Notice that, in epidemiological terms, the dependency of the recovery of infected on the interaction with a specific type of neighbour is a novelty in this kind of models. Where direct intervention is modeled as vaccination, it is not carried by some node in the graph, but it is imposed exogenously.

defined as the average number of secondary infections that occur when one infective is introduced into a completely susceptible host population ([49]). Whenever $\mathscr{R}_0 < 1$ the population will be disease free in equilibrium, viceversa when $\mathscr{R}_0 > 1$ there will be a disease outbreak. The determination of $\mathscr{R}_0$ is central for assessing the efficacy of surveillance policies and the impact of control strategies, as the minimal objective would be to keep $\mathscr{R}_0 < 1$ in order to avoid outbreaks. In this paper we determine $\mathscr{R}_0$ as the conditions under which the Disease Free Equilibrium (DFE), namely the equilibrium where $x_I^* = 0$, is stable. By linear stability analysis we know that a fixed point is stable if all the eigenvalues of the Jacobian evaluated at the fixed point are negative, or complex with negative real parts. If the (real part) of the largest eigenvalue of the DFE is negative and no eigenvalue is zero, then DFE is stable. It follows that we can derive the Basic Reproduction Number $\mathscr{R}_0$ as the parameter relation that makes largest eigenvalue negative:

$$\mathscr{R}_0 = \frac{\beta(1+\rho)}{\epsilon + \gamma x_R} \tag{3.2}$$

LEMMA **1** *Assuming all eigenvalues are non-zero, if the largest eigenvalue of the Disease Free Equilibrium, $\hat{\lambda}_{DFE} < 0$, then the reproduction number $\mathscr{R}_0 < 1$ and the Disease Free Equilibrium is locally asymptotically stable.*

□

Notice that here it is assumed that Non Susceptible and Repressors are constant in the population, which is not unreasonable in a short period and close to Disease Free Equilibria. In a more extreme situation of high conflict in the society, an Endemic Equilibrium with high level of Infected and Repressors it would be reasonable to allow for transmission among all compartments.[3] [121] also models the interaction between NS and S compartments, and this could be analogously done here, even if the choice of the transmission rates seems somehow arbitrary.

3.4 The static regular graph model

The model in 3.1 is quite simple, allows for relatively straightforward conclusions and we can easily find an analytic $\mathscr{R}_0$. Its relative simplicity comes from the central assumption that every individual in the population has the same probability of interacting with every other individual (random matching). Here we remove the random matching assumption and we introduce some constraint to the interaction process using a network of contacts:

[3] For example in a civil war the army could also be susceptible to switch against the leading authority, but this would be a different model.

individuals can interact only with their neighbours, that is with the set of adjacent nodes in the graph. The graph is non directed (if A interacts with B, B interacts with A) and non weighted (the frequency of interactions among neighbours is uniform). Moreover for simplicity it is also assumed the graph is regular, that is the number of neighbours is constant for all individuals.

In what follows we explain the derivation of a version of (3.1) on a regular graph of degree $k \geq 3$ using the Pair Approximation method. As in [80, 55] we first focus on the single node level, and then derive the differential equations for the model in terms of pairs. The transition between the states can be described by

$$\begin{array}{ccccc} S & \xrightarrow[I_n]{\beta} & I & \xrightarrow[R_n]{\gamma} & S \\ & & \downarrow{\scriptstyle \epsilon} & & \\ & & S & & \end{array} \tag{3.3}$$

which means that susceptible individuals can be infected at a rate β by any of their infected neighbour I_n and infected can be cured by a repressor neighbour at a rate γ, or they can spontaneously recover switching to the susceptible state at rate ϵ.

The time evolution of the above stochastic process can be described by the differential equations:

$$\begin{aligned} \dot{P}_t(S_x) &= -\beta \textstyle\sum_{y \in \mathcal{N}(x)} P_t(S_x, I_y) + \gamma \sum_{y \in \mathcal{N}(x)} P_t(I_x, R_y) + \epsilon P_t(I_x) \\ \dot{P}_t(I_x) &= \beta \textstyle\sum_{y \in \mathcal{N}(x)} P_t(S_x, I_y) - \gamma \sum_{y \in \mathcal{N}(x)} P_t(I_x, R_y) - \epsilon P_t(I_x) \end{aligned} \tag{3.4}$$

where $P_t(i_x, j_y)$ is the joint probability to have state i at x and state j at y at time t, $P_t(i_x)$ is the probability of having state i at x at time t and $\mathcal{N}(x)$ is the neighbourhood of site x. Notice that equations (3.4) are not limited to regular graphs only, as long as we know the graph structure we can write N (number of nodes in the graph) such equations and fully describe the model. By assuming a regular graph we know that all the nodes have the same number of neighbours[4] and we can write the above equations in terms of pair probabilities (see [65]) $p_{ij} = \frac{1}{k} \sum_{y \in \mathcal{N}(x)} P_t(i_x, j_y)$ where we drop for convenience the indexing on time. Call x_i the fraction of nodes in state i, we rewrite (3.4) as:

[4] In the case of an arbitrary, non regular graph, we can just use the average degree $\hat{k}$, in this case adding another layer of approximation.

$$\begin{aligned} \dot{x}_S &= -\beta k p_{SI} + \gamma k p_{IR} + \epsilon x_I \\ \dot{x}_I &= \beta k p_{SI} - \gamma k p_{IR} - \epsilon x_I \end{aligned} \tag{3.5}$$

Clearly 3.5 are not closed as they depend on pair probabilities p_{SI} and p_{IR}, which in turn depend on triplets, and those on higher order structures, creating an infinite chain of dependencies which would make the system unsolvable. In order to track down the change in the pair densities p_{ij} we need to take in consideration all those events that determine a change in the pair densities (this technique is sometimes called "bookeeping" [4]) There are four possible states, hence there are 10 pairs[5] The following diagram represents the possible transitions between couples. In this simple version of the model transitions only happen between states I and S, still nodes in state R and NS affect the probability of these events happening.

$$\begin{array}{ccccc} S,S \rightleftharpoons S,I & & S,R & & S,NS \\ \uparrow\downarrow & & \uparrow\downarrow & & \uparrow\downarrow \\ I,I & & I,R & & I,NS \\ & & & & \\ & & R,R & & R,NS \\ & & & & \\ & & & & NS,NS \end{array} \tag{3.6}$$

As it is usually assumed in PA models, we do not consider the possibility of a simultaneous change in both nodes of the pair, that is we exclude transitions $ii \to jj$ and $ii \leftarrow jj$.

By way of example here we present the derivation of the equation for the dynamics of the pair RI, that is the pair of a Repressor and an Infected. At the pair level there is a "direct" event that reduces the number of RI pairs: at rate γ the node in state I switches to state I due to the action of other node of the pair, R. This happens with probability p_{RI} Moreover, at rate ϵ-nodes in state I switch to state S ("spontaneous recovery"), independently of their neighbourhood: if the node "recovered" is in a pair RI this event will reduce the number of RI pairs. So the density of pairs RI decreases with probability $p_{RI}(\gamma+\epsilon)$. In addition to "direct" events we also need to take into account "indirect" events caused by the neighborhood of the pair. A new pair RI will form as a vertex in state R has a

[5]The number of distinct pairs over n states is given by $\binom{n+1}{2}$, where we assume that $p_{ij} = p_{ji}$

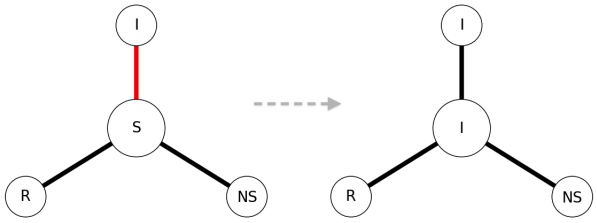

Fig. 3.1 Example of indirect effect changing a pair RS into RI

neighbouring pair SI that becomes II at rate β: the probability of this event given by the density of triples p_{RSI}, where $p_{ijh} = \frac{1}{k-1}\sum_{w\in\mathcal{N}^x(y)} P_t(i_x, j_y, h_w)$ and $\mathcal{N}^x(y)$ is the set of neighbours of y excluded x and again indexing on time is dropped . A pair RI will be destroyed at rate γ if the node in state I has another neighbour (outside the pair) in state R, and this happens with probability p_{RIR}. The pair RI has $(k-1)$ pairs that indirectly affect its dynamics, as among the k neighbours of the node in state I one is the node in state R at the other end of the pair itself.

$$\begin{aligned} \dot{p}_{RI} &\overset{infection}{+=} \beta(k-1)p_{RSI} \\ &\overset{recovery}{-=} \epsilon p_{RI} \\ &\overset{surveillance}{-=} \gamma[(k-1)p_{RIR} + p_{RI}] \end{aligned} \tag{3.7}$$

Hence the differential equation for the density of pairs RI is:

$$\dot{p}_{RI} = \beta(k-1)p_{RSI} - \gamma(k-1)p_{RIR} - (\epsilon+\gamma)p_{RI} \tag{3.8}$$

In order to solve the equations it is necessary to find a closure, that is to express higher order correlations in terms of lower order correlations. The simplest closure is the Mean Field, where $p_{ij} = p_i p_j$ and the structural property of the graph are completely overlooked. Uncorrelated Pair Approximation instead performs better than mean field, and in some cases also allows for closed form solutions.

With Pair Approximation we choose a triples closure, that is we aprroximate triple densities by pair densities. Assuming that pairs are uncorrelated (that is there is negligible clustering in the network), we can then express the density of a generic triple as:

$$p_{ijl} = \frac{p_{ij}p_{jl}}{x_j} \tag{3.9}$$

Where p_{ijl} is the density of triples of vertices in states i, j and l. Under the non-correlation assumption this is just a result of the application of Bayes theorem (see [80]). Using closure in (3.9) we can rewrite (3.8) as:

$$\dot{p}_{RI} = \beta(k-1)\frac{p_{RS}p_{SI}}{x_S} - \gamma\frac{p_{RI}^2}{x_I} - (\epsilon+\gamma)p_{RI} \tag{3.10}$$

and equation (3.4) as:

$$\dot{x}_S = -\beta k p_{SI} + \gamma k p_{RI} + \epsilon x_t \tag{3.11}$$

As can be seen in (B.1), the dynamics of our system depend on the pairs p_{SS}, p_{SI}, p_{RI}, p_{II}, p_{SNS}, p_{INS}, where we already used that $p_{ij} = p_{ji}$. We can use the following identities to reduce the dymension of the system:

$$\begin{aligned} x_S &= p_{SI} + p_{SR} + p_{SNS} + p_{SS} \\ x_{NS} &= p_{NSI} + p_{NSR} + p_{NSNS} + p_{NSS} \\ x_R &= p_{RI} + p_{RR} + p_{RNS} + p_{RS} \\ x_I &= p_{II} + p_{IR} + p_{INS} + p_{IS} \end{aligned} \tag{3.12}$$

from which follows that $1 = p_{RR}+p_{NSNS}+p_{II}+p_{SS}+2(p_{SI}+p_{SR}+p_{SNS}+p_{NSI}+p_{NSR}+p_{IR})$. Define the "local density" of neighbours in state i from the perspective of a node in state j as the conditional probability:

$$q_{i|j} = \frac{p_{ij}}{x_j} \tag{3.13}$$

where clearly:

$$q_{i|j} = q_{j|i}\frac{x_i}{x_j} \tag{3.14}$$

$$\sum_i q_{j|i} = 1 \tag{3.15}$$

Notice also that in this version of the model x_R and x_{NS} are constant, we can write the dynamics of the pairs as:

$$\begin{aligned}
\dot{p}_{SI} &= -p_{SI}\left[\beta(k-1)\frac{p_{SI}}{x_S} + \beta + \gamma(k-1)\frac{p_{RI}}{x_I}\right] + p_{SS}\beta(k-1)\frac{p_{SI}}{x_S} \\
&\quad + p_{II}\left[\gamma(k-1)\frac{p_{RI}}{x_I} + \epsilon\right] \\
\dot{p}_{RI} &= p_{RS}\beta(k-1)\frac{p_{SI}}{x_S} - p_{RI}\left[\gamma(k-1)\frac{p_{RI}}{x_I} + \gamma + \epsilon\right] \\
\dot{p}_{RS} &= -p_{RS}\beta(k-1)\frac{p_{SI}}{x_S} + p_{RI}\left[\gamma(k-1)\frac{p_{RI}}{x_I} + \gamma + \epsilon\right] \\
\dot{p}_{SNS} &= -p_{SNS}\beta(k-1)\frac{p_{SI}}{x_S} + p_{INS}\left[\gamma(k-1)\frac{p_{RI}}{x_I} + \epsilon\right] \\
\dot{p}_{INS} &= p_{SNS}\beta(k-1)\frac{p_{SI}}{x_S} - p_{INS}\left[\gamma(k-1)\frac{p_{RI}}{x_I} + \epsilon\right]
\end{aligned} \tag{3.16}$$

The master equations from which (3.16) is derived are explained in more details in the appendix (B.1). It can be useful to express this system in terms of the conditional probabilities $q_{i|j}$. By using a simple chain rule, $dq_{i|j}/dt$ is given by

$$\frac{dq_{i|j}}{dt} = \frac{d(p_{ij}/x_j)}{dt} = \frac{1}{x_j}\frac{dp_{ij}}{dt} - \frac{p_{ij}}{x_j^2}\frac{dx_j}{d_t} \tag{3.17}$$

So the final system in terms of conditional probabilities is:

$$
\begin{aligned}
\dot{x}_S &= -\beta k q_{I|S} x_S + \gamma k q_{R|I} x_I + \epsilon x_I \\
\dot{q}_{I|S} &= q_{I|S}^2 \beta(2-k) - \gamma(k-1)\tfrac{x_I}{x_S} q_{R|I}^2 \\
&\quad + q_{I|S}\Big[\beta(k-2) - \beta(k-1) q_{S|NS}\tfrac{x_{NS}}{x_S} - 2\epsilon - 2\gamma(k-1) q_{R|I} \\
&\quad - \gamma k q_{R|I}\tfrac{x_I}{x_S} - \beta(k-1) q_{R|S}\Big] + \epsilon\Big[\tfrac{x_I}{x_S} - \tfrac{x_h}{x_S} q_{I|NS}\Big] \\
&\quad + q_{R|I}\Big[\gamma(k-1)\tfrac{x_I}{x_S} - \gamma(k-1)\tfrac{x_h}{x_S} q_{I|NS} - \epsilon\tfrac{x_I}{x_S}\Big] \\
\dot{q}_{R|I} &= \gamma q_{R|I}^2 - q_{R|I}\Big[\gamma + k\beta\tfrac{x_S}{x_I} q_{I|S}\Big] + \beta(k-1)\tfrac{x_S}{x_R} q_{I|S} q_{R|S} \\
\dot{q}_{R|S} &= q_{R|S}\Big[q_{I|S}\beta - \gamma k\tfrac{x_I}{x_S} q_{R|I} - \epsilon\tfrac{x_I}{x_S}\Big] + \gamma(k-1)\tfrac{x_I}{x_S} q_{R|I}^2 \\
&\quad + [\epsilon+\gamma]\tfrac{x_I}{x_S} q_{R|I} \\
\dot{q}_{S|NS} &= q_{I|NS}\Big[\gamma(k-1) q_{R|I} + \epsilon\Big] - \beta(k-1) q_{I|S} q_{S|NS} \\
\dot{q}_{I|NS} &= \beta(k-1) q_{I|S} q_{S|NS} - q_{I|NS}\Big[\gamma(k-1) q_{R|I} + \epsilon\Big]
\end{aligned}
\tag{3.18}
$$

where $x_I = \rho - x_S$ and recall that $\dot{x}_R = 0$, $\dot{x}_{NS} = 0$.

In deriving 3.18 we did not include the possibility of strategic behaviour, hence an individual in state i can't pretend to be in a different state j, but for some applications it is reasonable to allow for this possibility. This can be done by including some decision rule according to which individuals choose which state they want to reveal to their neighbours, given they know about their own state but not about the state of their neighbours. Let's consider an example in the case of the recruitment process. I-nodes have an interest in recruiting S-nodes, and in order to do so they have to reveal themselves. Viceversa they don't want to reveal themselves to a R neighbour, as they will suffer some sort of punishment. R-nodes will always pretend to be S in order to induce I neighbours to reveal themselves. Assuming that S and NS individuals have no incentive in lying, the only individuals facing a decision are I, who need to evaluate the consequences of their actions: they will not choose to reveal themselves if the cost of this action (punishment) is

higher than the benefit, which is given by the eventual recruitment of a neighbour. If we assume that the utility of a single recruitment is normalized to one, the decision rule will prescribe that the will reveal themselves if:

$$\frac{\gamma}{\beta} \leq \frac{p_{IS}}{p_{RI}} = \frac{q_{I|S}x_S}{q_{R|I}x_I} \tag{3.19}$$

This can be simply included in (3.18) by simply modifying (3.11) in:

$$\dot{x}_S = (-\beta k p_{SI} + \gamma k p_{IR})\eta_i + \epsilon x_I \tag{3.20}$$

where $\eta_i = 0$ if $\frac{\gamma}{\beta} \leq \frac{p_{IS}}{p_{RI}}$ and $\eta_i = 1$ otherwise. More refined decision rules can be considered, here we skip this complication and we concentrate on the simple mechanicistic dynamic.

3.5 Equilibria Stability and Basic Reproduction Number

The system in (3.18) can be integrated numerically, and given values for the parameters and initial conditions, one can find the trajectories of the local densities and the fractions of types in the population.

As in the complete graph case, we are interested in determining the dependency of the stability of the DFE on the parameters. A rigorous derivation of $\mathscr{R}_0$ for a SIR model under PA has been done in [120], here we adopt the simpler approach of linear stability analysis around the DFE to find the largest eigenvalue $\hat{\lambda}_{DFE}$, as in (3.3). Let us consider the different fixed points and their stability:

Case 1: No Susceptibles $x_S^* = 0$ is a fixed point in the trivial case $x_I^* = q_{I|S}^* = q_{R|S}^* = q_{I|NS}^* = q_{S|NS}^* = q_{R|I}^* = 0$, so $\rho = 0$. Clearly $x_S = 0$, $x_I = \rho$ it is not a fixed point unless $\epsilon = x_R = 0$, otherwise there is a transition from state I to S due to spontaneous exit. The eigenvalues in this case are $(0, \beta(k-2))$, where $\beta(k-2) > 0$ except when $\beta = 0$, so this is clearly unstable as expected.

Case 2: Endemic Equilibirum [EE] When the infection cannot be eradicated from the population, but persists in equilibrium we have an Endemic Equilibrium. We generally do not have analytical solutions, except for the trivial case $x_R^* = q_{I|NS}^* = q_{R|S}^* = q_{S|NS}^* = q_{R|I}^* = 0$, when we have:

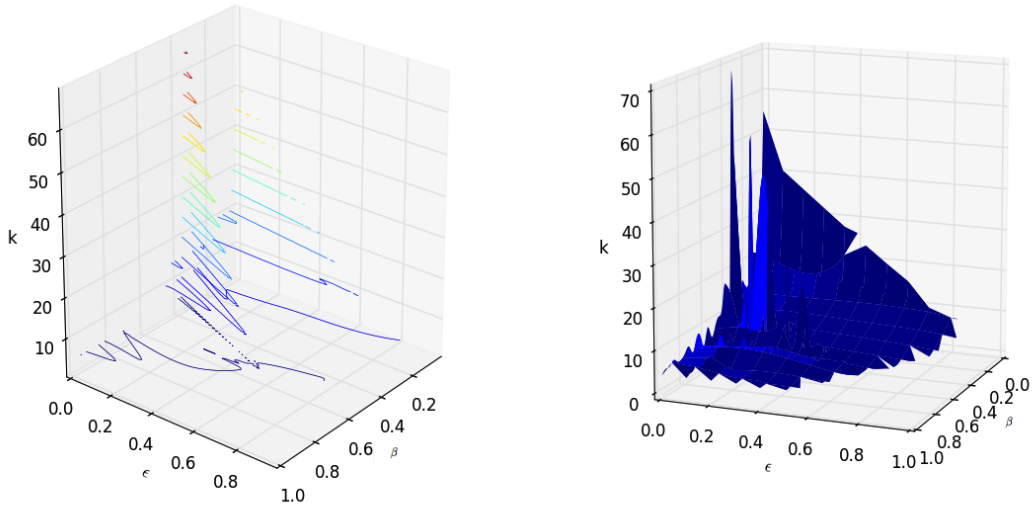

Fig. 3.2 *[Endemic Equilibrium]* Threshold map for endemic equilibrium as β, ϵ and k vary. The space above the blue curve is where the endemic equilibrium is unstable, while in the space below is stable. As connectivity increases the EE is stable only for very low infection and exit rates.

$$x_I^* = 1 - \rho \tag{3.21}$$

$$q_{I|S}^* = \frac{2\epsilon - \beta(k-2) \pm \sqrt{-(-2\epsilon + \beta(k-2))^2 + \frac{4\beta\epsilon(2-k)x_I^*}{x_S^*}}}{2\beta(2-k)} \tag{3.22}$$

$$x_S^* = \frac{\epsilon x_I^*}{\beta q_{I|S}^* k} = \frac{\epsilon\rho}{\beta q_{I|S}^* k + \epsilon} \tag{3.23}$$

Even in the trivial case the Jacobian is a dense matrix with non linear entries it is a hard task to find analytical solution for the eigenvalues, hence we need to evaluate the Jacobian numerically to perform linear stability analysis. We can then build a numerical stability threshold as shown in figure 3.2, where the stability of EE is evaluated as ϵ, β and k change. While for low connectivity ($k \leq 10$) there is a large combination of values for ϵ and β for which the EE is stable, for high connectivity the EE is stable only for values of ϵ and β very close to zero, as can be seen also in figure 3.5 for a given level of ϵ. In Figure 3.3 the stability of the EE is analysed as the infection rate and the spontaneous exit rate change. It can be seen that the set of stable EE, depending on the network degree and the initial conditions, is scattered around the locus $\beta = \epsilon$. This is intuitive as when $x_R^* = 0$, $\dot{x}_S = 0$ iff $\frac{\beta}{\epsilon} = \frac{x_I}{k q_{I|S} x_S}$.

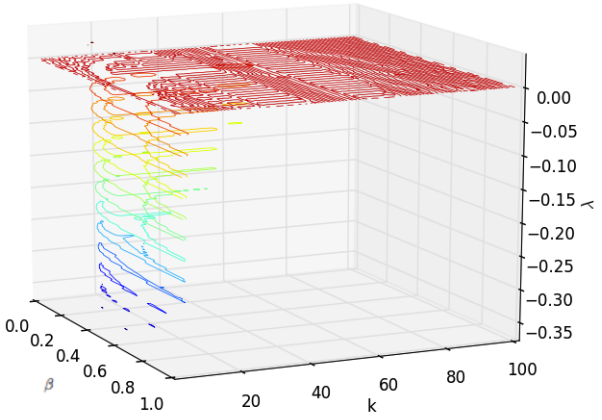

Fig. 3.3 *[Endemic equilibrium]* Here for a given level of exit rate, $\epsilon = 0.17$, the contour functions of the highest eigenvalue $\hat{\lambda}_{EE}$ as function of k and β. As k increases the endemic equilibrium becomes unstable (the red area at $\hat{\lambda}_{EE} = 0$) even for very low infection rates.

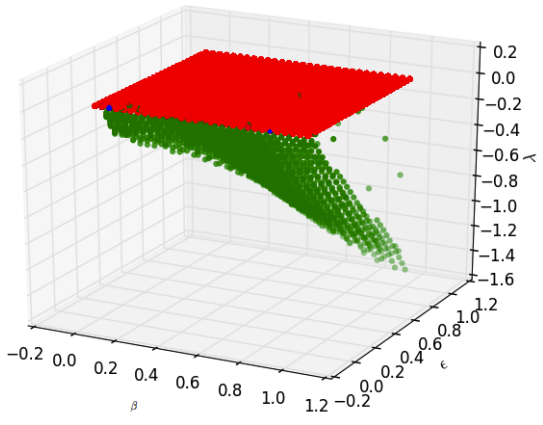

Fig. 3.4 *[Endemic Equilibrium]* The maximum eigenvalue $\hat{\lambda}_{EE}$ as a function of β and ϵ: most of the points are unstable (red area) while the set of stable points is a cloud around the locus $\beta = \epsilon$.

Case 3: Disease Free Equilibrium [DFE] $x_S^* = \rho$ and $x_I^* = 0$ is a fixed point, as in absence of infected individuals there is no source of infection in the population. As $x_I^* = 0$, in DFE we have $q_{I|S}^* = q_{R|I}^* = q_{I|NS}^* = 0$, but these identities are not enough to univocally determine $q_{S|NS}^*$ and $q_{R|S}^*$, as can be easily veryfied equating 3.18 to zero. $x_S^* = \rho$ and $x_I^* = 0$ is a fixed point, as in absence of infected individuals there is no source of infection in the population. In order to simplify stability analysis we evaluate the DFE where $q_{S|NS}^* = 0$ and $q_{R|S}^* = 0$. The resulting Jacobian is then:

$$J_{RFE} = \begin{bmatrix} -\epsilon & -\beta k\rho & 0 & 0 & 0 & 0 \\ -\frac{\epsilon}{\rho} & \beta(k-2)-2\epsilon & 0 & 0 & 0 & -\frac{\epsilon x_{NS}}{\rho} \\ 0 & -\gamma & 0 & 0 & 0 & 0 \\ 0 & 0 & 0 & 0 & 0 & 0 \\ 0 & -\gamma & 0 & 0 & 0 & \epsilon \\ 0 & -\gamma & 0 & 0 & 0 & -\epsilon \end{bmatrix} \tag{3.24}$$

which eigenvalues are $\left[0, -\epsilon, \frac{\beta(k-2)-3\epsilon \pm \sqrt{\beta^2k^2-4\beta^2k+4\beta^2+2\beta\epsilon k+4\beta\epsilon+\epsilon^2}}{2}\right]$ where 0 has multiplicity 3.

The presence of zero eigenvalues, that was clearly implied by the singularities in (3.24) implies that the Hartman-Grobman theorem does not apply hence negativity of the largest eigenvalue at DFE does not guarantee stability, and we need to perform further analysis as the stability of the equilibrium depend on non-linear terms. A closer look at the full eigenspace spanned by the eigenvectors of the Jacobian reveals that we can actually be satisfied with linear analysis, as the eigenvectors associated with the zero eigenvalues are $[0,0,0,1,0,0]$ with multiplicity 2 and $[0,0,0,0,1,0]$. The centre eigenspace spanned by these two eigenvectors correspond to the variables $q_{R|S}$ and $q_{S|NS}$: we don't know if they are stable at DFE, but we don't need to analyze further as variations in $q_{R|S}$ and $q_{S|NS}$ do not change x_I hence do not affect stability of the DFE, as long as all remaining non-zero eigenvalues are negative. The same holds if we remove the assumption that $q_{S|NS}^* = 0$ and $q_{R|S}^* = 0$.

LEMMA **2** *If at the Disease Free Equilibrium all the non-zero eigenvalues are negative the DFE is stable.*

Proof 1 *Define stable eigenspace E^s the space spanned by eigenvectors associated with eigenvalues with negative real part, and centre eigenspace E^c the space spanned by the eigenvectors associated with zero eigenvalues. If the (real part of) eigenvalues are either negative or zero, then the full eigenspace spanned by the eigenvectors of the Jacobian ad DFE can be decomposed in E^s and E^c. For the centre manifold theorem, there exist a*

unique centre manifold in the neighborhood of the DFE where the dynamics will eventually converge. Given that everywhere at the centre manifold $x_I^* = 0$, the DFE is stable.

As $k \geq 3$ the radicand of the last two eigenvalues is always positive, and rewriting the radicand the largest eigenvalue is:

$$\lambda = \frac{\beta(k-2) - 3\epsilon + \sqrt{\beta^2(k-2)^2 - 2\beta\epsilon(2+k) + \epsilon^2}}{2} \tag{3.25}$$

If we call $\theta = \sqrt{\beta^2(k-2)^2 - 2\beta\epsilon(2+k) + \epsilon^2}$, then we can define the basic reproduction number as:

$$\mathscr{R}_0 = \frac{\beta(k-2) + \theta}{3\epsilon} \tag{3.26}$$

If $\mathscr{R}_0 < 1$ the radicalization free equilibrium is locally asymptotically stable.

In order to study stability we evaluate $\hat{\lambda}_{DFE}$ numerically, as β, k and ϵ change. Figure 3.5 shows that there exist no threshold for infection rates greater than 0.6, and for $0 \leq \beta \leq 0.6$ the threshold exists only when ϵ is sufficiently large (and greater than β). Otherwise the population will always be subject to invasion by a disease. Where the threshold exists, we can see that even for very low infection rates, if connectivity is high the DFE is largely unstable. This can be seen by noticing that the threshold for $k \geq 10$ is flattened around $\beta = 0$. This is confirmed by the map of $\hat{\lambda}_{DFE}$ against β, k and ϵ in figure 3.6.

Notice that in (3.3) there is the assumption that an I-node "caught" by a R neighbour change its state to S. This assumption is necessary as the equations (3.18) hold for a static network, it is only the states of its node that change while both connections and number of nodes remains constant. While this is equivalent to assume that there is no acquired immunity, like in STDs, it is questionable if, in a recruitment model, this is a meaningful assumption. It could be interpreted as an effective propaganda by the R-nodes after which the individual does try to recruit other individuals to the cause anymore. This would be less appropriate in case we are modeling terrorist recruitment: if a terrorist is caught it is arrested, hence removed from the graph. In order to preserve the necessary assumption on the static network, and allow for removal, we should assume that the infected node is removed from the graph and replaced by a new node in the same position, with the same set of connections, whose state is determined by a stochastic function over $\{I, S, NS, R\}$. In the following section we are going to do better than that by endogenizing the graph, modeling both new node arrivals and node removal.

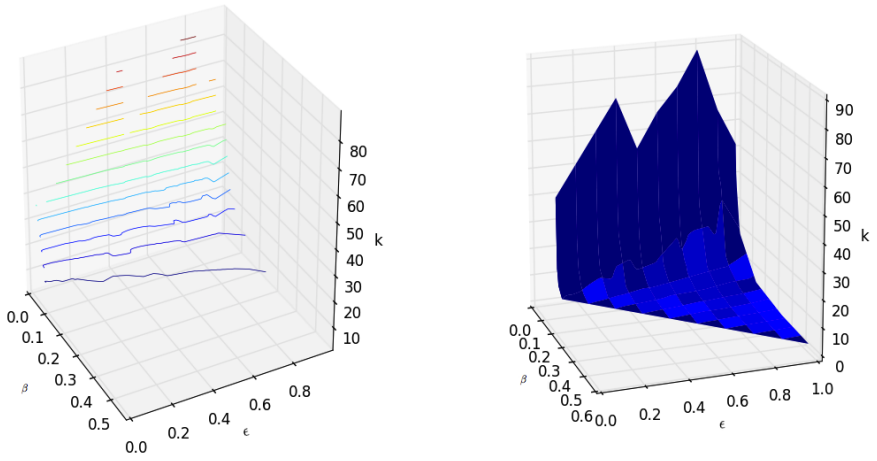

Fig. 3.5 *[Disease Free Equilibrium]* Map of the epidemic threshold as a function of β, ϵ and k (right) and corresponding contour functions (left). $\mathscr{R}_0 > 1$ in the space above the curve, where the DFE is unstable, viceversa it is stable in the space below.

3.6 Adaptive Networks

In the model developed in the previous section we assumed that the network is static, so it just constitutes a constraint to the disease (or recruitment) dynamic. The dynamical process happening on the network may also determine changes of the network structure, for example because infected nodes are isolated when recognized, so that the disease does not spread, or because they are removed from the network in the recruitment. In this section we model both the dynamics on the network and the dynamics of the network, that is the coevolution of infection process and contact topology, using adaptive networks. There is an increasing literature on adaptive networks [98], [40], [115], [111] with applications mainly to voter models and epidemiological models. The simplest version of epidemiological adaptive networks model the evolution of the graph as stochastic rewiring: S-nodes delete their links with I-nodes at a fixed rate and reconnect either to other S-nodes only or at random. The former case determine isolation of I-nodest that slows the diffusion of the epidemics, while in the latter isolation is clearly less effective. Usually nodes cannot be removed unless they die for natural cause or as a consequence of the disease.

Adopting the framework used in 3.4 we develop a simple adaptive network epidemic dynamic similar to [68] recruitment model. Our contribution is to introduce the new

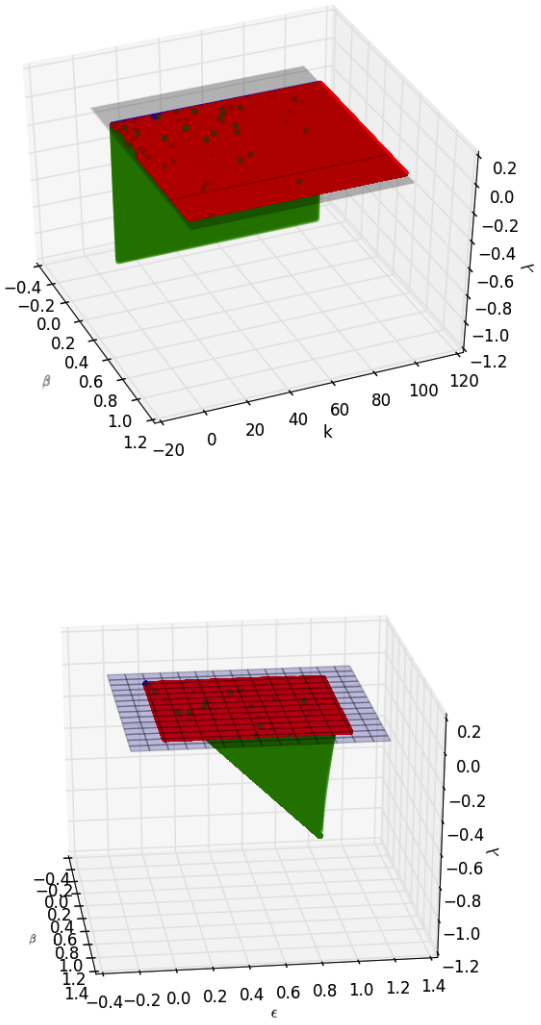

Fig. 3.6 *[Disease Free Equilibrium]* Maximum eigenvalue of the DFE, $\hat{\lambda}_{DFE}$ when β and k vary and when ϵ and k vary respectively. The gray shaded plane is the level where the maximum eigenvalue is zero, red points indicate stability, green points instability.

R-class, and to make node removal depending on interaction with R-neighbours, so determined by the graph structure, instead of being due to exogenous death rate. We start with a random regular network of degree k. New individuals arrive at rate μ and are in state $i = \{I, NS, S\}$ with probability P_i, where $\sum_i P_i = 1$. Every new node that arrives is endowed with a number of edges equal to the average connectivity in the graph κ, that will connect to κ distinct nodes avoiding self and double connections. The arrival process can be seen as births or immigration, and it is assumed that R-nodes can't arrive spontaneously. The underlying stochastic process describing infection is the same as in the previous section, except that now when a R-node interacts with an I-node, with probability γ the I node is removed from the network. The stochastic process is described in diagram 3.27 where $\otimes$ represent removal and $\bigcirc$ arrival.

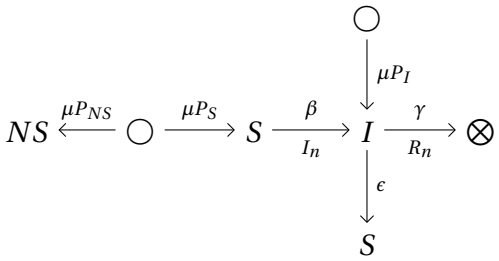

(3.27)

When a new node arrives κ new connections are created. The simplest way of model how these connections are created would be to assume they are done at random, so that the probability of a new arriving node of type i to establish a link with a node of type j (call it $P(i, j)$ would be proportional to the fraction of the individuals of type j in the population. A more realistic rule would be that nodes with higher degree have a higher probability of attracting new connections, usually called preferential attachment [5] which is well assessed in the literature for its capacity of generating scale-free graphs (for a review of different formation rules see [94]). Social networks often show a tendency of similar individuals to associate (homophily) [101] and we think that in this context that would be the most appropriate mechanism. In this model the only dimension along which node differ is their state, if there is homophily an individual in state i creates a link with an individual in the same state with probability that exceeds the fraction of people in that state, namely $P(i, i) > x_i$. We simply model this by defining $P(i, i) = x_i + \hat{h}$ and $P(i, j) = x_j - \frac{\hat{h}}{3}$ for $j \neq i$, so that $\sum_j P(i, j) = 1$. By following the same logic used in section 3.4 and taking in considerations all the event that happen at node and pair level, we can write the master equations for node and pair densities. While in the previous model the number of nodes and links was fixed, here it changes because of removal and new node arrival, so we need to renormalize node densities like in [28]. Consider for example the

density x_S, given that nodes arrive at rate μ and are in state S with probability P_S, there will be a corresponding loss of x_S density of $\mu P_S x_S$, viceversa because of infected node removal at a rate γp_{RI} all densities are renormalized upwards, so x_S increases by $\gamma p_{RI} x_S$. Note that a node removal event implies that on average κ links are lost, while when a new individual arrives κ new links are formed, hence pair densities need to be renormalized as well. Consider for example the evolution of pairs p_{SI}: with rate μ, κ new links are formed, that will be between an S and I-node with probability $P_I P(IS) + P_S P(SI)$. Because of new node formation every pair density needs to be renormalized: density p_{SI} decreases by $\mu\kappa p_{SI}$, and increases by $\kappa\gamma p_{RI} p_{SI}$ because of infected nodes removal. The same applies for all other pair densities. Notice that the average degree is constant as the number of edges grows linearly with the number of nodes[6], so the dynamical system is described by the following equations:

[6]This is a desirable property as [3] shows that whenever the number of edges is linear in the number of nodes a general family of inhomogeneous graphs can be generated, and many property of the graphs in this family can be easily determined, like the dimension of the giant component.

$$
\begin{aligned}
\dot{x}_S &= \mu P_S - \beta\kappa p_{SI} + \epsilon x_I + x_S(-\mu + \gamma p_{RI}\kappa) \\
\dot{x}_I &= \beta\kappa p_{SI} + \mu P_I - \epsilon x_I - \gamma\kappa p_{RI} + x_I(-\mu + \gamma p_{RI}\kappa) \\
\dot{x}_R &= \gamma p_{RI} x_R \kappa + -\mu x_R \\
\dot{x}_{NS} &= \mu P_{NS} + x_{NS}(-\mu + \gamma p_{RI}\kappa) \\
\dot{p}_{SI} &= \beta(\kappa-1)\tfrac{p_{SS}p_{SI}}{x_S} - \beta(\kappa-1)\tfrac{p_{SI}^2}{x_S} - \beta p_{SI} - \gamma(\kappa-1)\tfrac{p_{SI}p_{RI}}{x_I} \\
&\quad + \epsilon(p_{II} - p_{SI}) + \mu\kappa(P_I(x_S - \hat{h}/3) + P_S(x_I - \hat{h}/3) - p_{SI}) + \kappa\gamma p_{RI} p_{SI} \\
\dot{p}_{RI} &= \beta(\kappa-1)\tfrac{p_{RS}p_{SI}}{x_S} - \gamma(\kappa-1)\tfrac{p_{RI}^2}{x_I} - (\gamma\kappa + \epsilon) p_{RI} \\
&\quad + \mu\kappa(P_I(x_R - \hat{h}/3) - p_{RI}) + \kappa\gamma p_{RI}^2 \\
\dot{p}_{RS} &= -\beta(\kappa-1)\tfrac{p_{RS}p_{SI}}{x_S} + (\epsilon+\gamma) p_{RI} + \mu\kappa(P_S(x_R - \hat{h}/3) - p_{RS}) + \kappa\gamma p_{RI} p_{RS} \\
\dot{p}_{SNS} &= -\beta(\kappa-1)\tfrac{p_{SI}p_{SNS}}{x_S} + \epsilon p_{INS} + \kappa\gamma p_{RI} p_{SNS} \\
&\quad + \mu\kappa(P_S(x_{NS} - \hat{h}/3) + P_{NS}(x_S - \hat{h}/3) - p_{SNS}) \\
\dot{p}_{INS} &= \beta(\kappa-1)\tfrac{p_{SI}p_{SNS}}{x_S} - \epsilon p_{INS} + \mu\kappa(P_I(x_{RS} - \hat{h}/3) + P_{NS}(x_I - \hat{h}/3) - p_{INS}) \\
&\quad + \kappa\gamma p_{RI} p_{INS} \\
\dot{p}_{II} &= \beta p_{SI} + \beta(k-1)(\tfrac{p_{IS}^2}{x_s} - \tfrac{p_{II}p_{RI}}{x_I}) - 2\epsilon p_{II} + \mu\kappa(2P_I(x_I + \hat{h}) - p_{II}) + \kappa\gamma p_{RI} p_{II} \\
\dot{p}_{SS} &= -\beta(k-1)\tfrac{p_{SS}p_{SI}}{x_S} + \epsilon p_{SI} + \epsilon^2 p_{II} + \mu\kappa(2P_S(x_S + \hat{h}) - p_{SS}) + \kappa\gamma p_{RI} p_{SS}
\end{aligned}
\tag{3.28}
$$

The various components of the equations are explained in detail in the appendix.

3.7 Basic Reproduction Number

As we have done with the static network model, we find the Basic Reproduction Number by analyzing the stability of the Disease Free Equilibrium [DFE]. It is easy to see that a DFE exists only if $P_I = 0$, so if the arrival rate of I-nodes is zero (which can be interpreted as effective control at the borders to prevent entrance of I-nodes). Assuming no homophily, and using that at the DFE $x_I^* = 0$ also $p_{SI}^* = p_{RI}^* = p_{II}^* = p_{INS}^* = 0$, from (3.28) we can then find the DFE levels $x_S^* = P_S$, $x_R^* = 0$ and $x_{NS}^* = P_{NS}$, $p_{SS}^* = 2P_S^2$. The eigenvalues of the Jacobian at DFE are $-k\mu$ and $-\mu$ with multiplicity 3, $-\epsilon - \gamma k - k\mu$; $-2\epsilon - k\mu$, $-\epsilon - k\mu$; $\frac{1}{2}\Big[-2\epsilon - (1+k)\mu + \beta[2(k-1)P_S - 1] + \theta\Big]$ and $\frac{1}{2}\Big[-2\epsilon - (1+k)\mu + \beta[2(k-1)Ps - 1] - \theta\Big]$ with multiplicity 1, where $\hat{\theta} = \sqrt{(k-1)^2\mu^2 + [\beta - 2\beta(k-1)P_S]^2 + 2\beta\mu[k-1+P_S(4k-2)]}$. With positive γ, ϵ and μ we need just to focus on the last two eigenvalues as all the others are strictly negative. Moreover as $k \geq 3$ it follows that $\theta \geq 0$, so the largest eigenvalue is:

$$\hat{\lambda}_{DFE} = \frac{-2\epsilon - (1+k)\mu + \beta[2(k-1)P_S - 1] + \hat{\theta}}{2} \tag{3.29}$$

from which we can write the basic reproduction number for the adaptive model as:

$$\mathscr{R}_0 = \frac{2\beta(k-1)P_S + \hat{\theta}}{2\epsilon + \beta + \mu(k+1)} \tag{3.30}$$

The first thing we can notice is that stability of the DFE does not depend on γ and that it is obviously increasing in ϵ. Analyzing (3.30) numerically we see that κ has a huge impact on stability, whenever $\kappa > 10$ the DFE is unstable unless P_S or β (or both) are very low (3.7). When $P_S > 0.2$ the DFE is never stable under the given ϵ and β. For any given level of $P_S < 0.2$ stability of the DFE is given for higher values of μ as can be seen in (3.8a). It is quite counterintuitive that the more the graph increases the easier keeping the DFE stable, hence this aspect requires further analysis to better understand where it originates in the model. When the rate of S-nodes arriving is close to zero, then the DFE is stable for all values of μ. Viceversa The higher the arrival rate of S-nodes for a given level of μ the more unstable the DFE, but the picture changes if the infection rate decreases: in (3.8b) we see that when β is very low, then stability is ensured even for high arrival rates of suscepbile nodes, viceversa for low P_S, the DFE is stable even for high infection rate. Overall for a realistic low μ the DFE is largely unstable in the (β, P_S) space, except for points where at least one of the two coordinates is very close to zero.

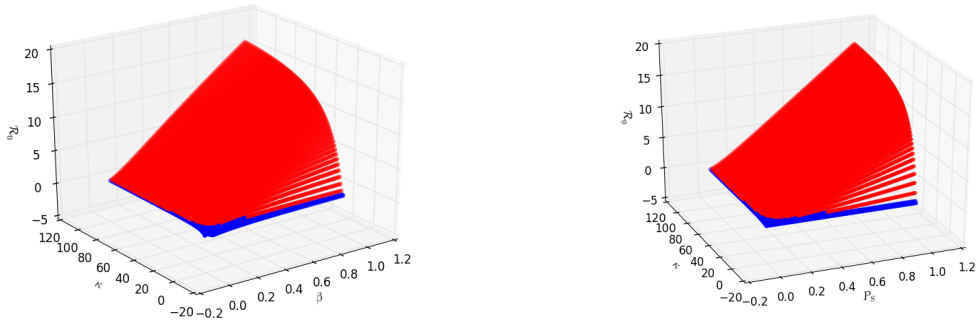

(a) (b)

Fig. 3.7 $\mathscr{R}_0$ for $\epsilon = 0.1, \mu = 0.1, P_S = 0.5$ (a) and $\epsilon = \mu = 0.1, \beta = 0.5$ (b). The red area indicates instability of the DFE, the blue area stability.

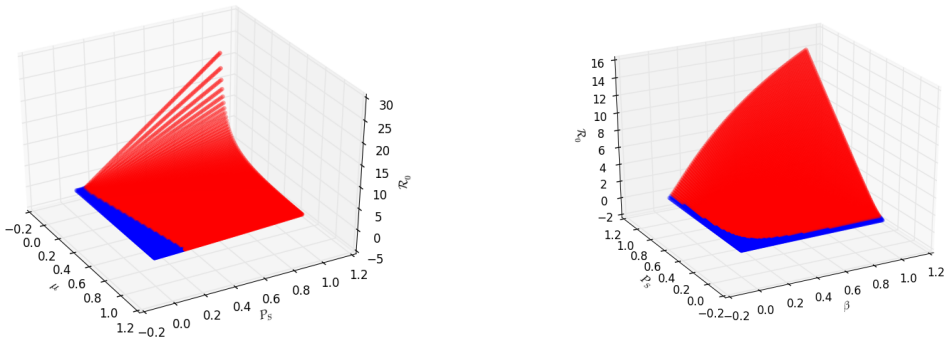

(a) (b)

Fig. 3.8 $\mathscr{R}_0$ for $\epsilon = 0.1, k = 10$, $\beta = 0.5$ (a) and $\epsilon = \mu = 0.1, k = 10$ (b). The red area indicates instability of the DFE, the blue area stability.

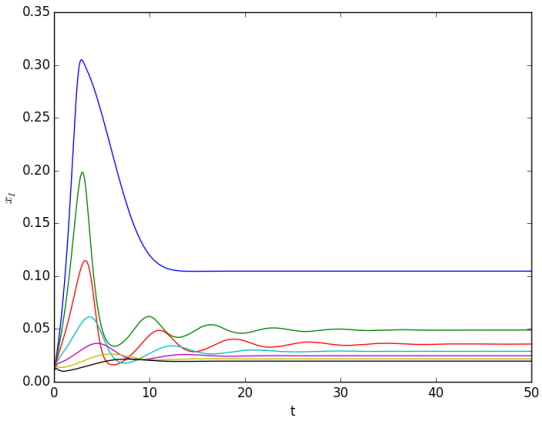

Fig. 3.9 Trajectories of x_I for different initial values of x_R, with $\epsilon = \mu = 0.1, k = 5$, $\beta = \gamma = 0.5$, $P_S = P_I = 0.5$ and $0.15 \leq x_R(0) \leq 0.7$. The higher the initial value of x_R, the lower the equilibrium value of x_I.

3.8 Numerical Analysis

Given it is not possible to find analytical solutions for the Endemic Equilibrium [EE] we proceed to analyze the system numerically in dependence of the initial conditions and parameters. Where it is not otherwise specified, the benchmark values are $\beta = 0.5 = \gamma$, $\mu = \epsilon = h = 0.1$, $P_S = P_I = 0.5$ and $P_{NS} = 0$. Initial infection level is assumed at $x_I(0) = 0.01$ and surveillance is relatively high at $x_R(0) = 0.2$. A general *caveat* is that being all the variables between 0 and 1 we need to be careful not to choose parameters in a way that make the equations stiff. High values of both ϵ and μ at the same time cause rapid variation in small time steps that may lead to stiffness. Choosing (at least one of) these values in the low range solves the issue. Homophily also can cause stiffness if $h > 0.2$. We see that depending on parameters and initial conditions there are a Low Infection EE [LEE] and a High Infection EE [HEE]. The EE varies little and appears to be consistently below 0.1 in most of the parameter space, while HEE shows more variability depending on parameters, from above the LEE to a maximum level of $x_I^* = 1 - x_R$.

Population initial conditions: Initial conditions have a relatively low impact on the equilibrium level x_I^* given the parameters. The initial level of surveillance $x_R(0)$ is the variable that has a larger impact on the EE, as can be seen in (3.9), and not surprisingly higher initial levels of surveillance (provided surveillance is sufficiently effective, that is γ is not too low) corresponds to lower level of infection in equilibrium. This is true under the above parameter specification as long as the initial value of x_R is not less than 0.15, otherwise the fraction of infected explodes. Extreme cases of high γ and low β reduce the minimum

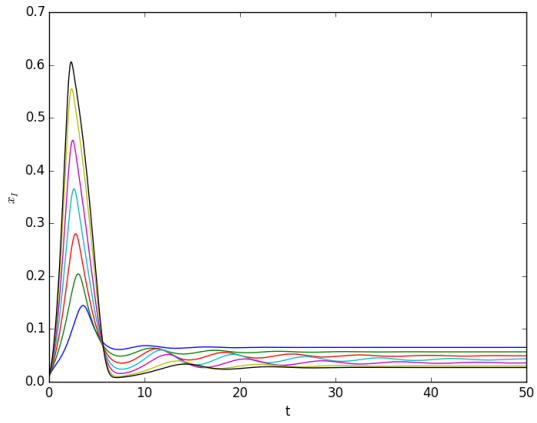

Fig. 3.10 Trajectories of x_I for different initial values of x_S, with $\epsilon = \mu = 0.1, k = 5$ $\beta = \gamma = 0.5$, $P_S = P_I = 0.5$. The lower the initial value of x_S, the higher the equilibrium value of x_I.

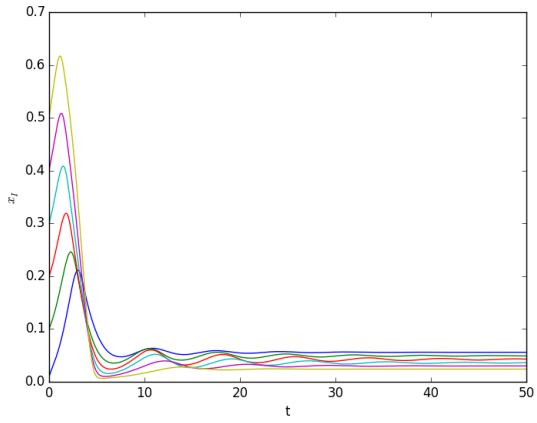

Fig. 3.11 Trajectories of x_I for different initial values of x_I, with $\epsilon = \mu = 0.1, k = 5$ $\beta = \gamma = 0.5$, $P_S = P_I = 0.5$. The lower the initial value of x_I, the higher the equilibrium value of x_I.

level of necessary surveillance. Unrealistic level of extremely high surveillance bring to the immediate extinction of the infection.

This is relatively trivial, while the dependency of x_I^* on the initial fraction of susceptible and infected nodes respectively is less intuitive, as x_I^* shows an inverse relation with both $x_I(0)$ and $x_S(0)$. As can be seen in figure (3.10) and (3.11) there is a clear relation between the peak that x_I reaches in the initial phase of the dynamics and the equilibrium level: the higher the peak the lower the equilibrium level. In (3.10) it is the higher fraction of susceptibles that drives the boost in the fraction of infected up to the point in which almost all susceptibles are infected while in (3.11) there is a constant shift upwards corresponding to the increment of $x_I(0)$, until almost all the susceptibles are infected. Once the population is almost entirely made of I and R-nodes then x_I falls quite rapidly towards the low level equilibrium. A tentative explanation can be the effectiveness of the surveillance that is represented by a higher value of γ: half of the time an I-node interacts with some R neighbour it is successfully removed, and even if the infection rate per contact is exactly the same (which is what boosts the infections initially), the removal stops the possibility of other infections.

State of arriving nodes: When $P_I > 0$ there is no DFE, as $\dot{x}_I \neq 0$. Let us consider two cases, namely when NS-nodes arrival rate is always zero and the case in which all arrival rates (but that of R-nodes) are positive. When $P_I > 0$, $P_S > 0$ and $P_{NS} = 0$ there exists an equilibrium where a small fraction of the population is infected. In what follows the parameters are set at $\beta = \gamma = 0.5$, $\epsilon = \mu = 0.1$. While μ and ϵ have a negligible and very marginal impact respectively on trajectories of x_I, setting β and γ can change the picture completely, as we will see later. Assume also that the arrival rates are the same for both S and I-nodes. This holds as long as γ is high enough. So with $P_S = P_I$ and β and γ are in the low infection equilibrium is always below $x_I^* = 0.1$, and there is no limit cycle, by changing the arrival rates we can, in some case, have oscillations around a low equilibrium level of x_I. When $P_I \leq P_S \leq 2P_I$, x_I shows damped oscillation towards the low level equilibrium. If the arrival rate of susceptible nodes is more than twice that of the infected nodes, $P_S > 2P_I$, provided $\gamma \geq 0.2$ then the trajectory of x_I^* oscillates around the low level equilibrium, with oscillations amplitude that is increasing in the difference $P_S - 2P_I$.

The picture changes if the arrival rates of susceptible, infected and non susceptible nodes are all non zero. (3.13) gives an example of the dependency of x_I^* on the arrival rates in the case $x_I(0) = 0.01$, $x_R(0) = 0.2$,$x_S(0) = 0.3$, but numerical analysis show that this behaviour is quite regular across different initial conditions given we keep the other parameters constant. The colors represents the position on the (P_I, P_S, P_{NS}) unitary simplex: green stands for $P_{NS} = 1$, red for $P_S = 1$, blue for $P_{NS} = 1$. Figure (3.13b) shows

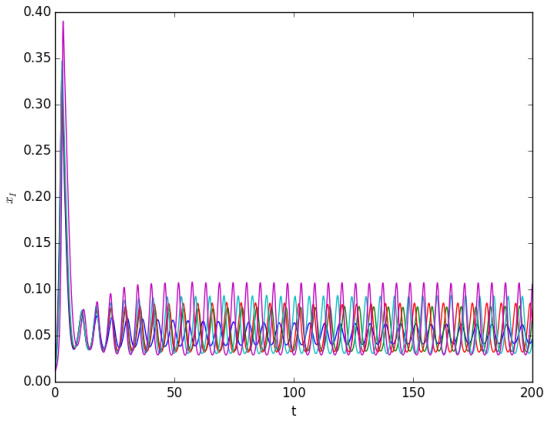

Fig. 3.12 Whenever $P_S > 2P_I$ the population of infected oscillates in the proximity of the low disease equilibrium. Trajectories here have all initial values of $x_I = 0.01, x_S = 0.3, x_R = 0.2$ While P_S and P_I change. The amplitude of the oscillation increases with $P_S - P_I$.

that when $P_{NS} = 1$ not surprisingly $x_I^* = 0$, and when $P_{NS} = 0$ or $P_S = 0$ or P_I=0, namely the faces of the simplex, the equilibrium is the low level. Notice also that when $P_{NS} = 0$ and $P_S > 0.6$ there are only few equilibria (we are in the parameter space where x_I keeps oscillating around the low level equilibrium). Quite interestingly most of the internal surface of the simplex, that is points where all the three arrival rates are positive, are mapped to the vertical triangle in (3.13b): there is a continuous map between the inside surface area of the simplex and x_I^*, with x_I^* increasing as P_{NS} decreases, and reaching its max where P_S is close to 1.

Infection rate and surveillance effectiveness: Whenever γ is less than 0.2, irrespective of the infection rate there is a drastic change in the dynamics and all but R-nodes become infected, as can be seen in (3.14b). Clearly when $0.2 \leq \gamma \leq 1$ the equilibrium level of x_I changes little with β, and as long as $\beta >> 0$, x_I^* is consistently less than 0.1, increasing with γ and decreasing with β. When the infection rate β is very close to zero x_I^* is just below 0.4 and when $\beta = 0$, it jumps close to 0.7. When $\gamma < 0.2$ then the equlibrium values of x_I^* increase around the point where are all infected but the repressor (around 0.8 in this case). Notice that while the low equilibrium increases with β, the high equilibrium decreases with β, showing a relation similar to that in (3.10),(3.11). In case the fraction of repressor is very low, then γ makes little difference, and the equilibrium level of x_I^* is continuously increasing with β, as shown in 3.14a, where $x_R(0) = 0.01$.

Frequency of arrivals Provided $P_{NS} = 0$ the infected fraction of the population in equilibrium is increasing with μ, as can be seen in (3.15a), where $\mu \in (0, 0.4)$. For higher values of μ at $\epsilon = 0.1$ equations become stiff. It is reasonabe to assume low arrival rates.

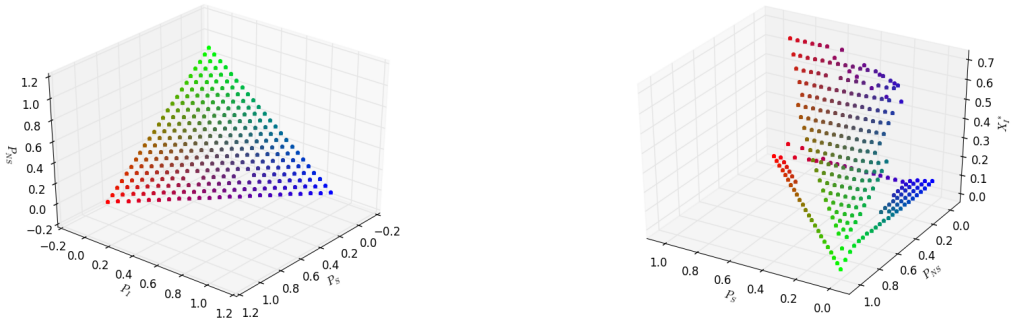

(a) (b)

Fig. 3.13 Dependency of x_I^* as the arrival rates change. In the equilibria in figure (b) initial conditions were $x_R(0) = 0.01$, $x_S(0) = 0.3$, $x_R = 0.2$. Figure (a) maps the point in the (P_S, P_I, P_{NS}) unitary simplex to colors.

Connectivity Changing average connectivity κ has a relatively significant impact on x_I^* for very low values ($\kappa < 10$) and no effect after $\kappa \geq 20$. It is somehow counterintuitive that for low connectivity level the equilibrium level of infection is higher, and for very high connectivity x_I^* it's practically zero (3.15b).

Homophily Homophily has a small negative impact when ranges in the acceptable values that prevent the equations to become stiff (3.16a). This is intuitive as if new I-nodes create more links with other I-nodes and S-nodes with other S-nodes then I-nodes have less chances to spread the infection. Interestingly for very low spontaneous exit rate ϵ and homophily $h > 0.1$ x_I shows cyclic behaviour, with amplitude of the oscillations increasing in h. The explanation is that at very low spontaneous exit rate both infection and removal acts mainly through neighbourhood relations, and because of homophily some segregation among groups emerges: if one of the nodes in an "island" of susceptible nodes is infected then most of the group will become infected, and this boosts x_I. As the fraction of I-nodes increased, the likelihood of interaction with R-nodes is higher hence removal rate is higher, and this brings x_I down again, but at the same time it brings also the removal rate down, hence x_I can increase again because of new infections.

Spontaneous exit Higher ϵ corresponds to lower x_I^* (3.16b).

Dependency of equilibria on parameters is summarized in table (3.8).

Equilibrium	Parameter Space	Value
LEE	$\gamma > \gamma_{min}$ $\beta > \beta_{min}$ $P_{NS} = 0$ or $\{P_{NS} < P^{NS}_{min}$ & $P_S < P^{S}_{min}\}$	$0 < x^*_I < 0.15$ Increasing with μ, β, P_S Decreasing with ϵ, γ and weakly with κ
HEE	$\gamma \leq \gamma_{min}$ $\beta \leq \beta_{min}$ $P_{NS} > P^{NS}_{min}$ or $\{P_{NS} < P^{NS}_{min}$ & $P_S > P^{S}_{min}\}$	$x_I(LEE) < x^*_I < 1 - x_R$ Increasing with μ, β, P_S Decreasing with ϵ, γ and weakly with κ
DFE	iff $P_I = 0$	$x^*_I = 0$, $x^*_R = 0$ $x^*_{NS} = P_{NS}$, $x^*_S = P_S$

Table 3.1 Summary of parameters effect on the infection level at equilibrium.

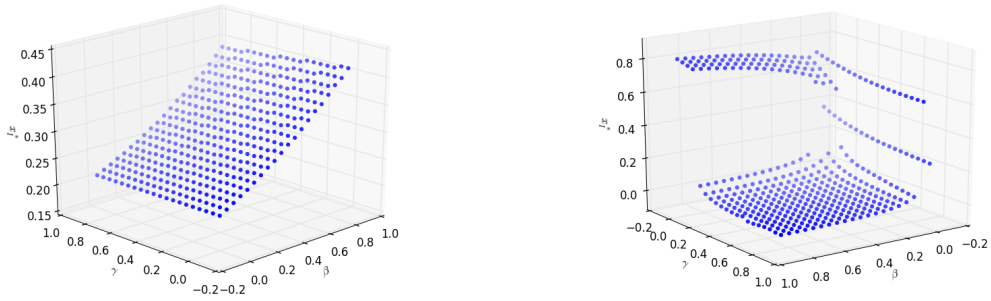

(a) (b)

Fig. 3.14 Change of x^*_I as λ and β change for (a) $x_R(0) = 0.01$, (b) $x_R(0) = 0.1$

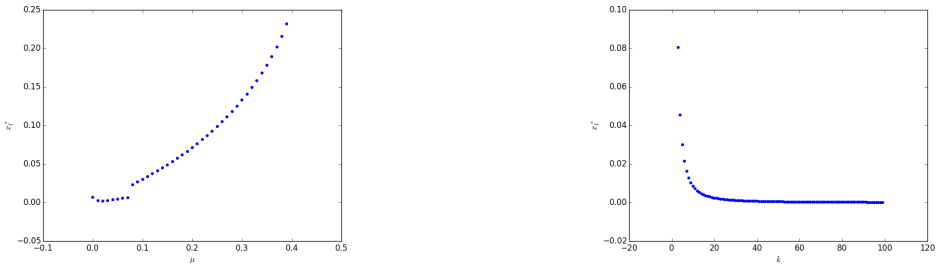

(a) (b)

Fig. 3.15 Impact of node arrival rate (a) and average connectivity (b) on x^*_I. With high κ x^*_I approaches zero, but never touches it if $P_I > 0$.

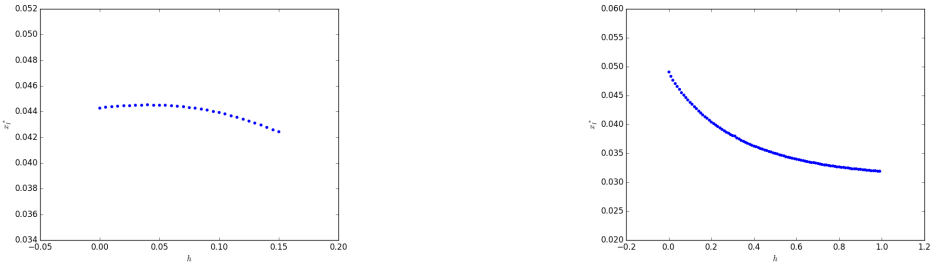

(a) (b)

Fig. 3.16 Dependency of x_I^* on homphily (a) and spontaneous exit rate (b)

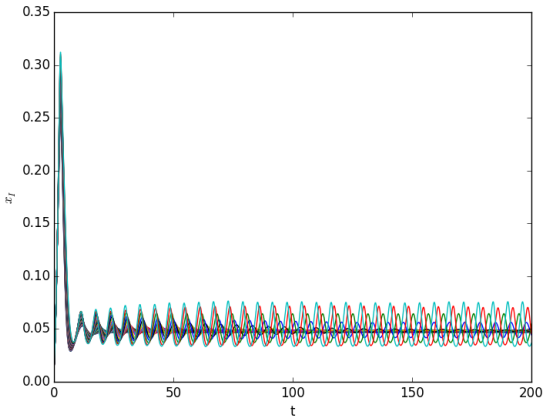

Fig. 3.17 Diverging oscillations caused by low ϵ and high homophily (b)

3.9 Best Response Maps

In this section we suggest how a social planner may elaborate a strategy to minimize or eliminate the infection, based on the results of the models presented. We assume that the social planner can choose the surveillance level and can influence the spontaneous exit ϵ. We do not model how ϵ can be influenced, as this would require a theory of the process examined (the motivations for which terrorists leave the organization are likely to be different from those who leave a political party), and here we are not trying to understand why it happens but at most how it happens. Reasonably ϵ is function of the incentives to leave (an amnesty for all the terrorists) and, possibly of the socio-economic opportunities individuals have: social and economic inequality, as well as fractionalization are likely to incerase the level of conflict, as elegantly explained in [33] who show that the equilibrium level of conflict in a society can be given by a linear function of inequality, group fractionalization and polarization.

As regards surveillance, there would be an obvious cost in recruiting and training the personnel that the social planner needs to consider, but even more, if surveillance is performed by a police force, there is another aspect to take in consideration: the ideological conflict has its *raison d'être* in some discontent with the status quo, and increasing surveillance is very likely to increase this discontent undermining power legitimacy. In his model of civil violence [30] model *this trade-off* with a "grievance" function, simply given by the product of a measure of social or economic privation and the perceived illegitimacy of the leading authority. Here we simply model this by making the fraction of Susceptible individuals in the population an increasing function of the surveillance level: the fraction of unsatisfied people depends on an exogenous variable α and of the amount of surveillance chosen by the social planner x_R. α is the minimum level of dissatisfaction, that here we assume fixed in the short term and not under control of the social planner, while the maximum level of dissatisfaction is reached when there are no more non susceptible individuals in the population (assuming that those encharged of surveillance are always loyal). Consider the modified generalized logistic function $\mathscr{L}$:

$$\mathscr{L}(x_R) = \alpha + \frac{x_{NS} - x_R}{(1 + Qe^{-b\gamma x_R})^{\frac{1}{v}}} \text{ for } x_R \in (0, R^{\text{MAX}}) \tag{3.31}$$

The above function, illustrated in (3.9) starts at α when $x_R = 0$, then increases with x_R and reaches a maximum at the positive root of $ve^{bx} + Q(bx + v - bx_{NS}) = 0$, then decreases. In (3.9) parameters are chosen so that when $x_R \in (0,1)$, $\mathscr{L} \in (0,1)$. The function can be interpreted this way: if the social planner decides to increase surveiillance x_R, she will recruit her agents among the non susceptible individuals, thus leading to a decrease in

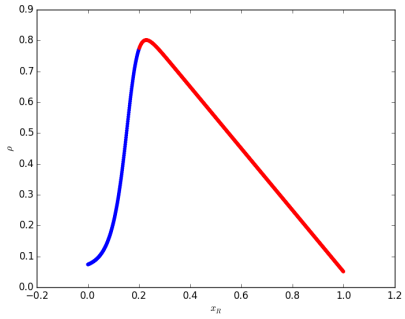

Fig. 3.18 Modified logistic for $x_R \in (0,1)$, $b\gamma = 50$, $Q = 4 \cdot 10^3$, $\upsilon = 2$. In blue the values on the interval $x_R \in (0, R^{)}$

x_{NS} (this explains the numerator of the second term of (3.31). Moreover, the increase in surveillance will cause a loss in legitimacy of the social planner, leading to a further decrease in x_{NS} and a corresponding increase in susceptible individuals. The increase in x_S above the already existent level α is given by the second term of (3.31). For our application the only meaningful interval is $x_R \in (0, R^{\text{MAX}})$, where R^{MAX} is the level of x_R such that $x_{NS} = 0$. A further increase in x_R leads to negative x_{NS} which makes no sense. Notice that R^{MAX} is located before the maximum of the function (see 3.9).

We are going to use the above function to model the initial fraction of susceptible nodes in order to build a Best Response map for the social planner.

The best case scenario for the social planner is the complete absence of infection in the population, hence her first best would be to ensure that the DFE remains stable, that is to say that $\mathscr{R}_0 < 1$. In the case of the non spatial model $\mathscr{R}_0$ (3.2) depends on ϵ, x_R, γ and ρ so the social planner would just choose x_R and γ and provide incentives to determine ϵ such that $\mathscr{R}_0 < 1$. Assuming that $\rho = \mathscr{L}(x_R) + x_I(0)$, and fixing the inital fraction of infected at $x_I(0) = 0.01$ and $\gamma = 0.5$, figure (3.19) shows an example of a Best Response map in the non spatial case. (3.19) shows that when ϵ is low, the DFE is unstable for low levels of surveillance. At the levels of x_R necessary for stability, (3.19a) shows that the unsatisfaction in the population is very high, that is the population at DFE is made mostly of R and S individuals.

In the adaptive mode case $\mathscr{R}_0$ is given by (3.30), assuming the social planner can observe the β, P_S, μ and k and just act on ϵ to make the DFE stable. It is also reasonable that the social planner have some control on the borders, so that the arrival rate of susceptible can be determined, even if with some error. Controlling the borders requires personnel, so we could also model the arrival rate of susceptibles as a function decreasing in x_R,

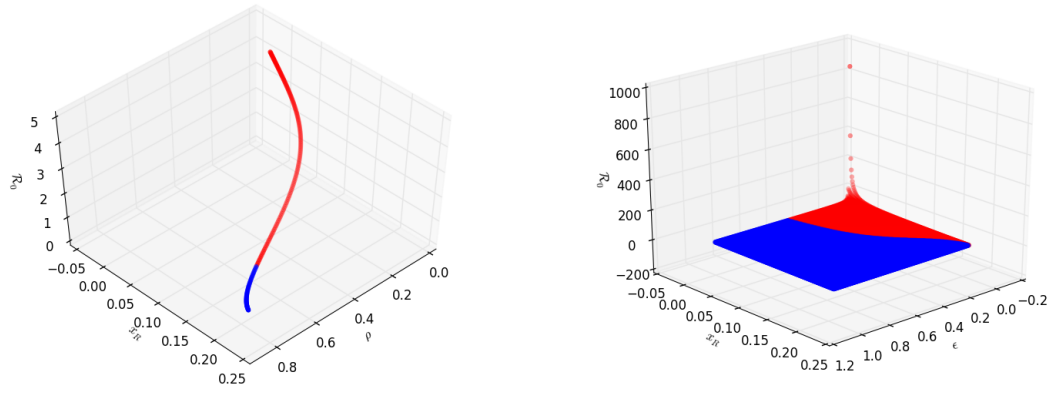

(a) (b)

Fig. 3.19 Best Response map (fully-mixed) when $\gamma = \beta = 0.5$: red corresponds to instability of DFE, blue to stability. (a) depicts how x_R choice impact on ρ, given $\epsilon = 0.1$, (b) shows the best response map when also ϵ can vary.

$P_S = f(x_R)$ with $\frac{\partial f}{x_R} < 0$, so that the social planner can choose the desired combination of x_R and ϵ.

In case the social planner cannot guarantee $P_I = 0$, then the DFE equilibrium does not exist, and the next best alternative is the LEE, and possibly the minimum LEE. A best response map can then be constructed having some information on the initial condition and the parameters. Assuming that $x_S(0) = \mathscr{L}(x_R)$, and using the usual set of parameter values (3.20b) shows in blue the combination of x_R and ϵ that guarantees the LEE.

3.10 Conclusions

In this paper a recruitment model with surveillance has been studied, using the framework of epidemiological compartmental models. Under each model thresholds conditions are derived, determining the parameter space where a susceptible population is resistent to the invasion of a new ideology. The paper shows how considering the population topology changes the thresholds and the behaviour of the dynamics. It has been found that in the fully-mixed population the threshold depends directly on the magnitude of surveillance, while when the population interactions are constrained by a graph, that is both in the static network and in the adaptive network, the threshold does not depend on surveillance. While in both the static and the adaptive network increasing average connectivity makes invasion of the new ideology easier, in the adaptive network case high connectivity levels can be sustained with low infection rates or low S-nodes arrival rate. The main differences

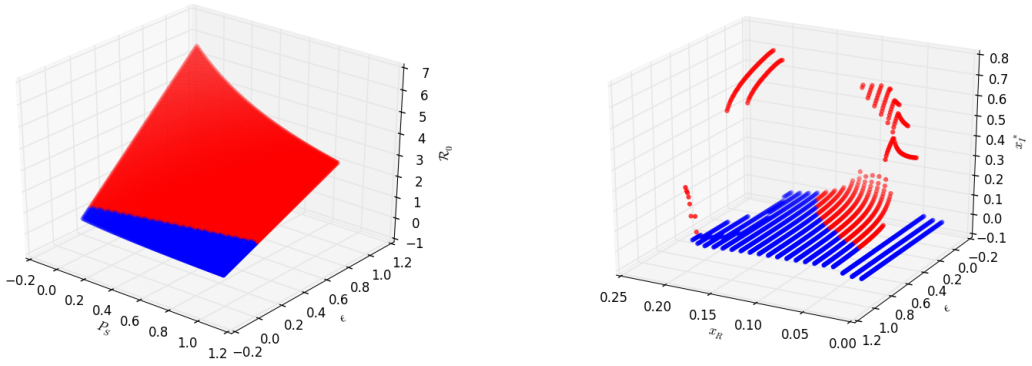

(a) (b)

Fig. 3.20 Best Response map (adaptive) for the DFE (a) at $\mu = 0.1 = \epsilon$, $\beta = 0.5$, $k = 10$ and for the LEE (b). Blue indicates BR.

between the static and adaptive network are that the dynamic graph threshold is less sensitive to the spontaneous exit rate ϵ, and that increasing the graph dimension *ceteris paribus* improves stability of the DFE. The adaptive network model shows two types of EE. In one equilibrium the invading ideology groupsurvive but it is very small, and survives only because it is to small to be detected and eliminated. If conditions are favorable the invading ideology can also take over the entire population, or survive in equilibrium at a consistently high level: depending on parameters there is a continuum of equilibria where the invading group can constitute any fraction of the population above 0.1. The adaptive network dynamics may also generate cycles around the equilibria in the appropriate range of arrival rates and level of homophily. The paper finally suggest how to use the results of the models to develop a response strategy of a social planner who wants to prevent the invasion of the new ideology or, whenever this is not possible, to minimize the invading ideology group. The model constitutes a basic framework, and many different aspects can subject of further studies. A promising research line regards the introduction of strategic behaviour of agent both regarding the actions of recruitment and surveillance and the way individuals remove or add new links, as well as adding further heterogeneity in nodes, for example allowing for different values of β. It would also be interesting to link the facility with which a new ideology can conquer new susceptibles with some inequality measure at a society level.

Chapter 4

Edgeworth Process on Networks

This paper is a joint work with my supervisor, Prof. Paolo Pin

Abstract

We define a class of pure exchange Edgeworth trading processes that under minimal assumptions converges to a stable set in the space of allocations, and characterize the Pareto set of these processes. Choosing a specific process belonging to this class, that we define fair trading, we analyze the trade dynamic between agents located on a weighted networks. We determine the conditions under which there always exists a one-to-one map between the set of networks and the set of stable equilibria. This result is used to understand which is the effect of the network topology on the trade dynamics and on the final allocation for the case of Cobb-Douglas utility function. We find that the position in the network affects the distribution of the utility gain given the initial allocations.

4.1 Introduction

One of the essential subjects of economics is analyzing prices and allocations in markets. The centrality of the subject has been clear since the first attempt to produce rigorous mathematical modeling of the functioning of a market. Nonetheless the most diffused approach in mathematical economics, namely general equilibrium theory, lasts on the fundamental assumption that individuals have no market power, hence take prices as given, *de facto* ruling out any significative analysis of prices. In the walrasian competitive equilibrium all trading in decentralized exchange takes place at the final equilibirum prices, while in real world agents discover equilibrium prices only by making mutually advantageous transaction at disequilibrium prices Foley [39]. Most of the equilibrium models are hence lacking a proper out-of-equilibrium analysis, where the assumption of perfect competition prevents agents from actually change prices. In order to circumvent the impasse given by the impossibility of a real price dynamics, the fictitious figure of the "auctioneer" had to be introduced. Models with the auctioneer are usually called *tâtonnement* models, which suffer from important lack of reality where agents constantly recontract instead of trading and so only prices are changing out of equilibrium while quantities are fixed Fisher [38]. Despite the diffusion of equilibrium models, economists

have been aware of their limitations since many years, for a recent critical review see Petri and F. Hahn [93]. Several alternatives have been proposed: in the early sixties there was an important effort in modeling out-of-equilibrium dynamics, even if in a simple and still non realistic way, while still guaranteeing existence and stability of the equilibrium. These models are called *non-tâtonnement* processes, or trading processes. Uzawa [122], Hahn [46] introduced the so called "Edegworth process" where they gave an explicit treatment of out-of-equilibrium trade. By allowing both prices and quantities to adjust out of equilibrium a fundamental difference emerges with previous walrasian models: equilibrium is path-dependent, and out of equilibrium dynamics change the equilibrium set, while in a walrasian process equilibrium is determined solely by the initial holdings, independently of the path of the process. Edgeworth processes rest on one fundamental, reasonable assumption: trade takes place if and only if there is an increase in utility by trading. Hahn [46] assumes that agents needs non-zero endowments of each good, and trade only if there is at least one individual who gains and no individual who loses. Under the assumption of strictly concave utility function Hahn proves that the pure exchange mechanism is approaching in the limit a Pareto optimum. Uzawa [122] formulates a more general Edgeworth's barter process, where individual transacts at each stage under the restriction that total quantities of each good stay constant in the economy and a transaction happens if and only if at least one part becomes better off. Uzawa proves that this process always converges to a Pareto-Optimum. Fisher [38] while recognizing that Edgeworth process is able to capture, even if to a limited extent, price adjustment, raises two main critiques regarding the assumption of utility-increasing trades at each step. First, as all parties need to gain something in order to have trade, it can be the case that only very big coalition can have mutually advantageous trade, hence the presence of coalition formation costs may prevent trade from actually happening. The second critique regards the impossibility of Pareto-increasing trades of taking account of the behaviour of arbitraging agents who try to take advantage from the opportunities arising in disequilibrium. The first critique was addressed by Madden [69], who proves that there is always an Edgeworth exchange for some pair of agents if there is an Edgeworth exchange at all. The second critique is potentially more cogent, and it is necessary to be more cautious, still it appears there would be nothing to prevent from considering expectations of future gains as part of the utility function, hence allowing for Pareto-improving speculative trade as well. Fisher [37] develops a more sophisticated model without auctioneer, where money is assumed to be just a medium of exchange, and agents have two roles at the same time: they act as "dealers" in one commodity, setting its the price and then waiting for others to come and make exchanges. For the remaining

commodities agents are then customers, who search among the dealers to find those with better price. The dealers propose their price, and eventually adjust the price after the search. The dealers in choosing their own price think *as if* they are in equilibrium, so there is a question if this is actually modeling price adjustment out of equilibrium. Another relevant work in this litterature is Hurwicz et al. [52, 53] who construct an iterative decentralized process in environments free of externalities. It is a stochastic model, where every trade leading to a Pareto superior allocation has a positive probability of being picked, whilst the individual particular trades are of measure zero if the set of trades is continuous. Participants pick a trade, according to a probability distribution, among those not inferior to their current endowment. Their set of feasible trade is then given by this probabilistically selected bid and the intersection between all the other trades which are not inferior to her current endowment and a cube centered on the bid. Compatible bids, so potential trades, are the points in the interesection of two participants' such cubes. Here randomization plays a role, as the referees chooses a random point in this intersection. This process converges stochastically to a Pareto Optimum and it is usually more stable than *tâtonnement* processes. Notice that this bidding process has some of the characteristics of *non-tâtonnement* processes, as trade is utility increasing and actually take places during the process. At the same time trade happens only when demand and supply are in balance thanks to the intervention of a fictious referee, which resembles the walrasian auctioneer. Among other stochastic models it is also worth mentioning Gintis [42], who studies out-of-equilibrium price and quantity adjustment process for a decentralized market economy with production, where the economy is modeled as a Markov process, and stability is found under certain conditions.

If the assumption of agents having no market power is removed, then it is then necessary to model how agents agree on the division of the gains from their transaction, and hence how prices emerge. The two main approaches to the theory of bargaining, namely the non-cooperative and the cooperative approach, originate from the same person: John Nash. Nash [76] proposed a theory of axiomatic bargaining having a unique solution for the situation in which two agents have access to a set of alternatives on which they have different preferences. If they are not able to agree on any of the alternative they will receive what is the established disagreement point in the feasible set. This paper inspired the cooperative game theory approach to bargaining, with the proposals of several different solutions. The second paper Nash [77] inspired an important number of successive contributions aimed at establishing non-cooperative foundations of competititive equilibrium. Just to mention few of the many relevant works Rubinstein [99], Rubinstein and Wolinsky [100], Gale [41],Sabourian [103]. As Thomson [118] points out, while the (cooperative)

Nash solution has possibly been the most successfull, other two solution concepts have received also considerable attention by the economist: the egalitarian solution and the Kalai-Smorodinsky solution. Kalai [59] propose a solution which, once established a vector of weights for individual utilities, selects the maximal point in the feasible set where utility gains from the disagreement point are proportional to these weights. The egalitarian solution is a particular case of this, where the weights are equal. The solution proposed by Kalai and Smorodinsky [60] chooses the maximal point of the feasible set which is proportional to the profile of maximal payoffs that agents can separately reach among the feasible points that dominate the disagreement point. This can be intended as a normalized version of the egalitarian solution Thomson [118]. Both alternative solutions satisfy weak Pareto-optimality.

This paper has some continuity with the cited literature as we adopt a version of the Edgeworth barter process, and we define a class of trading processes that under a limited number of assumptions converge to an equilibrium. In our model we do not have prices explicitly, but prices are the rate of exchange between goods, and they can change at any moment along the process, as you would expect in a real trade. Also there is no gravitation towards equilibrium prices because equilibria are path-dependent. In the family of the trading processes that satisfy our assumption we restrict the attention on a very specific form of trade, and we adopt the egalitarian solution as the rule according to which agents share utility gains when they trade. There are evidences in many real word bargaining practices where the agents divide the "fixed pie" equally, in particular in the practice of sharecropping where despite the parties involved very often have different bargaining power, nonetheless the fifty-fifty rule is dominant in many social groups. Young [127] gives an evolutionary foundation of such a rule in a contest without common knowledge and without learning, where agents choices are based only on the precedent choices of other agents. The process is characterized by a positive feedback that can eventually reach stability on a fixed division rule. The choice of a specific trading rules is without loss of generality, as our results are true under more general assumptions, as it will be clear in the rest of the paper.

Our paper is very close to Cowan and Jonard [24], who model knowledge diffusion as a barter process in which agents exchange different types of knowledge. Agents meet their neighbours repeatedly and in case there is room for trade, that is there is a differential in two dimensions of knowledge, they trade, each receiving a constant share of the knowledge differential. At the end of the trade both parties have an increased utility, as utility increases with knowledge levels. They show that diffusion of knowledge is maximized where the

proportion of links between an agent and other agents not in his neighbourhood is between 1 and 10 percent of all direct links between agent pairs.

The main contribution of this paper is to fill a gap in the literature on trade, that is providing a dynamical model of trade on a network. There are many reasons why we want to consider the network structure of the agents, starting with the fact that real trades are shaped and influenced by the structure of relationship between agents: not everybody can interact with everybody else due to geography, social relationships, technological compatibility. Quoting Fisher: "disequilibrium considerations have something to do with the institutional structure of transactions and the way in which markets are organized". We are interested in modeling an economy where the individual market power matters, and clearly market power also crucially depends on the position in the network. The local nature of many markets and their dependence on the global structure is another characteristics of real markets that can be analysed with a network formulation, and there are many interesting questions that can be analysed in this contests, that are subject of a very active area of research in economics. For an exhaustive review of these contributions see Manea [70]. Our paper differs from all these models as we do not model strategic interaction among agents, and in this sense our model is extremely simplificative, but we are able of characterizing the dynamics on a network with a treatable and relatively simple convergent dynamical systems, providing a novel contribution to the literature. Moreover we prove a version of the Second Welfare Theorem for networks, contributing to the analysis of the effect of the network structure on final allocations and the distribution of welfare.

The paper is structured as follows: in the first section we define our family of bilateral trading processes, and we provide a characterization of the Pareto set to which these processes converge. We then choose a specific trading rules, namely the egalitarian rule, proving that the trade so defined belong to the family of trades of our interest. In the second section we extend trading to more agents, and we introduce the network structure as a weighted network. In the third and last section we analyze the Cobb-Douglas case, and we construct the set of equilibria for this specific case, giving some examples of the effect of the topology on the final allocation.

4.2 The model

4.2.1 Pure Exchange

There are $n \geq 2$ agents, and we will generally refer to an agent $i \in \{1,\dots,n\} \equiv N$, and $m \geq 2$ goods, and we will generally refer to a good $k \in \{1,\dots,m\} \equiv M$. Agents can only have non-negative quantities of each good, and we are considering a pure exchange economy with no production, so that the total resources in the economy are fixed and given by the sum of the agents' endowments. The endowment of agent i is a point in the positive ortant of $\mathbb{R}^m$, call this space $P = \{x \in \mathbb{R}^m_+\}$ where the $k-$th coordinate represents the quantity of good k. Assume time is continuous and goods are infinitely divisible, and let $x_{ik,t}$ be the endowment of agent i at time t for good k. In this way $\vec{x}_{i,t} \in \mathbb{R}^m$ is the m–dimensional vector of agent i's endowment, while $\vec{x}_{k,t} \in \mathbb{R}^n$ is the n–dimensional vector of all agents' endowments of good k. As we assumed there is no production, nor can the goods be disposed of, the sum of the elements of each such vector $\vec{x}_{k,t}$ is constant in time. The initial allocations of the economy are then represented by the n vectors of agents' endowment at time zero, call them $\{\vec{x}_{1,0},\dots,\vec{x}_{n,0}\}$. All agents' allocations at a given point in time can then be represented by an $(m \times n)$ matrix with all non-negative entries, call it $\mathbf{X}_t$. In the following we may not express the time variable t, when it does not create ambiguity. Hence an unrestricted state of the economy at any time t is a point in the positive orthant of an $\mathbb{R}^{mn}$ space, given by the Cartesian product P^n . As we assumed that resources are fixed in the economy at a point $w \in \mathbb{R}^m$ (where the k-th coordinate is the total quantity of good k in the economy), the state space of our interest is a subset of P^n, call it $W = \{x \in P^n : \sum x_i = w\}$, which is an open subset of an affine subspace with compact closure in $(\mathbb{R}^m)^n$ Smale [114].

Any agent i is characterized by a differentiable, strictly increasing utility function U_i from $\mathbb{R}^m$ to $\mathbb{R}$. It is also assumed that preferences are strictly convex. Given $x_t \in W$, a point in the space of the economy at some point in time t, call $\vec{U}(x_t)$ its corresponding n–dimensional vector of utilities. We call $\mu_{ik,t} \equiv \partial U_i(\vec{x}_{i,t})/\partial k$ the marginal utility of agent i, with endowment $\vec{x}_{i,t}$, with respect to good k. Define as $\mu_{i,t}$ the gradient of the utility function for agent i at time t, that is the vector of all her marginal utilities. All the gradients can be aggregated in a $m \times n$ matrix of all the marginal utilites at a given point in time, call it $\mathbf{M}_t$. The vector of strictly positive marginal utilities $\vec{\mu}_{i,t}$, is proportional to any vector of marginal rates of substitutions with respect to any good $\ell \in \{1,\dots,m\}$.

To give the geometrical intuition of the space of the economy, notice that it is the surface of an (m)-dimensional convex polytope with 2^m vertices (ie an hyperrectangle) or alternatively a point on one of its $(m-1)$-dimensional facets. Notice also that we can define a geometrical multidimensional version of the Edgeworth box. Consider that given

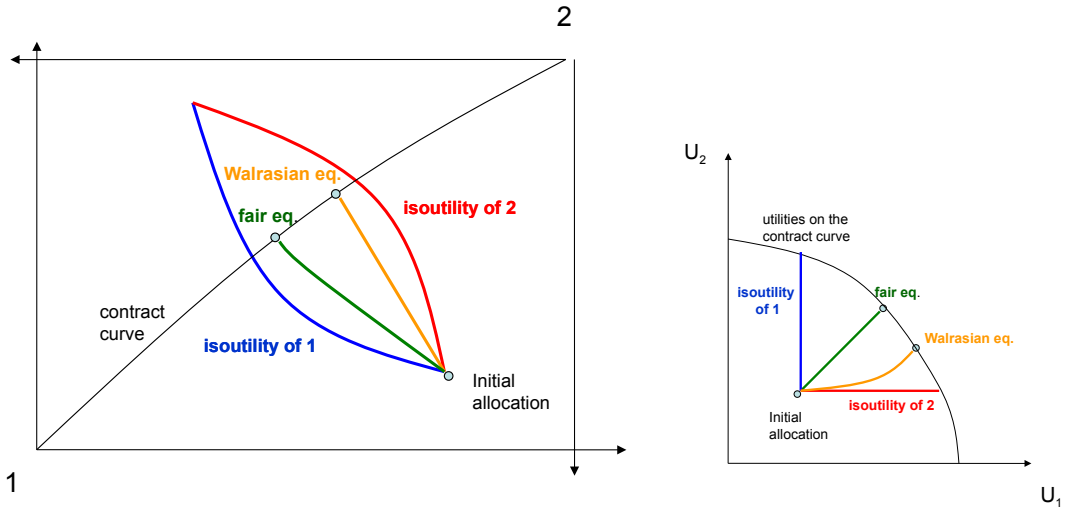

Fig. 4.1 Example of the difference between a Walrasian equilibrium and a fair equilibrium in the Edgeworth box and in the space of utilities.

the total quantity of good k, call it $\bar{k}$, every possible allocations of this among the n agents is a point in the convex hull $\Gamma = \{\theta_0\bar{k} + \cdots + \theta n\bar{k} | \theta_i \geq 0, i \in (0,n), \sum_i \theta_i = 1\}$, that is to say a point in the $(n-1)$ regular simplex with edge lenght $\bar{k}$. The same holds for each of the m goods (with possibly different $\bar{k}$ of course). Notice also that the traditional Edgeworth box is nothing but the Cartesian product of two 1-simplices (that is to say of two segments of a line), as can be seen in figure. Recall that a Cartesian product of simplices is called a simplotope, and denote as Δ^n an n-dimensional simplex,

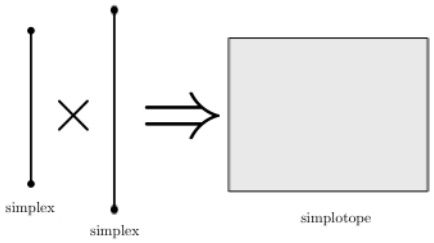

Fig. 4.2 Modified from Shoham and Leyton-Brown [112], shows the Cartesian product of two 1-simplices. Notice the analogy with the Edgeworth Box.

Definition 3 *The multi-dimensional equivalent of the Edgeworth Box for a pure exchange economy with n agents and m goods is a simplotope* $\Lambda = \prod_{j=1}^{m} \Delta_i^{(n-1)}$, *where* $\Delta_j^{(n-1)}$ *is the*

$(n-1)$ *regular simplex with edge of length equal the total quantity of good* j*. The Edgeworth Box is of dimension* $(n-1)m$*.*

In the pure exchange economy defined above, the contract curve is given by the set of all those allocation where all marginal utilities are proportional, i.e.

$$\mathscr{W} = \left\{\mathbf{X} : \forall\ i, j \in N,\ \exists k \in \mathbb{R},\ k \neq 0,\ s.t.\ \mu_i(\vec{x}_i) = k\mu_j(\vec{x}_j)\right\}\ . \tag{4.1}$$

Proposition 3 *Smale [114] If preferences are convex and monotonic then the set of Pareto Optima is homoeomorphic to a closed* $(n-1)$ *simplex.*

For a proof of [3 see Smale [114], or the appendix (C). Remember that a diffeomorphism implies an homeomorphism but not viceversa, and the assumptions in [3 are standard in economics, and are indeed minimal: no assumption on the commodity space, very few restriction on the utility. In order to obtain a diffeomorphism it is enough to assume convexity[1] of the function and of the commodity space. It is shown that if preferences are C^2 and convex it is possible to find utility representations that admit a convex space, for an exhaustive discussion and proofs see Mas-Colell [71]. Notice that in our case the assumptions of the proposition are satisfied: the state space of interest is an open subset of an affine subspace with compact closure in $\mathbb{R}^{mn}$ Smale [114]. Moreover, we also assumed preferences to be convex, so the indifference curves are convex. The convexity assumption makes the problem much easier to deal with, but in case this assumption is relaxed we can still characterize the Pareto Set, that will be a $(n-1)$ stratified set, that is a manifold with borders and corners, see Wan [124], de Melo [27].

4.2.2 Trading

Define *trading* between agents in N as a continuous dynamic over the endowments, which is based on marginal utilities. Formally it will be a set of differential equations of the form:

$$\frac{d\vec{x}_{i,t}}{dt} = f_i\left(\mathbf{M}_t\right)\ , \tag{4.2}$$

where function f_i from $\mathbb{R}^{n\times m}$ to $\mathbb{R}^m$, satisfies the following 3 properties, for any set $\mathbf{M}_t = \left(\vec{\mu}_{1,t}, \vec{\mu}_{2,t}, \ldots \vec{\mu}_{n,t}\right)$ of feasible marginal utilities:

- **Zero sum:** the sum $\sum_{i=1}^{n} \vec{f}_i$ is equal to the null vector $\vec{0}$.

[1] Note that in [11 there is the assumption of convexity of the functions. No confusion should rise as we recall that a standard convex multiobjective problem is a minimization of convex functions, viceversa a maximization of concave function

- **Trade:** if there are at least two vectors of marginal utilities, $\vec{\mu}_{i,t}$ and $\vec{\mu}_{j,t}$, which are linearly independent, then at least one between $\vec{f}_i$ and $\vec{f}_j$ is different from $\vec{0}$.
- **Positive gradient:** for any agent i it will always be the case that $\vec{\mu}_{i,t} \cdot \vec{f}_i \geq 0$, with strictly positive sign if there is trade.

The assumption of *zero sum trade* guarantees that we are in a pure exchange economy without consumption or production of new goods, as the amount of all the goods remain unchanged in any step of the process. The assumption of *trade* guarantees that there is actually trade, unless we are in a Pareto optimal allocation, where the marginal rate of substitution between any two goods would be the same for any couple of agents. Finally, the assumption of *positive gradient* guarantees that any marginal exchange represents a Pareto improvement for any agent $i \in N$. That is because

$$\begin{aligned} \frac{dU_i}{dt} &= \sum_{k=1}^{m} \frac{dU_i}{dx_{ik}} \frac{dx_{ik}}{dt} \\ &= \vec{\mu}_{i,t} \cdot f_i(\mathbf{M}_t) \geq 0 \end{aligned} \tag{4.3}$$

Generalizing Hahn [47], it is easy to show that all and only the fixed points of the dynamical system defined in (4.2), are Pareto optimal allocations. That is because the function

$$\bar{U}(\mathbf{X}_t) \equiv \sum_{i=1}^{n} U_i(\vec{x}_{i,t}) \tag{4.4}$$

can be seen as a potential. It is bounded in its dominion of all possible allocations, it strictly increases as long as there is trade (i.e. out of equilibrium), and it will be stable when there are no two agents who could both profitably exchange goods between them. At the limit $\bar{U}$ will converge for sure to a value, say $\bar{U}^*$, corresponding to an allocation $\mathbf{X}^*$. As preferences are strictly convex, there will be no trade in $\mathbf{X}^*$.

The fixed points of the above dynamical system are reached by a sequence of infinitesimally small trades from an initial state, hence the set of the solutions of the trade mechanism, call it the Stable Pareto Set, is an open subset of the Pareto Set defined above Smale [114]

Note that at this stage there is no assumptions that endowments do not become negative, that is to say we are not requiring a condition like $\frac{dx_{ik}}{dt} > 0$ as $x_{ik} \to 0$. This will depend on the initial endowment $\mathbf{X}_t$ of the agents and or their utility functions. As any marginal exchange represents a Pareto improvement for any agent $i \in N$, we will implicitely assume that any Pareto improvement starting from the initial conditions will lie in the region of non–negative endowments.

Examples that satisfies these properties are the classical Walrasian *tâtonnement* process, as well as non-*tâtonnement* processes, as can be find in Hahn [47] and Hurwicz et al. [52, 53].

4.3 *Fair trading* between two agents

There is an entire family of trading mechanisms satisfy the very general assumptions of zero sum, trade and positive gradient. The moment in which we choose a trading mechanism we are implicitly making assumptions on some bargaining rule that has been fixed by the agents participating the trade. This may seem a restiction, and to some extent it is a restriction, still we can come out with different trading mechanisms corresponding to different bargaining solutions. We define a mechanism that we call *fair trading*, that is based on the Kalai egalitarian solution Kalai [59], were we assume that when there is possibility for a Pareto improvement, agents trade if and only if they equally split the gains in utility from the trade.

Trading is bilateral, so assume for now that there are only two agents, so that $N = \{1,2\}$, and $m \geq 2$ goods. By the zero sum property we have that $\vec{f}_1 = -\vec{f}_2$. We are restricting our attention to the case where marginal utility from trading, is equally split among the two agents. The pareto improvement from trading is defined in (4.3), so we are requiring that:

$$\vec{\mu}_{1,t} \cdot f_1\left(\vec{\mu}_{1,t}, \vec{\mu}_{2,t}\right) = \vec{\mu}_{2,t} \cdot f_2\left(\vec{\mu}_{1,t}, \vec{\mu}_{2,t}\right) \ . \tag{4.5}$$

By the zero sum property this is satisfied if

$$\left(\vec{\mu}_{1,t} + \vec{\mu}_{2,t}\right) \cdot f_1\left(\vec{\mu}_{1,t}, \vec{\mu}_{2,t}\right) = 0 \ , \tag{4.6}$$

which simply means that marginal trade has to be orthogonal to the sum of marginal utilities.

There is a full sub–space of dimension $m-1$ that is orthogonal to the sum of the two marginal utilities. Here we consider a single element that lies in the sub–plane generated by $\vec{\mu}_{1,t}$ and $\vec{\mu}_{2,t}$. We assume that trade for agent 1, $\vec{f}_1$, is the orthogonal part of $\vec{\mu}_{1,t}$ with respect to $\vec{\mu}_{1,t} + \vec{\mu}_{2,t}$ (or the vector rejection of $\vec{\mu}_{1,t}$ from $\vec{\mu}_{1,t} + \vec{\mu}_{2,t}$). In formulas it is

$$f_1\left(\vec{\mu}_{1,t}, \vec{\mu}_{2,t}\right) = \vec{\mu}_{1,t} - \frac{\vec{\mu}_{1,t} \cdot \left(\vec{\mu}_{1,t} + \vec{\mu}_{2,t}\right)}{|\vec{\mu}_{1,t} + \vec{\mu}_{2,t}|^2} \left(\vec{\mu}_{1,t} + \vec{\mu}_{2,t}\right) \tag{4.7}$$

where $|\cdot|$ is the Euclidean norm in $\mathbb{R}^m$.

Proposition 4 *In a fair trading between two agents, the istantaneous trade of one agent is equal to the additive inverse of the instantaneous trade of the other agent.*

The above proposition is trivial, and it is easy to check that:

$$f_2\left(\vec{\mu}_{1,t},\vec{\mu}_{2,t}\right)=\vec{\mu}_{2,t}-\frac{\vec{\mu}_{2,t}\cdot\left(\vec{\mu}_{1,t}+\vec{\mu}_{2,t}\right)}{|\vec{\mu}_{1,t}+\vec{\mu}_{2,t}|^2}\left(\vec{\mu}_{1,t}+\vec{\mu}_{2,t}\right)=-f_1\left(\vec{\mu}_{1,t},\vec{\mu}_{2,t}\right) \tag{4.8}$$

because

$$f_1\left(\vec{\mu}_{1,t},\vec{\mu}_{2,t}\right)+f_2\left(\vec{\mu}_{1,t},\vec{\mu}_{2,t}\right)=\left(\vec{\mu}_{1,t}+\vec{\mu}_{2,t}\right)-\frac{|\vec{\mu}_{1,t}+\vec{\mu}_{2,t}|^2}{|\vec{\mu}_{1,t}+\vec{\mu}_{2,t}|^2}\left(\vec{\mu}_{1,t}+\vec{\mu}_{2,t}\right)=\vec{0} \tag{4.9}$$

Proposition 5 *The fair trading mechanism between two agents defined as in* (4.7) *satisfies zero sum, trade and positive gradient.*

It is easy to check that the fair trading specified in (4.7) satisfies the trade condition, as it is equal to $\vec{0}$ only if $\vec{\mu}_{1,t}=k\vec{\mu}_{2,t}$, for some $k\in\mathbb{R}$.

To see that it also satisfies positive gradient, note that a sufficient condition for having a non-negative change in marginal utility:

$$\vec{\mu}_{1,t}\cdot\left(\vec{\mu}_{1,t}-\frac{\vec{\mu}_{1,t}\cdot\left(\vec{\mu}_{1,t}+\vec{\mu}_{2,t}\right)}{|\vec{\mu}_{1,t}+\vec{\mu}_{2,t}|^2}\left(\vec{\mu}_{1,t}+\vec{\mu}_{2,t}\right)\right)\geq 0 \tag{4.10}$$

is that $\|\vec{\mu}_{1,t}\cdot\left(\vec{\mu}_{1,t}+\vec{\mu}_{2,t}\right)\|\leq|\vec{\mu}_{1,t}||\vec{\mu}_{1,t}+\vec{\mu}_{2,t}|$, where $\|\cdot\|$ is the classical norm in $\mathbb{R}$. But last inequality is the Cauchy–Schwarz inequality, which is always strict, being 0 if and only if $\vec{\mu}_{1,t}$ and $\vec{\mu}_{2,t}$ are linearly dependent, that is when there is no trade.

Note here that any $\alpha f_1\left(\vec{\mu}_{1,t},\vec{\mu}_{2,t}\right)$, with $\alpha>0$ would go, but we stick to the normalized case with $\alpha=1$. In general, this parameter α will represent the *speed* at which the dynamical system is moving, so there will be no loss in generality in assuming it equal to 1.

We have then proved that the fair trading mechanism is a bilateral pure exchange mechanism satisfying the required three assumptions.The two agents trade over $m\geq 2$ goods, starting from some initial allocation $\mathbf{X}_0\in\mathbb{R}^{m\times 2}$ and evolving according to the following system of differential equations in matrix form, based on (4.2) and (4.7):

$$\frac{d\mathbf{X}_t}{dt}=\left(\vec{\mu}_{1,t}-\frac{\vec{\mu}_{1,t}\cdot\left(\vec{\mu}_{1,t}+\vec{\mu}_{2,t}\right)}{|\vec{\mu}_{1,t}+\vec{\mu}_{2,t}|^2}\left(\vec{\mu}_{1,t}+\vec{\mu}_{2,t}\right),\vec{\mu}_{2,t}-\frac{\vec{\mu}_{2,t}\cdot\left(\vec{\mu}_{1,t}+\vec{\mu}_{2,t}\right)}{|\vec{\mu}_{1,t}+\vec{\mu}_{2,t}|^2}\left(\vec{\mu}_{1,t}+\vec{\mu}_{2,t}\right)\right) \tag{4.11}$$

This dynamical system is well defined, as $\vec{\mu}_{1,t}$ and $\vec{\mu}_{1,t}$ are defined in $\mathbf{X}_t$, and are based on the utilities U_1 and U_2. However, this system is not linear in $\mathbf{M}_t$.

THEOREM **1** *[Cauchy-Lipschitz] If f_i is uniformly Lipschitz continuous for all i and continuous in t then the dynamical system has a unique solution given initial conditions.*

Proof 2 *Any textbook, see for example O'Regan [91].*

If the dynamical system has a unique solution is then invertible, this means that we can go back to initial conditions

4.4 More agents

Suppose now that there are more than two agents, so that $n \geq 3$. Trade is always bilateral, and *fair trading* implies that for every trade the marginal utility from trading has to be equally split among the parts:

$$\left(\vec{\mu}_{i,t} + \vec{\mu}_{j,t}\right) \cdot f_i\left(\vec{\mu}_{i,t}, \vec{\mu}_{j,t}\right) = 0 \quad \forall i, j \in N, i \neq j \tag{4.12}$$

This must hold for all of the $n-1$ possible couples where trader i is involved, so that individual i's instantaneous trade $\vec{f}_i$ lies in a sub–space of dimension $m-n+1$, if it exists. This clearly imposes a first constraint on the minimal possible amount m of goods.

Moreover, by the zero sum property, we need that the sum of all the istantaneous trades cancels out, $\sum \vec{f}_i = 0$. This is an additional constraint, that will be satisfied only if the dimension of the sub–space where $\vec{f}_i$ lies is more than one. So the minimum number of goods that guarantees the existence of fair trading is such that $m-n+1 \geq 2$, or that $m \geq n+1$.

Proposition 6 *If $n \geq 3$ then fair trading mechanism exists if and only if $m \geq n+1$*

EXAMPLE **1** *3 traders*

Suppose that for a certain allocation all the three vectors of marginal utilities of the traders are linearly independent. Say $\vec{\mu}_1 = (2,1,1)$, $\vec{\mu}_2 = (1,2,1)$ and $\vec{\mu}_3 = (1,1,2)$. $\vec{f}_1$ has to be orthogonal to both $\vec{\mu}_1 + \vec{\mu}_2 = (3,3,2)$ and $\vec{\mu}_1 + \vec{\mu}_3 = (3,2,3)$, so that it will be of the form $\vec{f}_1 = k(5,-3,-3)$, for some $k \in \mathbb{R}$. Similarly we will have $\vec{f}_2 = h(-3,5,-3)$, for some $h \in \mathbb{R}$, and $\vec{f}_3 = \ell(-3,-3,5)$, for some $\ell \in \mathbb{R}$.
To balance trading we need also that $\vec{f}_1 + \vec{f}_2 + \vec{f}_3 = (0,0,0)$, but as they are linearly independent vectors, this is possible only for $k = h = \ell = 0$, which means no trading, even if marginal utilities are not proportional. □

REMARK **1** *If the fair trading is between two traders* ($n = 2$) *then two goods* ($m \geq 2$) *are sufficient to guarantee the existence of trade*

The above can be easily verified, with two traders each trade $\vec{f}_1$ and $\vec{f}_2$ by construction is orthogonal to the same vector $\vec{f}_1 + \vec{f}_2$, so that they will never be linearly independent.

Previous example shows that if $m \leq n$, and $m \geq 3$, then fair trading is not possible. If the number of goods where instead $m = n+1$, then every candidate $\vec{f}_i$ would lie on a plane, and there would always exist a non–trivial solution for the zeros sum property because we would have a homogeneous system of linear equations with n linear equations in $n+1$ variables. If m is even greater, then existence would result *a fortiori*.

4.4.1 The network environment

What happens if $m \leq n+1$, if for instance there are only 2 goods and many agents? In this case we consider a market mechanism that allows for distinct couples to match and trade with some exogenously fixed probability in every instant of time. When they meet they will trade according to the unique fair trading mechanism defined in Section 4.3.

We assume an exogenously fixed vector $\vec{p}$ of probabilities among the n agents. At every instant in continuous time agent i is picked with probability p_i, and then i will trade with another of the $n-1$ nodes with uniform probability. In this way the couple of agents i and j may be matched to trade with probability $\frac{p_i+p_j}{n-1}$.

As randomness is confined to instantaneous moments in continuous time, we can express them just as weights by which the different matchings are considered. We can apply (4.7), that we will call $\vec{f}'$ and (4.11), to have a dynamical system of the form[2]

$$\frac{d\mathbf{X}_t}{dt} = \left(\sum_{i \in N} \frac{p_1 + p_i}{n-1} f_1'\left(\vec{\mu}_{1,t}, \vec{\mu}_{i,t}\right), \sum_{i \in N} \frac{p_2 + p_i}{n-1} f_2'\left(\vec{\mu}_{2,t}, \vec{\mu}_{i,t}\right), \ldots, \sum_{i \in N} \frac{p_n + p_i}{n-1} f_n'\left(\vec{\mu}_{n,t}, \vec{\mu}_{i,t}\right) \right) \tag{4.13}$$

As for the case of 4.11, this system is not linear. $\vec{f}_i$ is a linear combination of all the pairwise f_i's, based on the probabilities.

Proposition 7 *The fair trading mechanism on a network satisfies zero sum, trade and positive gradient properties.*

Zero sum holds as for every couple i and j, which is matched with weight $\frac{p_i+p_j}{n-1}$, $f_i = -f_j$ by construction, as discussed in Section 4.3.

[2] Here we consistently define that $f_i'\left(\vec{\mu}_{i,t}, \vec{\mu}_{i,t}\right) = \vec{0}$.

Trade holds because, for every couple i and j such that $\vec{\mu}_i$ and $\vec{\mu}_j$ are linearly independent, we can consider trader k such that $p_k > 0$. i and j will trade with k with positive weight, and if $\vec{\mu}_i$ and $\vec{\mu}_j$ are linearly independent, then at least one of them is linearly independent with $\vec{\mu}_k$, suppose it is j. From fair trading between two agents, as discussed in Section 4.3, we have that the marginal utility of that trader from that matching is strictly increasing. Then, as no other trading can generate negative marginal utilities, it means that the overall marginal utility of that trader from all matchings is strictly increasing. And this can happen only if there is trade, i.e.

$$\vec{f}_j = \sum_{i \in N} \frac{p_j + p_i}{n-1} f'_j\left(\vec{\mu}_{j,t}, \vec{\mu}_{i,t}\right) \neq \vec{0} \ . \tag{4.14}$$

Finally, positive gradient comes from the fact that $\vec{f}_i$ is a linear combination of f'_is, so that

$$\vec{\mu}_{i,t} \cdot \vec{f}_i = \sum_{j \in N} \frac{p_i + p_j}{n-1} \vec{\mu}_{i,t} \cdot f'_j\left(\vec{\mu}_{i,t}, \vec{\mu}_{j,t}\right) \ , \tag{4.15}$$

which is strictly positive as soon as there is trading.

The matching mechanism defined above generates a family of weighted networks, that can be thought as linear combination of stars. The least connected case possible is when the probability vector has only one entry equal to one. In this case one of the agents is picked with probability 1 and interact with any other with uniform probability, so that she is the core of a weighted star where each edge has weight $1/(n-1)$. In case in the vector $\vec{p}$ there is more than one entry which is non-zero the corresponding network is a star with a number of nodes in the core equal to the number of non-zero entries in $\vec{p}$. If all the entries in $\vec{p}$ are non-zero then the resulting network is a complete weighted network. [insert figure]

4.5 Analogous of the second welfare theorem for networks

In this section we will prove that there is a one to one mapping between the simplex of probabilities and the Pareto Set obtained as a result of the fair trade dynamics. Also, we will prove that this map has no holes (is simply connected) and so we can produce a version of the second welfare theorem for networks.

Define as $\mathscr{W}$ the set of stationary point of a dynamics based on marginal utilities, that is the subset of the Pareto Set that is reached by the trade dynamics defined by $\vec{f}$

THEOREM **2** *If f is continuous in t, x, p and Lipschitz in x with Lipschitz constant independent of t and p, then the solution $x(t, p, x(t_0))$ is continuous in $(t, p, x(t_0))$ jointly.*

Proof 3 *Being x continuous in p,$x(t_0)$ and uniformly in t, then the solution $x(t, p, x(t_0))$ is also continuous in t for given p and $x(t_0)$, we can equivalently say that the map $(p, x(t_0)) \to x(t, p, x(t_0))$ is continuous, so standard arguments imply that x is continuous in $t, p, x(t_0)$ jointly.*

THEOREM **3** *Given a pure exchange economy, with monotonic, continuous, convex preferences, and a trade dynamics defined by a Lipschitz continuous function, if x^* is a point in the Pareto Set $\mathcal{W}^N$ of the stable points of the dynamics, then there exist a weighted network g that, given the initial allocations, implements a sequence of trades that ends up in x^*.*

Proof 4 *Lipschitz continuity guarantees existence and uniqueness of solutions by (1), and uniqueness implies invertibility. Call $\bar{x}(t, p)$ the solution of the dynamical system defined by $f(t, x, p)$, with initial conditions $x(t_0) = x_0$. If we introduce a new variable $s \in \mathbb{R}^n$, and define as $\hat{x} = [x, s] \in \mathbb{R}^{mn+n}$ and $\hat{f}(t, \hat{x}) = [f(t, x, p), 0] \in \mathbb{R}^{nm+n}$, we can now define the initial condition as $\hat{x}(t_0) = [x_0, p]$, which means we are imposing $s(t_0) = p$, but parameters are not changing in time, so $s(t) = p$ for all t and the solution of the dynamical system defined by $\hat{f}(t, \hat{x})$ with initial condition $\hat{x}(t_0)$, is $\hat{x}^*(t, p) = [\bar{x}(t, p), p]$. This means we can transform parameters into initial conditions.*

Now define an initial time τ and final time t and assume that both lie in an interval $[a, b]$. Assume also that all the solutions $\hat{x}^*(t, p)$ exist in this interval (we can choose the interval arbitrarily so that all our solutions exist). Then define a map from a subset $\mathcal{U} \subset \mathbb{R}^{nm+m}$ into R^{nm+m}

$$S_\tau^t = x(t, \tau, \hat{x}(\tau)) \tag{4.16}$$

This map the initial value $\hat{x}(\tau)$ to the solution at time t. By (2) $x(t, \tau, \hat{x}(\tau))$ is continuous in $(t, \tau, \hat{x}(\tau))$. By uniqueness, it is invertible and its inverse is continuous. So $S_\tau^t : \mathcal{U} \to \mathcal{W}^N$ is a homeomorphism (that is one-to-one, onto, continuous, with continuous inverse).

From this follows our result: for any choice of the initial allocation and of the parameter p defining the network, there is one solution in $\mathcal{W}^N$, and for any such solution there is an allocation and a network that generated it through the trade dynamics

The above proofs follow standard arguments in the theory of ordinary differential equations. For reference, see E.A. Coddington [29], Burke [17]

LEMMA **8** *The map from initial allocations and network to the Pareto Set, $S_\tau^t : \mathcal{U} \to \mathcal{W}^N$ is simply connected.*

Proof 5 *$\mathscr{U}$ is a convex subset of $\mathbb{R}^{n+m}$ as a product of two convex subset of $\mathbb{R}^n$ and $\mathbb{R}^m$ respectively, so $\mathscr{U}$ is simply connected. Being $\mathscr{U}$ and $\mathscr{W}^N$ homoeomorphic, and given $\mathscr{U}$ is simply connected, this is a necessary and sufficient condition for $\mathscr{W}^N$ to be simply connected.*

Hence we proved that there is a continuous, invertible with continuous inverse map between the set of initial conditions (initial allocations and network) and that this map has no holes (it is simply connected). Notice also that as we did in the proof of theorem (3), that is transforming parameters into initial conditions, we can transform initial conditions into parameters, so that we can study the effect of the network topology fixed the initial allocations.

We are also able to characterize the set of Pareto Optima that are the resulting stable points of the fair trade dynamics

Proposition 9 *The set of stationary points of a fair trading dynamics on networks, $\mathscr{W}^N$ is a subset of the Pareto Set which is homeomorphic to a closed $(n-1)$ simplex.*

Proof 6 *The proof is trivial. $\mathscr{W}^N$ is a strict subset of $\mathscr{W}$ as the stable point of the trading dynamics are Pareto Optima and all those allocations in $\mathscr{W}$ where agents are worse off than their initial allocation in the dynamics are not in $\mathscr{W}^N$. Given that the set $\mathscr{W}$ is homeomorphic to a $(n-1)$ simplex and that $\mathscr{W}^N$ is continuous and simply connected, $\mathscr{W}^N$ is also homeomorphic to a $(n-1)$ simplex.*

The assumption of Lipschitz continuity is central in our context in order to ensure existence and uniqueness of the solution. Notice that although sufficient, Lipschitz continuity is not necessary for the existence of a solution continuous in the initial conditions, see for example Henry [48]. Lipschitz continuity is a strong form of uniform continuity which puts a condition on the rate of change of the function, or in other words it puts a bound on its first derivatives. In the case of our interests then a function may fail to be Lipschitz close to the boundary of the good space, that is to say where x is close to zero, where the rate of change of the function f can be very high. We rule this cases out by properly choosing the utility function, where the failure of Lispchitz assumption would not necessarily invalidate our results where there still exist a unique solution to the dynamical system defining trade.

4.5.1 A numeric example: the Cobb-Douglas case

In this section we present some numerical examples in the case of three agents trading two goods for which they have Cobb-Douglas preferences. By constructing the contract curve it will be shown that the stable points of the fair trading mechanism are diffeomorphic to

a $n-1$ simplex, as in the case contemplated in the appendix (C). We will also construct the one-to-one map between the simplex of the probabilities and the fair contracts as stated by theorem (3).

The state space of the trade dynamics in the network case is the cartesian product between the $n-1$ unitary simplex (which represents the space of probabilities with which agents are picked) and the space of commodities, that is $\Delta^{n-1} \times W \subset \mathbb{R}^{nm}$. One of the main results in the paper is that each point in the simplex, given an initial point in the commodity space, can be mapped into solution which, at a final time, corresponds to a point on the contract curve.

Suppose that the three agents have a Cobb-Douglas utility function (so convex preferences are satisfied) with constant return to scale, so $U_i(x) = x_1^{\alpha_i} x_2^{1-\alpha_i}$. This implies that the functions are concave, so in this case the Pareto Set is a curved $(n-1)$ simplex, or equivalently it is diffeomorphic to a unitary simplex.

Call α_i the exponent of the utility function for agent i, and $x_i(0) = (x_{i,1}, x_{i,2})$ the initial allocation for agent i. The probability space is represented by a unitary 2-simplex, where the barycentric coordinates of a point represent the probability triple (p_1, p_2, p_3).

Each point in the simplex is associated with a different color: red for the point $(1,0,0)$, blue for $(0,1,0)$, green for $(0,0,1)$. The probability simplex is represented as a color gradient of blue, red and green: each point has a different color, and starting from the three vertices they fade into each other, in a way that the magnitude of the component of blue, red and green in a color is proportional to the magnitude of the corresponding vertex coordinate. The (barycentric) coordinates of each point in the simplex represent the probability each agent is picked to trade. Every such point is mapped to a weighted graph according to the matching mechanism defined in section (4.4.1): given the probabilities (p_1, p_2, p_3), the edge between agents (i, j) has weight $(p_i + p_j)/2$. The triangle on the right of figure (4.3) shows this mapping: a point on the probability simplex is mapped to a point of the same color on the simplex of topologies. Notice that according to the matching rule above, in the extreme cases where the probability for one agent is 1 and the others' are zero (any of the three vertices of the probability simplex) the corresponding graph is a weighted star, where the agent with $p_i = 1$ is the core. All the other points in the simplex correspond to weighted complete graph. As a result notice that the topology simplex has vertices $(0.5, 0.5, 0), (0, 0.5, 0.5), (0.5, 0, 0.5)$. In the first case represented in figure (4.4) assume that the utility functions are determined by $\alpha_1 = 0.5$, $\alpha_2 = 0.4$, $\alpha_3 = 0.6$, while the initial allocations are such that agent three has the highest endowment of both goods, agent two has the lowest endowment of good 1 and endowment of good 2 higher than agent 1 that is $x_{3,1} > x_{1,1} > x_{2,1}$ and $x_{3,2} > x_{2,2} > x_{2,1}$. Note that with 3 agents and 2 goods

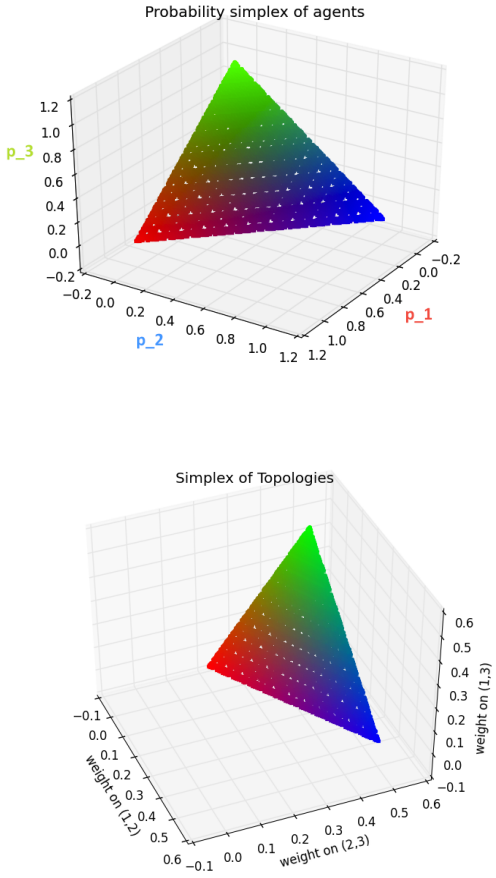

Fig. 4.3 Probability simplex (left) and corresponding simplex of topologies (right). Red corresponds to $p_1 = 1$, blue to $p_2 = 1$, green to $p_3 = 1$. The magnitude of the component of green, blue and red for each point is proportional to the magnitude of the corresponding probability.

the Edgeworth Box is a simplotope in 4 dimensions, so we cannot visualize it. We can represent the contract curve in the space of the agents' utilities, that is a tridimensional space. From the results obtained we know that the set of stable points of the trading dynamics, $\mathscr{W}^N$, is a subset of the contract curve (4.1), that it is homeomorphic to a 2-simplex. From the computations we that in the case of Cobb-Dougals, we have that the set of stable equilibria is not only homeomorphic but diffeomorphic to a 2-simplex.

Proposition 10 *With Cobb-Douglas utility function the set of stable point of a fair trading dynamics is diffeomorphic to a* $(n-1)$ *simplex.*

Consider figure (4.4): the leftmost simplex represents the space of topologies, each point in that space represents a weighted graph between the agents. Each topology is then

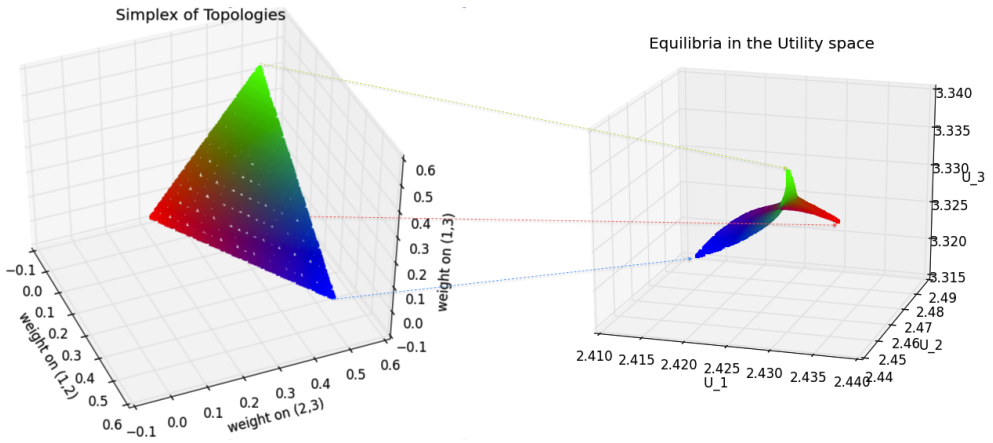

Fig. 4.4 Mapping between simplex of topologies and the corresponding equilibria. Only the three vertices are shown, map is according to colors

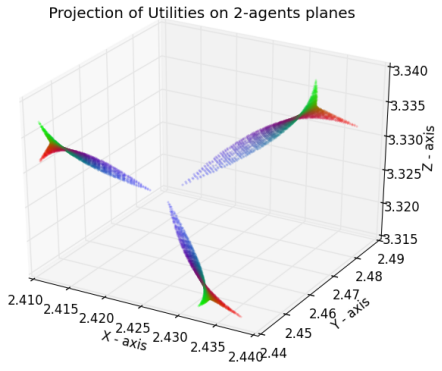

Fig. 4.5 Projection of equilibria in the space of utility on agents' planes

mapped to the corresponding equilibrium of the dynamical system defined by the fair trading mechanism, represented in the space of utilities on the right of the figure. The map between the two spaces is determined by colors, while the three vertices are explicitly mapped. The figure on the right, that is the set of equilibria $\mathscr{W}^N$ in this case, is a curved 2-simplex, with the vertices of the simplex of topologies that are mapped in the vertices of $\mathscr{W}^N$. Figure (4.5) shows the projections of the set of equilibria on the planes of the utility of two agents respectively, and makes the diffeomorphism more evident.

The computations confirm our results: the map between the network topologies and the set of equilibria is continuous, and there is a diffeomorphism between the simplex of topologies and the set of equilibria: each initial network is mapped by our dynamical process described in (4.13) into a point of the curved simplex representing the set of equilibria. Notice also that the points corresponding to the three vertices in the probability

simplex, that is to say cases in which the probability of being picked is 1 on one agent and zero on the others, so the cases in which the network is a weighted star with weights 0.5 on each edge, corresponds to points in which the utility of the core of the star is maximized. The effective level of utility will depend on the initial allocation, but in all the cases will be the highest possible given the initial allocation.

In the example in figure (4.4) agent 3 has the highest initial endowment, and ends up having the highest level of utility in all the possible cases, ranging from 3.315 in its minimum, when the network is a star in which agent 2 is the core (blue vertex), to 3.330 in its maximum (when agent 3 is the core of the star). From this we can infer that the trade with agent 1 is the most advantageous for agent 3, as well as for agent 2, as also her utility hits the minimum point when she can't trade with 3, and then increases when they trade on networks in which most of the interactions are between 2 and 3 (there is higher weight on this edge, as represented in the blue area). Clearly there is an asymptote in the growth of agent 1 utility moving towards a star in which agent 3 is the core (green area) and viceversa for agent 3 moving towards a star for which 1 is the core (red area). Looking at figure (4.5), utility of agent 1 is represented on the x axis, and utility of agent 3 on z axis: the figure has a twist in correspondance of the green area, where the utility of 1 stabilizes around 2.430(+) and utility of 3 steeply increases till its maximum, while in correspondance of the red area utility of 1 stabilizes around 3.330(+) while utility of 1 reaches its maximum.

In figure (4.6) we start at a different point in the space of goods. The initial allocations are such that $x_{1,1} > x_{2,1} > x_{3,1}$ and $x_{2,2} > x_{1,2} > x_{3,2}$ that is agent 1 and 2 have a lot of both goods and agent 3 is the poorest in both goods. As before each agent maximizes her utility when she is the core of a star. Agent 3 is the one who is worse off by being a periferal node when agent 1 or agent 2 are the core. This is not surprisingly as she is the one with the worst initial allocation. Viceversa utilities for agents 2 and 3 hit their minimum when agent 3 is in the core. By going towards the points in which the frequency of trades is mainly between agents 1 and 2 (the networks represented by the edge between the red and blue vertices in figure (4.3)) their utility is close to the maximum, meaning that both rich agents prefer trading among themselves because they can extract more utility, instead of trading with the "poor" agent only.

In figure (4.7) it is possible to observe the shape of the equilibrium points in the space of commodity one and commodity two respectively, helding the other commodity constant. As we would expect this is also a curved simplex, with each agent getting the highest quantity of each commodity (the vertices of the curved simplex) when they are the core of a star network.

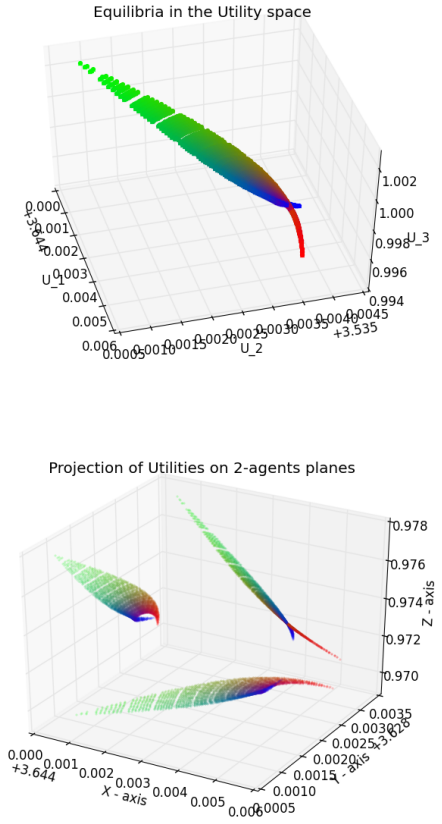

Fig. 4.6 Equilibria of the fair trading represented on the space of utilities for the case $\alpha_1 = \alpha_2 = \alpha_3 = 0.5$ (left) and projection on two-agents' planes.

We then consider the case of extreme inequality in which agent 1 starts with a lot of both goods and agents 2 and 3 have a much inferior initial allocation, more precisely $x_{1,1} > x_{3,1} > x_{2,1}$ and $x_{1,2} > x_{2,2} = x_{3,2}$, results are represented in figure (4.8) for the case of a Cobb-Douglas with $\alpha_1 = \alpha_2 = \alpha_3 = 0.5$, and in figure (4.9) for the case in which they all prefer good 2 than good 1, that is their utility functions are such that $\alpha_i = 0.2$ for $i = 1,2,3$. The first thing that we can notice is that the space of equilibria looks relatively similar in both cases, so that the initial allocation matters much more than the preferences, provided preferences are homogeneous across agents. Given the disproportion in initial allocations utility of agent 1 is greater than the two "poor" agents for all possible network topologies, while agent 2 and 3 maximize their utility when they are the core of a weighted star, as expected. Nonetheless notice that both agent 2 and 3 will prefer to be in the perifery of the star where agent 1 is the core than being in the perifery of the star where any of the other "poor" agent is in the core, even if the richest agent is maximizing her utility in this

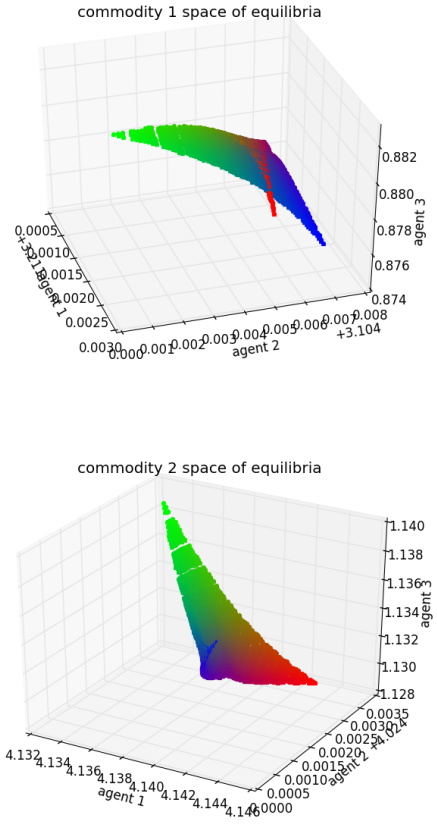

Fig. 4.7 Set of equilibria of a fair trading on the space of one commodity only

case. This is because both agents 2 and 3 prefer to have a consistent number of trades with agent 1, that is they will always prefer to trade in networks in which the weight of the edge connecting them with agent 1 is higher *ceteris paribus*, and this determines the "boomerang" shape of the set of equlibria.

Now consider the case in which agent 1 is still the richest, but the initial allocation is much less unequal than the previous two cases. The initial allocations in this case are $x_{1,1} > x_{2,1} > x_{3,1}$ and $x_{1,2} > x_{2,2} > x_{3,2}$, so agent 3 is the poorest. The results are represented in figure (4.9), preferences are the same as before. We can see how the picture drastically changes: now agent 2 worst position is when she is a periferal node of a star where agent 1 is the core, and the higher the frequency of trade in which agent 1 is involved, the lower agent's 2 utility. Agent 3, the most disadvantaged, is worst off when she is in the perifery of a star with 2 in the core, she would rather prefer agent 1 to be the core. In general her utility will decrease the higher the weight on the edge between 2 and 1.

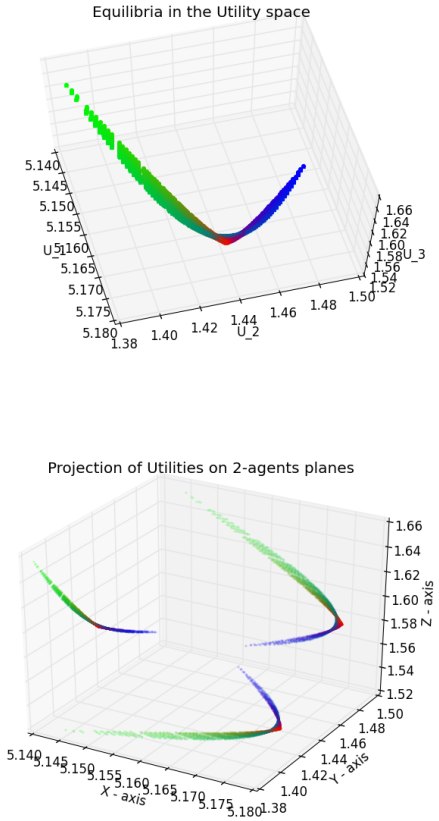

Fig. 4.8 $\alpha_1 = \alpha_2 = \alpha_3 = 0.5$, extreme inequality: agent 1 is rich agents 2,3 are poor.

To summarize the results obtained in this section, we have found that the utility of an agent depends crucially on her position in the network: it is maximized when the agent is the core of a weighted star *ceteris paribus*. When there is inequality in initial allocation, but there is not much variation between the two "poor" agents, then the disadvantaged agents prefer networks where they interact more with the richest agent over networks where they interact most of the times among them. When the inequality is extreme and there is a "middle income" agent and an "extremely poor" agent, the "middle income" may extract more utility by interacting with the "extremely poor" agent, while will not prefer to be in networks where she interact only with the richest agent because in this case her utility gain will be minimum. Viceversa the most disadvantaged agent will prefer to trade more with the richest agent than with the "middle income" agent. These results are related to Borondo et al. [14], who find a clear relation between the structure of the network and the meritocracy of the society, in the sense that when the network is sparse then individuals' compensations depends on the position in the network instead of their

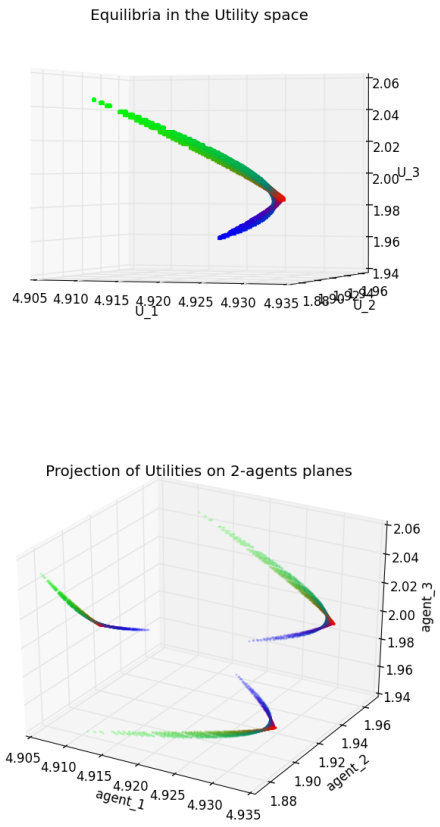

Fig. 4.9 $\alpha_1 = \alpha_2 = \alpha_3 = 0.2$, extreme inequality: agent 1 is rich agents 2,3 are poor

ability to produce value. Similar result is obtained in a coalitional setting by [123] who find a connection between network sparseness and inequality by studying how the extremal Lorenz distribution changes under different network topologies.

4.6 Conclusions

This paper studies an Edgeworth process on a weighted graph, where agents can continuously exchange their endowments with their neighbours, according to their utility functions. We define a family of trade dynamic which fixed points coincide with the Pareto Set, and choose a specific mechanism in this family, according to which individuals equally split the utility gain of every trade. This choice is without loss of generality as the results obtained hold for all mechanisms in the defined family. Under usual assumptions on the structure of preferences we prove a version of the Second Welfare Theorem on Networks: for any network in the space of finite weighted networks, there exists a sequence of Pareto

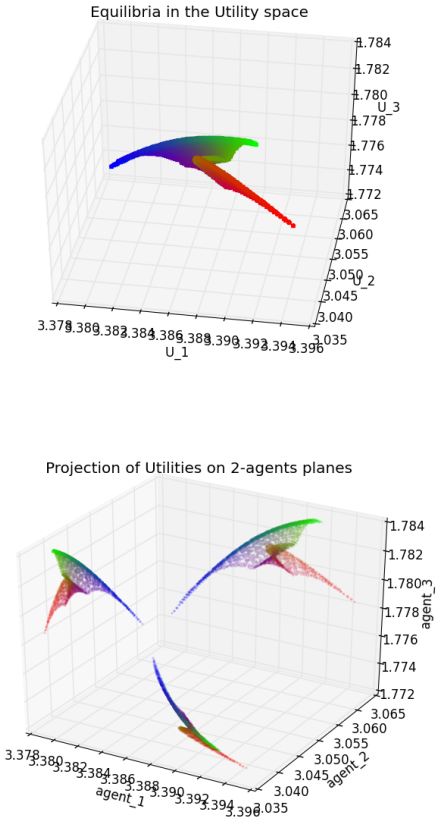

Fig. 4.10 $\alpha_1 = \alpha_2 = \alpha_3 = 0.2$ moderate inequality: agent 1 richer than agents 2 and 3.

improving trades which ends in the Pareto Set. Assuming Cobb-Douglas preferences we build numerical examples of the mapping between the network topology and the final allocation in the Pareto Set, and provide a brief analysis of the impact of the topology on the final allocation. This aspect can be further analyzed to include network related measures of inequality, to understand the link between deprivation in endowments and deprivation in opportunities determined by the position on the network.

References

[1] A. Cherif, H. Yoshioka, W. N. and Bose, P. (2009). Terrorism: Mechanism of radicalization process, control of contagion and counter-terrorist measures. *American Economic Review*.

[2] A. S. Mata, S. F. (2015). Multiple transitions of the susceptible-infected-susceptible epidemic model on complex network. *Physical Review*, 91.

[3] B. Bóllobas, S. J. and Riordan, O. (2007). The phase transition in inhomogeneous random graphs. *Random Structures & Algorithms*, 31:3–122.

[4] Baalen, M. V. (2000). Pair approximations for different spatial geometries. *In: The Geometry of Ecological Interactions: Simplifying Spatial Complexity, Cambridge University Press*, pages 359–387.

[5] Barabási, A. and Albert, R. (1999). Emergence of scaling in random networks. *Science*, 286:509–512.

[6] Barabasi, A.-L. and Albert, R. (1999). "Emergence of Scaling in Random Networks". *Science*, 286:509–512.

[7] Barthélemi, A. B. M. and Vespignani, A. (2008). *Dynamical processes on complex networks*. Cambridge University Press.

[8] Bauch, C. (2002). A moment closure method for sexually transmitted disease transmission through a concurrent partnership network. *Proceedings of the Royal Society*, 267:2019–2027.

[9] Bender, E. and Canfield, E. (1978). The asymptotic number of non-negative integer matrices with given row and column sums. *Journal of Combinatorial Theory, Series A*, 24:296–307.

[10] Bernoulli, D. (1760). Essai d'une nouvelle analyse de la mortalité causée pal la petite vérole, et des avantages de l'inoculation poir la prévenir. *Histoire de L'Acad.Roy.Sci. (Paris)*, pages 1–45.

[11] Bollobás, B. (1980). A probabilistic proof of an asymptotic formula for the number of labelled regular graphs. *European Journal of Combinatorics*, 1:311–316.

[12] Bollobás, B. (1981). Random graphs. *Combinatorics*, ed. H.N.V. Temperley, London Mathematical Society Lecture Note Series, 52, Cambridge University Press:80–102.

[13] Bollobás, B. (1998). *Modern Graph Theory*. Springer, Graduate texts in mathematics.

[14] Borondo, J., Borondo, F., Sickert, C., and Hidalgo, C. (2014). "To Each According to its Degree: The Meritocracy and Topocracy of Embedded Markets'. *Scientific Reports*, 4 (3784):DOI: 10.1038/srep03784.

[15] Bowles, S. (2006). *Microeconomics, Behavior, Institutions, and Evolution*. Princeton University Press, first edition.

[16] Bowles, S. and Gintis, H. (2011). *A Cooperative Species: Human Reciprocity and Its Evolution*. Princeton University Press.

[17] Burke, J. (2015). "ODEs: Continuity and Differentiability of Solutions'. *University of Washington, Mathematics Department*, http://www.math.washington.edu/~burke/crs/555/555_notes/continuity.pdf.

[18] C. Ballester, A. Calvó-Armengol, Y. Z. (2006). Who's who in networks. wanted: the key player. *Econometrica*, 74:1403–1417.

[19] Castellano, C. and Pastor-Satorras, R. (2010). Thresholds for epidemic spreading in networks. *Physical Review Letters*, 105.

[20] Cavalli-Sforza, L. and Feldman, M. (1981). *Cultural transmission and evolution: a quantitative approach*. Princeton University Press.

[21] Chakrabarti, D. et al. (2008). Epidemic thresholds in real networks. *ACM Transactions on Information and System Security*, 10.

[22] Clauset, A. and Gleditsch, K. (2012). The developmental dynamics of terrorist organizations. *Plos One*, 7.

[23] Clewley RH, Sherwood WE, L. M. and JM, G. (2007). Pydstool, a software environment for dynamical systems modeling. *URL http://pydstool.sourceforge.net*.

[24] Cowan, R. and Jonard, N. (2004). "Network Structure and The Diffusion of Knowledge'. *Journal of Economic Dynamics & Control*, 28:1557–1575.

[25] D. Chakrabarti, Y. Wang, D. W. and Faloutsos, C. (2003). Epidemic spreading in real networks: an eigenvalues viewpoint. *22nd International Symposium on Reliable Distributed Systems (SRDS'03)*.

[26] D. Juher, J. R. and Saldaña, J. (2013). Outbreak analysis of an sis epidemic model with rewiring. *Journal of Mathematical Biology*, 67:411–432.

[27] de Melo, W. (1976). "On the Structure of the Pareto Set of Generic Mappings". *Bol. Soc. Brasil. Mat.*, 7 (2):121–126.

[28] Demirel, G. and Gross, T. (2012). Absence of epidemic thresholds in a growing adaptive network. *Physics and Society*.

[29] E.A. Coddington, N. L. (1955). *Theory of Ordinary Differential Equations*. McGraw-Hill.

[30] Epstein, J. M. (2002). Modeling civil violence: an agent-based computational approach. *Proceeding National Academy of Sciences USA*, 99:7243–7250.

[31] Erdős, P. and Rényi, A. (1959). On random graphs. *Publicationes Matematicae Debrecen*, 6:290–297.

[32] Erdős, P. and Rényi, A. (1960). On the evolution of random graphs. In *PUBLICATION OF THE MATHEMATICAL INSTITUTE OF THE HUNGARIAN ACADEMY OF SCIENCES*, pages 17–61.

[33] Esteban, J. and Ray, D. (2011). Linking conflict to inequality and polarization. *American Economic Review*, 101:1345–1374.

[34] Esteban, J. and Ray, D. (2012). The evolutionary logic of terrorism: Understanding why terrorism is an inevitable human strategy in conflict. *In: The Psychology of Counterterrorism (Cass Series on Political Violence), Oxford: Routledge*.

[35] Euler, L. (1741). Solutio problematis ad geometriam situs pertinentis. *Commentarii Academiae Scientiarum Imperialis Petropolitanae*, 8:128–140.

[36] F.C. Santos, J.M. Pacheco, T. L. (2006). Evolutionary dynamics of social dilemmas in structured heterogeneous populations. *PNAS*, 103:3490–3494.

[37] Fisher, F. (1972). "On Price Adjustment Without an Auctioneer. *The Review of Economic Studies*, 39 (1):1–15.

[38] Fisher, F. (2003). Disequilibrium and Stability'. In Petri, F. and Hahn, F., editors, *General Equilibrium, Problems and Prospects*. Routledge, London, UK.

[39] Foley, D. (2010). "What's Wrong with the Fundamental Existence and Welfare Theorems?'. *Journal of Economic Behavior & Organization*, 75:115–131.

[40] G. Demirel, F. Vazquez, G. B. and Gross, T. (2014). Moment-closure approximations for discrete adaptive networks. *Physica D: Nonlinear Phenomena*, 15:68–80.

[41] Gale, D. (2000). *Strategic Foundations of General Equilibrium, Dynamic Matching and Bargaining Games*. Cambridge University Press, Cambridge, UK.

[42] Gintis, H. (2012). The Dynamics of Pure Market Exchange'. In M. Aoki, K. Binmore, S. D. and Gintis, H., editors, *Complexity and Institutions: Markets, Norms, and Corporations*. Palgrave Macmillan.

[43] Gleeson, J. (2013). Binary-state dynamics on complex networks: Pair approximation and beyond. *Physical Review X*, 3.

[44] Gleeson, J. et al. (2012). Accuracy of mean-field theory for dynamics on real-world networks. *Physical Review E*, 85.

[45] H. Matsuda, N. Ogita, A. S. and Satō, K. (1992). Statistical mechanics of population - the lattice lotka-volterra model. *Progress of Theoretical Physics*, 88:154–161.

[46] Hahn, F. (1962). "On the Stability of a Pure Exchange Equilibrium. *International Economic Review*, 3 (2):206–213.

[47] Hahn, F. (1982). Stability. In Arrow, K. and Intriligator, M., editors, *Handbook of Mathematical Economics*. North Holland, Amsterdam.

[48] Henry, C. (1973). "An Existence Theorem for a Class of Differential Equations with Multivalued Righthand Side'. *Journal of Mathematical Analysis and Applications*, 41:179–186.

[49] Hethcote, H. (2000). The mathematics of infectious diseases. *SIAM Review*, 42:599–653.

[50] Hofbauer, J. and Sigmund, K. (1998). *Evolutionary games and population dynamics*. Cambridge University Press.

[51] House, T. (2011). Modelling epidemics on networks. *arXiv:1111.4875*.

[52] Hurwicz, L., Radner, R., and Reiter, S. (1975a). "A Stochastic Decentralized Resource Allocation Process: Part i". *Econometrica*, 43 (2):187–221.

[53] Hurwicz, L., Radner, R., and Reiter, S. (1975b). "A Stochastic Decentralized Resource Allocation Process: Part ii". *Econometrica*, 43 (3):363–393.

[54] Ibsen-Jensen R., K. C. and Nowak, M. (2015). Computational complexity of ecological and evolutionary spatial dynamics. *PNAS*, 112:15636–41.

[55] J. Benoit, A. Nunes, M. T. d. G. (2006). Pair approximation models for disease spread. *Demophysics*, 50:177–181.

[56] J. Maynard-Smith, G. P. (1973). The logic of animal conflict. *Nature*, 246 (5427):15–18.

[57] Jackson, M. O. (2008). *Social and Economic Networks*. Princeton University Press, first edition.

[58] Jensen, M. K. and Rigos, A. (2014). Evolutionary games with group selection. *Working Paper of the University of Leicester*, 14.

[59] Kalai, E. (1977). "Proportional Solutions to Bargaining Situations: Intertemporal Utility Comparisons". *Econometrica*, 45 (7):1623–1630.

[60] Kalai, E. and Smorodinsky, M. (1975). "Other Solutions to Nash's Bargaining Problem". *Econometrica*, 43 (3):513–518.

[61] Keeling, M. and Eames, K. (2005). Networks and epidemic models. *Journal of The Royal Society Interface*, 2:295–307.

[62] Kermack, W. and McKendrick, G. (1927). A contribution to the mathematical theory of epidemics. *Proceedings of the Royal Society of London*, 115:700–721.

[63] Kuehn, C. (2016). *Moment Closure—A Brief Review*, pages 253–271. Springer International Publishing, Cham.

[64] Latora, V. and Marchiori, M. (2004). How the science of complex networks can help developing strategies against terrorism. *Chaos, Solitons & Fractals*, 20:69–75.

[65] Lebowitz, J. (2004). Pair approximation of the stochastic susceptible-infected-recovered-susceptible epidemic model on the hypercuibic lattice. *Physical Review E*.

[66] Lieberman E., C. H. and Nowak, M. A. (2005). Evolutionary dynamics on graphs. *Nature*, 433:312–316.

[67] Lovison, A. and Pecci, F. (2014). "Hierarichical Stratification of Pareto Sets". *arXiv:1407.1755*.

[68] M. Shkarayev, I. S. and Shaw, L. (2013). Recruitment dynamics in adaptive social netwokrs. *Journal of Physics A: Mathematical and Theoretical*, 46.

[69] Madden, P. (1978). "Why the Edgeworth Process Assumption Isn't That Bad?'. *The Review of Economic Studies*, 45:279–283.

[70] Manea, M. (Forthcoming). "Models of Bilateral Trade in Networks'. *The Oxford Handbook on the Economics of Networks*.

[71] Mas-Colell, A. (1990). *The Theory of General Economic Equilibrium*. Cambridge University Press, Cambridge, UK.

[72] McKay, B. and Wormald, N. (1991). Asymptotic enumeration by degree sequence of graphs with degrees $o(n^{1/2})$. *Combinatorica*, 11:97–117.

[73] Mesquita, B. D. (2005). The terrorist endgame: A model with moral hazard and learning. *Journal of Conflict Resolution*, 49:237–258.

[74] Miller, J. and Kiss, I. (2014). Epidemic spread in networks: Existing methods and current challenges. *Mathematical Modelling of Natural Phenomena*, 9:4–42.

[75] M.J. Keeling, D. R. and Morris, A. (1997). Correlation models for childhood epidemics. *Proceedings of The Royal Society*, 264:1149–1156.

[76] Nash, J. (1950). "The Bargaining Problem". *Econometrica*, 18 (2):155–162.

[77] Nash, J. (1952). "Two Persons Cooperative Games". *Econometrica*, 21 (1):128–140.

[78] Neumann, J. V. and Morgenstern, O. (1944). *Theory of Games and Economic Behavior*. Princeton University Press.

[79] Newman, M. (2002). The spread of epidemic disease on networks. *arXiv:cond-mat/0205009*.

[80] Newman, M. (2010). *Networks, An Introduction*. Oxford University Press.

[81] N.M. Ferguson, C. D. and Anderson, R. (1975). Transmission and control of arbovirus diseases. *Epidemiology K. L. Cooke, ed., SIAM, Philadelphia*, pages 104–121.

[82] N.M. Ferguson, C. D. and Anderson, R. (2001). The foot-and-mouth epidemic in great britain: Pattern of spread and impact of interventions. *Science*, 292:1155–1160.

[83] Nowak, M. (2006). *Evolutionary dynamics: exploring the equations of life*. The Belknap Press of Harvard University Press, first edition.

[84] Nowak, M. and May, R. B. (1964). The genetical evolution of social behaviour. i. *Journal of Theoretical Biology*, pages 1–16.

[85] Nowak, M. and May, R. B. (1992). Evolutionary game and spatial chaos. *Nature*, 359:826–829.

[86] Nowak, M. A. (2000). Evolutionary biology of language. *Philos Trans R Soc Lond B Biol Sci.*, 355:1615–1622.

[87] Nowak M.A., C. T. and Antal, T. (2010). Evolutionary dynamics in structured populations. *Philosophical Transaction of the Royal Society B*, 365:19–30.

[88] Ohtsuki, H. and Nowak, M. A. (2006). The replicator equation on graphs. *Journal of Theoretical Biology*, 243:86–97.

[89] Ohtsuki, H. and Nowak, M. A. (2008). Evolutionary stability on graphs. *Journal of Theoretical Biology*, 251:698–707.

[90] Ohtsuki H., J. P. and Nowak, M. A. (2007). Evolutionary graph theory: breaking the symmetry between interaction and replacement. *Journal of Theoretical Biology*, 246:681–694.

[91] O'Regan, D. (1997). *Existence Theory for Nonlinear Ordinary Differential Equations*. Springer Science+ Business Media, Dordrecht.

[92] Pastor-Satorras, R. and Vespignani, A. (2001). Epidemic spreading in scale-free networks. *Physical Review Letters*, 86:3200–3203.

[93] Petri, F. and F. Hahn, E. (2003). *General Equilibrium, Problems and Prospects*. Routledge, London, UK.

[94] Pin, P. and Rogers, B. (2015). Stochastic network formation and homophily. *Oxford Handbook on the Economics of Networks*.

[95] R. Axelrod, W. H. (1981). The evolution of cooperation. *Science*, 211:1390–1396.

[96] R. Pastor-Satorras, C. Castellano, P. V. M. and Vespignani, A. (2015). Epidemic processes in complex networks. *Review of Modern Physics*, 87.

[97] RH, C. (2012). Hybrid models and biological model reduction with pydstool. *PLoS Computational Biology*, 8:e1002628.

[98] Risau-Gusman, S. and Zanette, D. (2009). Contact switching as a control strategy for epidemic outbreaks. *Journal of Theoretical Biology*, 257:52–60.

[99] Rubinstein, A. (1982). "Perfect Equilibrium in a Bargaining Model'. *Econometrica*, 50 (2):97–109.

[100] Rubinstein, A. and Wolinsky, A. (1990). "Decentralized Trading, Strategic Behaviour and the Walrasian Outcome'. *The Review of Economic Studies*, 57 (1):63–78.

[101] S. Currarini, M. J. and Pin, P. (2009). An economic model of friendship: Homophily, minorities and segregation. *Econometrica*, 77:1003–1045.

[102] S. Tench, H. F. and Gill, P. (2016). Spatio-temporal patterns of IED usage by the Provisional Irish Republican Army. *European Journal of Applied Mathematics*, 27:377–402.

[103] Sabourian, H. (2004). "Bargaining and Markets: Complexity and the Competitive Outcome'. *Journal of Economic Theory*, 116:189–228.

[104] Sandholm, W. (2009). Evolutionary game theory. in *Encyclopedia of complexity and system science,* R.A. Meyers ed., pages 3176–3205.

[105] Sandler, T. and Arce, D. (2007). Terrorism: a game-theoretic approach. *Handbook of Defense Economics*, 2:775–813.

[106] Sandler, T. and Enders, W. (1995). Terrorism: Theory and applications. *Handbook of Defense Economics*, 1.

[107] Sandler, T. and Enders, W. (2012). *The Political Economy of Terrorism.* Cambridge University Press.

[108] S.C. Ferreira, C. C. and Pastor-Satorras, R. (2012). Epidemic thresholds of the susceptible-infected-susceptible model on networks: A comparison of numerical and theoretical results. *Physical Review*, 86.

[109] Schaub, E. and Darken, C. (2007). Utilizing biological models to determine the recruitment of the irish republican army. *International Journal of Social, Behavioral, Educational, Economic, Business and Industrial Engineering*, 1.

[110] Shakarian P., P. Roos, A. J. (2012). A review of evolutionary graph theory with applications to game theory. *BioSystems,* 107:66–80.

[111] Shaw, L. and Schwartz, I. (2010). Enhanced vaccine control of epidemics in adaptive networks. *Physical Review E*, 81.

[112] Shoham, Y. and Leyton-Brown, K. (2008). *Multiagent Systems.* Cambridge University Press, Cambridge, UK.

[113] Shoval, O. et al. (2012). "Evolutionary Tradeoffs, Pareto Optimality, and the Geometry of Phenotype Space". *Science*, 336 (6085):11571–1160.

[114] Smale, S. (1975). "Global Analysis and Economics I Pareto Optimum and a Generalization of Morse Theory". *Synthese, Mathematical Methods of the Social Sciences*, 31 (2):345–358.

[115] T. Gross, C. D. and Blasius, B. (2006). Epidemic dynamic on an adaptive network. *Physical Review Letters*, 96.

[116] T. House, M. K. (2011). Insights from unifying modern approximations to infections on networks. *J. R. Soc. Interface*, 8.

[117] Taylor, P. and Jonker, L. (1978). Evolutionary stable strategies and game dynamics. *Mathematical Biosciences*, 40:145–156.

[118] Thomson, W. (2009). "Bargaining and The Theory of Cooperative Games: John Nash and Beyond'. *Working Paper, Rochester Center for Economic Research*, 554.

[119] T.P. Davies, H.M. Fry, A. W. and Bishop, S. R. (2013). A mathematical model of the london riots and their policing. *Nature Scientific Reports*, 3.

[120] Trapman, P. (2007). Reproduction numbers for epidemics on networks using pair approximation. *Mathematical Biosciences*, 210.

[121] Uwadia F., G. L. and Lambertini, L. (2006). A dynamical model of terrorism. *Discrete Dynamics in Nature and Society*, pages 1–32.

[122] Uzawa, H. (1962). "On the Stability of Edgeworth's Barter Process'. *International Economic Review*, 3 (2):218–232.

[123] W. Kets, G. Iyengar, R. S. and Bowles, S. (2011). Inequality and network structure. *Games and Economic Behavior*, 74:47–97.

[124] Wan, Y. (1978). "On the Structure and Stability of Local Pareto Optima in a Pure Exchange Economy". *Journal of Mathematical Economics*, 5:255–274.

[125] Wormald, N. (1999). Models of random regular graphs. *Surveys in Combinatorics*, J.D. Lamb and D.A. Preece, eds. London Mathematical Society Lecture Note Series, 276, Cambridge University Press:239–298.

[126] X. Luo, X. Zhang, G. S. and Jin, Z. (2014). Epidemical dynamics of sis pair approximation models on regular and random networks. *Physica A*, 410:144–153.

[127] Young, H. P. (1993). "The Evolution of Conventions". *Econometrica*, 61:57–84.

Appendix A

A.1 Evolutionarily Stable Strategy

Define *pure strategies* as the finite set of behaviours that a player in the game can adopt $Z = \{z_1, ..., z_n\}$ where n is the number of such strategies. Let a *mixed strategy* be a profile of ex-ante probabilities to play each pure strategy, $S_n = \{\mathbf{p} = [p_1, ..., p_n] \in \mathbb{R}^n : p_i \geq 0, \quad \sum_{i=1}^{n} p_i = 1\}$. Clearly a *pure strategy* can be seen as a degenerate *mixed strategy* with $p = e_i$, $i = 1, ..., n$. Suppose the game has two players only, and define as $\pi_{i,j}$ the payoff for a player adopting the pure strategy z_i facing a player adopting z_j. Hence all the possible payoffs can be collected in the payoff matrix $\Pi = [\pi_{i,j}]$. Considering $\mathbf{p}$ and $\mathbf{q}$ as two possible profiles of mixed strategy, the expected payoff of a player adopting $\mathbf{p}$ against a player adopting $\mathbf{q}$ is given by $\mathbf{p}\Pi\mathbf{q} = \sum_{ij} \pi_{ij} p_i p_j$. A *strict Nash Equilibrium* is defined as the strategy that is the unique best reply to itself, so $\mathbf{p}$ is a (strict) Nash Equilibrium if $\mathbf{p}\Pi\mathbf{p} > \mathbf{p}\Pi\mathbf{q}$ $\forall \mathbf{q} \neq \mathbf{p}$, that is to say the strategy which gives the highest expected payoff.
An Evolutionarily Stable Strategy [ESS] can be seen as a refined form of Nash Equilibrium. Following [50] we can give the definition of an ESS

Definition 4 *The strategy* $\mathbf{p}$ *is an ESS if, whenever in a population playing* $\mathbf{p}$ *a small fraction* ϵ *of mutant playing* $\mathbf{q}$ *is introduced, the resident population has an higher expected payoff than the mutant. That is to say*

$$\mathbf{p}\Pi(\epsilon\mathbf{q} + (1-\epsilon)\mathbf{p}) > \mathbf{q}\Pi(\epsilon\mathbf{q} + (1-\epsilon)\mathbf{p}) \tag{A.1}$$

with $\epsilon > 0$ *sufficiently small and* $\forall\, \mathbf{q} \in S_n$.

With $\epsilon \to 0$ we can say that $\mathbf{p}$ is ESS if the following two conditions hold:

$$\mathbf{p}\Pi\mathbf{p} \geq \mathbf{p}\Pi\mathbf{q} \quad \forall \mathbf{q} \in S_n \tag{A.2}$$

$$\text{if}\,\mathbf{p} \neq \mathbf{q}\,\text{and}\,\mathbf{p}\Pi\mathbf{p} = \mathbf{p}\Pi\mathbf{q}\,\text{then}\,\mathbf{p}\Pi\mathbf{q} > \mathbf{q}\Pi\mathbf{q} \tag{A.3}$$

(*A*.2) can be called an *equilibrium condition*, and it corresponds to the definition of a Nash Equilibrium (NE), while (*A*.3) is a *stability condition* that guarantees that the mutant cannot take over the population, requiring that in case the NE is not strict, the resident strategy performs better against the mutant than the mutant does against itself.
From these it is clear that (strict) NE $\iff$ ESS. The expected payoff in (*A*.1) are obtained assuming population is well-mixed, so that the probability of facing an individual playing a strategy $\mathbf{p}$ is given by the fraction of $\mathbf{p}$ in the population. In the case of a regular graph, the ESS is obtained by (A.2) and (A.3) with the transformed payoff matrix $\hat{\Pi}$. Thus the ESS condition on a regular graph of degree k is given by:

$$\mathbf{p}\hat{\Pi}\mathbf{p} > \mathbf{p}\hat{\Pi}\mathbf{q} \quad \forall \mathbf{q} \in S_n \tag{A.4}$$

The case $\mathbf{p}\hat{\Pi}\mathbf{p} = \mathbf{p}\hat{\Pi}\mathbf{q}$ is not taken in consideration because the values in B are obtained by approximation and, moreover, if the number of strategies $n \geq 4$ the class of games with equality in (*A*.4) is of measure zero.

Appendix B

B.1 Pair Equations, static network

The detailed bookeeping of the events that affects the dynamics of the pairs for the static network B.1 and the adaptive network B.2.

$$
\begin{aligned}
\dot{p}_{SI} &= \underbrace{\beta(k-1)\frac{p_{SS}p_{SI}}{x_S} - \beta(k-1)\frac{p_{SI}^2}{x_S} - \beta p_{SI}}_{\text{infection } (S\to I)} \\
&+ \underbrace{\gamma(k-1)\frac{p_{RI}p_{II}}{x_I} - \gamma(k-1)\frac{p_{SI}p_{IR}}{x_I}}_{\text{surveillance } (I\to S)} \\
&+ \underbrace{\epsilon(p_{II}-p_{SI})}_{\text{voluntary exit } (I\to S)} \\
\dot{p}_{RI} &= \underbrace{\beta(k-1)\frac{p_{RS}p_{SI}}{x_S}}_{(S\to I)} - \underbrace{\gamma(k-1)\frac{p_{RI}^2}{x_I} - (\epsilon+\gamma)p_{RI}}_{(I\to S)} \\
\dot{p}_{RS} &= \underbrace{\gamma(k-1)\frac{p_{RI}^2}{x_I}}_{(I\to S)} - \underbrace{\beta(k-1)\frac{p_{RS}p_{SI}}{x_S}}_{(S\to I)} + \underbrace{(\epsilon+\gamma)p_{RI}}_{(I\to S)} \\
\dot{p}_{SNS} &= \underbrace{-\beta(k-1)\frac{p_{SI}p_{SNS}}{x_S}}_{(S\to I)} + \underbrace{\gamma(k-1)\frac{p_{RI}p_{INS}}{x_I} + \epsilon p_{INS}}_{(I\to S)} \\
\dot{p}_{INS} &= \underbrace{\beta(k-1)\frac{p_{SI}p_{SNS}}{x_S}}_{(S\to I)} - \underbrace{\gamma(k-1)\frac{p_{RI}p_{INS}}{x_I} - \epsilon p_{INS}}_{(I\to S)}
\end{aligned}
\tag{B.1}
$$

B.2 Pair Equations, adaptive network

$$
\begin{aligned}
\dot{p}_{SI} &= \underbrace{\beta(\kappa-1)\frac{p_{SS}p_{SI}}{x_S} - \beta(\kappa-1)\frac{p_{SI}^2}{x_S} - \beta p_{SI}}_{\text{infection } (S\to I)} \\
&\quad \underbrace{-\gamma(\kappa-1)\frac{p_{SI}p_{IR}}{x_I}}_{\text{surveillance } (I\to S)} \\
&\quad + \underbrace{\epsilon(p_{II}-p_{SI})}_{\text{voluntary exit } (I\to S)} + \underbrace{\mu\kappa(P_I P(IS)+P_S P(SI))}_{\text{arrival}} \underbrace{-\mu\kappa p_{SI}+\kappa\gamma p_{RI}p_{SI}}_{\text{normalization}} \\
\dot{p}_{RI} &= \underbrace{\beta(\kappa-1)\frac{p_{RS}p_{SI}}{x_S}}_{(S\to I)} \underbrace{-\gamma(\kappa-1)\frac{p_{RI}^2}{x_I} - \epsilon p_{RI}}_{(I\to S)} + \underbrace{\mu\kappa P_I P(IR)}_{\text{arrival}} \underbrace{-\mu\kappa p_{RI}+\kappa\gamma p_{RI}^2}_{\text{normalization}} \\
\dot{p}_{RS} &= \underbrace{-\beta(\kappa-1)\frac{p_{RS}p_{SI}}{x_S}}_{(S\to I)} + \underbrace{\epsilon p_{RI}}_{(I\to S)} + \underbrace{\mu\kappa P_S P(SR)}_{\text{arrival}} \underbrace{-\mu\kappa p_{RS}+\kappa\gamma p_{RI}p_{RS}}_{\text{normalization}} \\
\dot{p}_{SNS} &= \underbrace{-\beta(\kappa-1)\frac{p_{SI}p_{SNS}}{x_S}}_{(S\to I)} + \underbrace{\epsilon p_{INS}}_{(I\to S)} \\
&\quad + \underbrace{\mu\kappa(P_S P(SNS)+P_{NS}P(NSS))}_{\text{arrival}} \underbrace{-\mu\kappa p_{SNS}+\kappa\gamma p_{RI}p_{SNS}}_{\text{normalization}} \\
\dot{p}_{INS} &= \underbrace{\beta(\kappa-1)\frac{p_{SI}p_{SNS}}{x_S}}_{(S\to I)} \underbrace{-\epsilon p_{INS}}_{(I\to S)} \underbrace{-\mu\kappa p_{INS}+\kappa\gamma p_{RI}p_{INS}}_{\text{normalization}}
\end{aligned}
\tag{B.2}
$$

B.3 Eigenvalues

In the general case of

$$
-\frac{1}{2\rho}\Big[\rho(2\beta+3\epsilon+\beta q_{R|S}(k-1)-\beta k)+\beta q_{S|NS}x_{NS}(k-1)\pm\Theta\Big] \tag{B.3}
$$

where

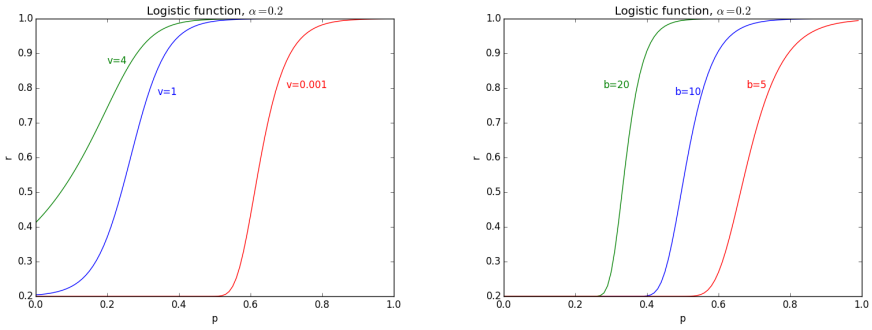

Fig. B.1 Examples of $\mathscr{GL}$ varying the parameters.

$$\Theta = \Big[\epsilon^2\rho^2 + 2\beta\epsilon\rho((2+k-q_{R|S}+kq_{R|S})\rho-(k-1)q_{S|NS}x_{NS}) + \beta^2((2+k(-1+q_{R|S})-q_{R|S})\rho+(-1+k)q_{S|NS}x_{NS})^2\Big]^{\frac{1}{2}} \tag{B.4}$$

The generalized logistic function is:

$$\mathscr{GL} = \alpha + \frac{\psi}{(1+Qe^{-bp})^{\frac{1}{v}}} \tag{B.5}$$

α and ψ are the lower and upper asymptotes, b is the growth rate (if $b=1$ the function is linear), $v>0$ determines if the maximum growth of the curve is closer to the lower or upper asymptote, and the values of Q and b chosen so that $r=\alpha$ when $p=0$.

Appendix C

Notice that finding the contract curve corresponds to solving a convex multiobjective optimization problem, and the solution in the contract curve are the Pareto Optima of this optimization problem. Here we present a proposition which is a stronger case than (3).

Proposition 11 *[Lovison and Pecci [67]] Let $X \subset \mathbb{R}^l$ open and convex. Let $f_i : X \longrightarrow \mathbb{R}$, $i = 1,\ldots,n$, $l \leq n$, be smooth and convex functions. Then the Pareto set is a curved $n-1$ simplex, i.e. it is diffeomorphic to an $n-1$ dimensional simplex, i.e. the convex hull of a set of n points in general position in $\mathbb{R}^n$. Each one of the vertices coincides with one of the optima of the n functions taken separately. Every $k-1$ facet of the curved simplex corresponds to the Pareto optimal set of the problem defined by a subset of k functions in $\{u_1,\ldots,u_n\}$.*

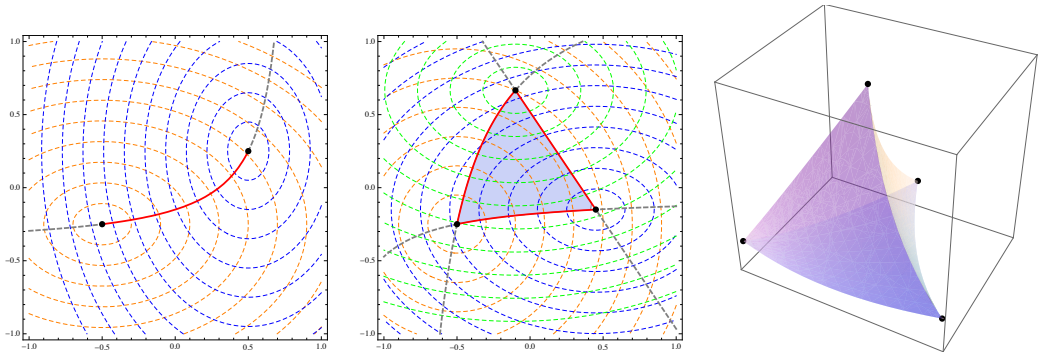

Fig. C.1 Taken from Lovison and Pecci [67], shows the case of the Pareto Set as in the convex case, respectively for 2 functions (leftmost graph), 3 functions and 4 functions.

Proposition [11] has been show geometrically by Shoval et al. [113].

Definition 5 *A function $f(x) : \mathbb{R}^n \to \mathbb{R}^n$ is Lipschitz continuous if there exists a constant L such that:*

$$|f(x) - f(x')| \leq L|x - x'| \quad \forall \quad x, x' \in \mathbb{R}^n$$

Definition 6 *A topological space X is pathwise-connected if and only if for every two points $x, y \in X$ there is a continuous function f from $[0,1]$ to X such that $f(0) = x$ and $f(1) = y$, in other words for any two points in X there is a path connecting them.*

Definition 7 *A space S is simply connected (or 1-connected) if it is pathwise-connected and if every map from the 1-sphere to S extends continuously to a map from the 2-disk, that is every loop in S is contractible.*

Here we also present a proof of (3), that the Pareto Set is homeomorphic to a$(n-1)$ simplex.

Proof 7 . *[[71]] Define as Δ the $(n-1)$ closed unitary simplex, $U = \{u \in \mathbb{R}^n : u(x) = (u_1(x_1), \ldots, u_n(x_n))\}$ the set of the utilities of the attainable allocations for all agents, and $\mathcal{W}$ the set of weak optimal allocations. U is convex, closed and bounded. Given that $u_i(0) = 0$ for all i and preferences are monotone, then 0 is in the interior of the set of the utilities and if $0 \leq v' < v \in U$ then v' is in the interior of U relative to $\mathbb{R}^n_+$. Hence for each $p \in \Delta$ there is a unique $u(p) \in \mathcal{W}$ such that $p = \alpha u(p)$ for some $\alpha > 0$. The map $p \to u(p)$ is continuous because U is compact, and this map is the homeomorphism we are looking for.*

List of Abbreviations

PA pair approximation
PD prisoner dilemma
NE Nash equilibrium
DFE disease free equilibrium
EE endemic equilibrium
HEE high infection endemic equilibrium
LEE low infection endemic equilibrium
EGT evolutionary game theory
EGrT evolutionary graph theory
BD birth-death
DB death-birth
IM imitation
ESS evolutionary stable strategy
MR multi-regular